0-315-01044-4

National Library of Canada | Bibliothèque nationale du Canada

Canadian Theses Division | Division des thèses canadiennes

Ottawa, Canada
K1A 0N4

48902

PERMISSION TO MICROFILM — AUTORISATION DE MICROFILMER

• Please print or type — Écrire en lettres moulées ou dactylographier

Full Name of Author — Nom complet de l'auteur

GLENN RICHARD CAMERON

Date of Birth — Date de naissance	Country of Birth — Lieu de naissance
13/12/46	CANADA

Permanent Address — Résidence fixe

7603 - 153 ST.
EDMONTON, ALTA
T5R 1N3

Title of Thesis — Titre de la thèse

A SOLID STATE GALVANIC CELL TO DETERMINE THERMODYNAMIC PROPERTIES OF GROUP VIB CARBIDES.

University — Université

UNIVERSITY OF ALBERTA

Degree for which thesis was presented — Grade pour lequel cette thèse fut présentée

M. Sc. IN METALLURGY

Year this degree conferred — Année d'obtention de ce grade	Name of Supervisor — Nom du directeur de thèse
1980	DR. T. H. ETSELL

Permission is hereby granted to the NATIONAL LIBRARY OF CANADA to microfilm this thesis and to lend or sell copies of the film.

The author reserves other publication rights, and neither the thesis nor extensive extracts from it may be printed or otherwise reproduced without the author's written permission.

L'autorisation est, par la présente, accordée à la BIBLIOTHÈQUE NATIONALE DU CANADA de microfilmer cette thèse et de prêter ou de vendre des exemplaires du film.

L'auteur se réserve les autres droits de publication; ni la thèse ni de longs extraits de celle-ci ne doivent être imprimés ou autrement reproduits sans l'autorisation écrite de l'auteur.

Date	Signature
Oct 9/80	A. Cameron

NL-91 (4/77)

National Library of Canada

Cataloguing Branch
Canadian Theses Division

Ottawa, Canada
K1A 0N4

Bibliothèque nationale du Canada

Direction du catalogage
Division des thèses canadiennes

NOTICE

The quality of this microfiche is heavily dependent upon the quality of the original thesis submitted for microfilming. Every effort has been made to ensure the highest quality of reproduction possible.

If pages are missing, contact the university which granted the degree.

Some pages may have indistinct print especially if the original pages were typed with a poor typewriter ribbon or if the university sent us a poor photocopy.

Previously copyrighted materials (journal articles, published tests, etc.) are not filmed.

Reproduction in full or in part of this film is governed by the Canadian Copyright Act, R.S.C. 1970, c. C-30. Please read the authorization forms which accompany this thesis.

AVIS

La qualité de cette microfiche dépend grandement de la qualité de la thèse soumise au microfilmage. Nous avons tout fait pour assurer une qualité supérieure de reproduction.

S'il manque des pages, veuillez communiquer avec l'université qui a conféré le grade.

La qualité d'impression de certaines pages peut laisser à désirer, surtout si les pages originales ont été dactylographiées à l'aide d'un ruban usé ou si l'université nous a fait parvenir une photocopie de mauvaise qualité.

Les documents qui font déjà l'objet d'un droit d'auteur (articles de revue, examens publiés, etc.) ne sont pas microfilmés.

La reproduction, même partielle, de ce microfilm est soumise à la Loi canadienne sur le droit d'auteur, SRC 1970, c. C-30. Veuillez prendre connaissance des formules d'autorisation qui accompagnent cette thèse.

THIS DISSERTATION HAS BEEN MICROFILMED EXACTLY AS RECEIVED

LA THÈSE A ÉTÉ MICROFILMÉE TELLE QUE NOUS L'AVONS REÇUE

THE UNIVERSITY OF ALBERTA

A SOLID STATE GALVANIC CELL TO DETERMINE THERMODYNAMIC PROPERTIES OF GROUP VIB CARBIDES

by

© GLENN R CAMERON

A THESIS

SUBMITTED TO THE FACULTY OF GRADUATE STUDIES AND RESEARCH

IN PARTIAL FULFILMENT OF THE REQUIREMENTS FOR THE DEGREE

OF MASTER OF SCIENCE

IN

METALLURGY

EDMONTON, ALBERTA

FALL 1980

THE UNIVERSITY OF ALBERTA

FACULTY OF GRADUATE STUDIES AND RESEARCH

The undersigned certify that they have read, and recommend to the Faculty of Graduate Studies and Research, for acceptance, a thesis entitled A SOLID STATE GALVANIC CELL TO DETERMINE THERMODYNAMIC PROPERTIES OF GROUP VIB CARBIDES submitted by GLENN R CAMERON in partial fulfilment of the requirements for the degree of MASTER OF SCIENCE in METALLURGY.

T. H. Etsell

Supervisor

J. E. Mather

Samuel A. Bradford

Date Oct. 2, 1980

DEDICATION

TO MARLENE

ABSTRACT

A galvanic cell employing calcia stabilized zirconia as the solid electrolyte was developed for the determination of the free energies of formation of the Group VIB carbides.

The initial cell designs using prepurified argon gas flowing over the anode and cathode compartments failed to produce stable, reproducible readings due to the oxygen content in the gas even though a titanium gettering furnace was incorporated into the design.

Subsequent evacuated cell designs overcame this problem and were used for the chromium carbide (Cr_3C_2), the molybdenum carbide (Mo_2C) and the tungsten carbide (WC) systems.

For the latter two systems, the temperature range capable of being studied was restricted at temperatures less than 800°C by the sluggishness of the cell reactions and at temperatures greater than 850°C by excessive cathode compartment pressures.

For the chromium system, similar low temperature restrictions applied, but the upper limit was bounded by the onset of electronic conductivity. Regression analysis of the free energy data for chromium carbide (Cr_3C_2) gave the expression:

$$\Delta G^0 = -15000 + 6.1T \text{ cal/mole}$$

which, when compared to previous investigations, is less negative but consistent with the results obtained from other emf studies.

ACKNOWLEDGEMENTS

I would like to express my sincerest appreciation to Dr. T.H. Etsell for his guidance and encouragement throughout the course of this research.

I would like to thank the staff of the Department of Mineral Engineering for their co-operation and assistance, in particular Messrs. T. Forman, B. Konzuk, H. Nerenberg, B. Smith, B. Snider and Mrs. C. Barker.

My thanks also to B. Flintoff for use of his computer programs, Dr. A. Block-Bolten for his advice and suggestions and Mrs. C. Best for her typing and proofreading.

I need also mention fellow graduate student P. Griffin whose conferences, companionship and criticisms were enjoyed and endured while writing this thesis.

Lastly, I am particularly indebted to my wife, Marlene, whose patience, understanding, support and encouragement were always sustaining.

Table of Contents

Chapter		Page
I.	LITERATURE REVIEW	1
	A. CHROMIUM CARBIDE	3
	INTRODUCTION	3
	THERMODYNAMIC DATA	4
	B. MOLYBDENUM CARBIDE	19
	INTRODUCTION	19
	THERMODYNAMIC DATA	19
	C. TUNGSTEN CARBIDE	24
	INTRODUCTION	24
	THERMODYNAMIC DATA	24
	D. SOLID ELECTROLYTES	28
	E. OXIDE ELECTROLYTES	29
II.	THEORY	31
	A. IONIC AND ELECTRONIC CONDUCTIVITY	31
	B. CONDUCTION DOMAINS	34
	C. THERMODYNAMIC MEASUREMENTS	35
	D. CELL REACTIONS	37
	CHROMIUM CARBIDE	37
	MOLYBDENUM CARBIDE	38
	TUNGSTEN CARBIDE	39
III.	EXPERIMENTAL	40
	A. MOLYBDENUM RESISTANCE FURNACE	40
	DESIGN AND CONSTRUCTION	40

B. CELL DESIGNS 42
ARGON FLOW CELLS 42
EVACUATED CELLS 45
C. CELL COMPONENT MIXTURES 47
D. CHEMICAL REAGENTS 47
CHROMIUM 48
MOLYBDENUM 48
TUNGSTEN 49
CARBON 49
ARGON 49
IV. RESULTS AND DISCUSSION 50
A. CHROMIUM CARBIDE 50
FLOW CELLS 50
EVACUATED QUARTZ CELL 52
EVACUATED ALUMINA CELLS 53
B. MOLYBDENUM CARBIDE 58
C. TUNGSTEN CARBIDE 62
D. HIGH TEMPERATURE QUENCH TESTS 63
E. EQUILIBRIUM PRESSURE CALCULATIONS 65
V. CONCLUSIONS 72
VI. RECOMMENDATIONS FOR FUTURE WORK 74
FIGURES 76
PHOTOGRAPHS 109
BIBLIOGRAPHY 118

LIST OF FIGURES

FIGURE.....PAGE

1. Chromium-carbon phase diagram.....77
2. Standard free energy compilation: Chromium carbide....78
3. Molybdenum-carbon phase diagram.....79
4. Standard free energy compilation: Molybdenum carbide..80
5. Tungsten-carbon phase diagram.....81
6. Standard free energy compilation: Tungsten carbide....82
7. Schematic representation of the partial ionic and electronic conductivities.....83
8. Schematic representation of the solid electrolyte region for calcia stabilized zirconia.....83
9. Partial conductivities as a function of component partial pressure.....84
10. Electrolytic domains of calcia stabilized zirconia and yttria doped thoria.....85
11. Molybdenum resistance furnace schematic.....86
12. Molybdenum resistance furnace - temperature profile...87
13. Second argon flow cell: Emf vs Temperature.....88
14. Evacuated quartz cell: Emf vs Temperature.....89
15. First evacuated alumina cell - Chromium system: Emf vs Temperature.....90
16. First evacuated alumina cell - Chromium system: Free energy vs Temperature.....91
17. Second evacuated alumina cell - Chromium system: Emf vs Temperature.....92

18. Second evacuated alumina cell - Chromium system:
Free energy vs Temperature.....93
19. First evacuated alumina cell - Molybdenum system:
Emf vs Temperature.....94
20. Second evacuated alumina cell - Molybdenum system:
Emf vs Temperature.....95
21. Second evacuated alumina cell - Molybdenum system:
Free energy vs Temperature.....96
22. Fourth evacuated alumina cell - Molybdenum system:
Emf vs Temperature.....97
23. Fourth evacuated alumina cell - Molybdenum system:
Free energy vs Temperature.....98
24. First evacuated alumina cell - Tungsten system:
Emf vs Temperature.....99
25. First evacuated alumina cell - Tungsten system:
Free energy vs Temperature.....100
26. Second evacuated alumina cell - Tungsten system:
Emf vs Temperature.....101
27. Second evacuated alumina cell - Tungsten system:
Free energy vs Temperature.....102
28. Theoretical partial pressures - Chromium system.....103
29. Theoretical partial pressures - Molybdenum system....104
30. Theoretical partial pressures - Tungsten system.....105
31. Cathode compartment - Chromium system
Theoretical total pressure and component weights.....106
32. Cathode compartment - Molybdenum system
Theoretical total pressure and component weights.....107

33. Cathode compartment - Tungsten system

Theoretical total pressure and component weights.....108

LIST OF PHOTOGRAPHS

NUMBER.....PAGE

1. Molybdenum resistance furnace and controller.....110
2. Argon purification train.....110
3. Argon flow cell.....111
4. Argon flow cell (assembled).....111
5. Evacuated alumina cell - close-up of cell top.....112
6. Anode compartment of evacuated chromium cell.....113
7. Bottom of zirconia electrolyte showing sintering of powder.....114
8. Sectioned zirconia electrolyte showing colour gradation.....115
9. Section of electrolyte tube.....116
10. Polished end of electrolyte tube.....116
11. Anode compartment of molybdenum cell.....117

I. LITERATURE REVIEW

There have been a number of reviews and compilations of equilibrium and thermodynamic data published but only a few are sufficiently well researched to be of great value. In this introduction each will be briefly dealt with chronologically and comments made, where applicable, describing their merits or deficiencies.

Beginning in 1937, Kelley[1] collected and correlated data on the thermodynamic properties of metal carbides and nitrides. In 1953 Richardson[2] published a survey of the available data on the thermodynamics of metal carbides, gaseous carbon compounds and solutions of carbon in iron. He also made an attempt to establish likely accuracies for each system quoted. Following Richardson, in 1963 Wicks and Block[3] compiled the thermodynamic properties of sixty-five elements as carbides, oxides, halides and nitrides.

In a series of monographs entitled Refractory Materials, the second volume published in 1967, The Refractory Carbides by Storms[4], contains data on the phase relationships, lattice parameters, chemical reactivity, hardness and thermodynamic properties of the refractory carbides. The seventh volume, Transition Metal Carbides and Nitrides by Toth[5], discusses many of the same properties, as well as including detailed phase diagrams for these carbides and nitrides.

In 1971 Reed[6] published Free Energy of Formation of Binary Compounds: An Atlas of Charts for High-Temperature

Chemical Calculations reviewing and updating the works of the previous authors.

Kubaschewski et al[7] have published a number of editions of Metallurgical Thermochemistry starting in 1951, the latest edition being the fifth, published in 1979. Their work contains a broad and comprehensive treatment of the theoretical basis of thermodynamic functions such as equilibrium constants, heat contents and heats of formation, entropy and Gibbs free energy of formation. Also covered are experimental methods for determining each of these entities as well as examples of thermochemical treatment of metallurgical problems. Finally, they have tabulated thermochemical data for the heats of formation and fusion, heat capacities, vapour pressure and standard Gibbs free energies of formation.

Also in 1979, Shatynski[8] reviewed and extended the previous surveys of Richardson, Wicks and Block, Reed and the fourth edition of Kubaschewski et al. Included in this work was the estimated accuracy for each value quoted.

This literature survey will concentrate on the Gibbs free energy data for the chromium, molybdenum and tungsten carbides taken from each of the aforementioned compilations as well as numerous other authors whose research was done specifically on the compounds of interest.

Each metal carbide will be discussed separately in order to make comparisons of the free energy data and experimental methods used by these authors.

Finally, the background of solid oxide electrolytes will be covered in order to illustrate their applicability to electromotive force measurements in solid state galvanic cells.

A. CHROMIUM CARBIDE

INTRODUCTION

There are three forms of chromium carbide well documented in the literature: Cr_3C_2, Cr_7C_3 and $Cr_{23}C_6$ as illustrated in the chromium-carbon phase diagram, Fig. 1. However, earlier sources[1,9-15] referred to carbides of the formulae Cr_5C_2 and Cr_4C. In subsequent investigations[16-21] these compounds were more correctly identified as Cr_7C_3 and $Cr_{23}C_6$, respectively. The error in the earlier identifications is understandable bearing in mind the date of the investigations (circa 1920), the experimental limitations at that time and the fact that the difference in carbon content between Cr_5C_2 and Cr_7C_3 is 0.55% and only 0.23% between Cr_4C and $Cr_{23}C_6$.

This thesis concentrates only on the carbide of the highest carbon content, Cr_3C_2, for two important reasons. Firstly, the Gibbs free energy of formation has been the subject of many more studies and is therefore better known. By studying this compound initially, the results obtained from the cell developed for this investigation could be thoroughly checked against known literature values.

Secondly, this carbide can be investigated directly in

a carbon-excess cell mixture yielding free energy data for that carbide alone. If mixtures of the higher carbides were to be used, accurate thermodynamic data for these systems would be required since the emf values would result from a combination of formation energies. There may also be an accompanying possibility of forming unwanted carbide combinations creating an ill-defined system if a mixture of the three carbides were to be used.

THERMODYNAMIC DATA

The carbides of chromium were first observed in 1893 when Moissan[22] prepared Cr_3C_2 and what he thought to be Cr_4C. One of the earliest studies of their thermodynamic properties was in 1919 when Slade and Higson[12] investigated the heat of reaction of "Cr_4C" by measuring the carbon monoxide pressure resulting from the reaction:

$$5Cr + CO = Cr_4C + CrO$$

Following in 1931, Schenck, Kurzen and Wesselkock[10] used methane gas to study the formation of carbides quoted as Cr_5C_2, Cr_7C_3, and Cr_3C_2. In 1933 Sauerwald, Teske and Lempert[11] refer in their work to the compound "Cr_4C". The data for these papers are summarized in a review by Kelley[1] in 1937. Ignoring the two erroneous compounds mentioned, the equation quoted for the reaction:

$$3Cr + 2C \text{ (graphite)} = Cr_3C_2$$

is $\Delta G^0 = -8550 - 5.03T$ cal

In a collection of papers in 1944, Kelley et al[14] conceded that the Cr_5C_2 quoted earlier was, in fact, Cr_7C_3.

They still maintained, however, that Cr_4C was the carbide of lowest carbon content. The data were summarized to determine expressions for the reactions:

$$1/3\ Cr_2O_3 + 13/9\ C = 2/9\ Cr_3C_2 + CO$$

where $\Delta G^0 = 60690 - 59.36T$

and for $3\ Cr + 2\ C = Cr_3C_2$

where $\Delta G^0 = -22330 - 9.9T\log T + 1.775\times10^{-3}T^2 + 0.296\times10^5T^{-1} + 27.43T$

In a report of investigations, Boericke[15] refers to free energy data for Cr_7C_3, Cr_4C and Cr_3C_2. For the latter reaction above, he gave virtually the same expression and claimed an estimated accuracy of 300 cal.

For some years following, only the heat capacity of Cr_3C_2 was studied, in 1952 by DeSorbo[23] and in 1954 by Oriani and Murphy[24].

Richardson[2] published a comprehensive survey of the available data up to 1953 making mention of the fact that up to that point, the free energy data were derived from heats of formation, heat capacies and equilibrium measurements. Since the heats of formation were derived from differences between large thermal quantities it was "small wonder that the relatively small differences between such large quantities commonly had large percentages inaccuracies".[2] Equilibrium measurements were also subject to error since it was assumed that the pressure due to carbon monoxide alone was being measured when, in fact, there could have been contributions from volatile oxides, carbon dioxide or from

the metal vapour itself. In these gas equilibrium measurements the gases to be analyzed were sampled in a cold part of the apparatus. Unless the gas mixture was circulated, there was a possibility of thermal segregation as was claimed to be the case in Boericke's[15] earlier work.

Richardson mentioned the work of Goldschmidt[18] as having corrected the compound Cr_4C cited in Boericke's paper to $Cr_{23}C_6$. However, Goldschmidt was not the original investigator, but simply reported the earlier findings of Westgren and Phragmen[21].

Richardson made use of the original equilibrium and thermal data from Boericke as well as entropies and heat capacities determined by Kelley et al[14] to recalculate the free energy expressions for the reactions:

I $\quad 23/6\ Cr + C = 1/6\ Cr_{23}C_6$

where $\quad \Delta G^0 = -16380 - 1.54T$

II $\quad 7/27\ Cr_{23}C_6 + C = 23/27\ Cr_7C_3$

where $\quad \Delta G^0 = -10050 - 2.85T$

III $\quad 3/5\ Cr_7C_3 + C = 7/5\ Cr_3C_2$

where $\quad \Delta G^0 = -3200 - 0.20T$

By combining his reactions I, II, and III in the following manner:

$(18/23)I + (81/161)II + (5/7)III$

one arrives at the expression:

$$\Delta G^0 = -20618 - 2.81T$$

for the reaction:

$$3Cr + 2C = Cr_3C_2$$

Kosolapova and Samsonov[18,28] investigated the preparation of Cr_3C_2 and Cr_7C_3 in 1959 by reacting the oxide with appropriate amounts of graphite. They did not, however, attempt to study the thermodynamic properties of these compounds.

In 1960 Elliott and Gleiser[27] published Thermochemistry for Steelmaking which tabulated physical properties, vapour pressures, standard heats and free energies of formation of selected compounds including the three chromium carbides. This work does not represent a major advancement, however, since the free energy data are derived from equilibrium data of Kelley et al.[14], Oriani and Murphy[24], and DeSorbo[23]; and the high temperature results are simply extrapolated from these sources.

In a review subsequent to the earlier work, Kelley and King[20] summarized the data of previous authors and corrected the previous report of Cr_4C to $Cr_{23}C_6$ with an accompanying recalculation of the entropy data although no evaluation of free energy expressions was made.

In 1961 Alekseev and Shvartsman[28] used the circulation method to study the equilibrium in the $Cr_{23}C_6$-Cr-H_2-CH_4 system to obtain a temperature dependence equation for the free energy of formation of $Cr_{23}C_6$ from chromium and graphite. Although this carbide is not the main one of interest in this study, it is nonetheless important since it represents the first attempt to directly measure the free energy of formation for a chromium carbide compound.

Alekseev and Shvartsman's final result was:

$$\Delta G^0 = -13600\pm400 - 0.2\pm0.4T$$

for the reaction:

$$23/6\ Cr(s) + C(s) = 1/6\ Cr_{23}C_6(s)$$

Fujishiro and Gokcen[28] were the first to study the free energy of formation of Cr_3C_2 using a graphite Knudsen effusion cell. The equilibrium pressure of gaseous chromium was measured resulting from the reaction:

$$1/3\ Cr_3C_2(s \text{ or } l) = 2/3C(graphite) + Cr(g)$$

They arrived at their free energy expressions by combining the equilibrium pressure measured with the free energy functions for gaseous chromium and graphite obtained from Stull and Sinke[25] and extrapolating the data for Cr_3C_2 from DeSorbo[23] and Oriani and Murphy[24] to their experimental temperatures. The resulting expressions were:

$$\Delta G^0 = 96982 - 29.86T$$

for $1/3\ Cr_3C_2(s) = Cr(g) + 2/3\ C(s)$

and $$\Delta G^0 = 89394 - 26.36T$$

for $1/3\ Cr_3C_2(l) = Cr(g) + 2/3\ C(s)$

In a later review by Storms[4], it was pointed out that nearly half of the weight loss was due to diffusion of chromium through the crucible walls rather than through the orifice. Although attempts were made to correct for it by using pure chromium as a blank, some uncertainty still remained.

Vintaykin[30] followed Fujishiro and Gokcen in determining the free energy of formation of Cr_3C_2 by

measuring its dissociation pressure in a Knudsen cell. He also recalculated the free energy expression for Cr_3C_2 using Fujishiro and Gokcen's results combined with the vapour pressure measurements on pure chromium made by Speiser et al[31] and Vintaykin[32] to arrive at:

$$\Delta G^0 = -9900 - 1.29T$$

His experimental procedure combined the Knudsen method with a radiometric determination of the amount of chromium sputtered onto a target. As pointed out in a later discussion of his investigation by Mabuchi, Sano and Matsushita[33], he apparently did not take the influence of scattering loss into account. The expression finally arrived at by Vintaykin for the formation of Cr_3C_2 was:

$$\Delta G^0 = -8200 - 7.0T$$

In 1963 Wicks and Block[3] assembled the thermodynamic properties of sixty-five elements that had been published up to and including 1959. Although they cite values for Cr_7C_3 and Cr_3C_2, it is interesting to note that they still quote values for the compound Cr_4C ignoring the basic work of Westgren and Phragmen[21] who, among others, established that Cr_4C was in fact $Cr_{23}C_6$. The free energy expression for the equation:

$$3\,Cr + 2\,C = Cr_3C_2$$

was calculated using heat capacity and heat of formation data from DeSorbo[23], Rossini et al[35] and Kelley[48] to give:

$$\Delta G^0 = -20450 - 0.47T\ln T - 0.18\times10^{-3}T^2$$
$$- 1.06\times10^5T^{-1} + 1.40T$$

Since their assemblage was based on older, less reliable data the value of its contribution to this study is diminished.

More recently, in 1965, Gleiser[38] used the same reaction as Kelley[14] to study chromium carbide:

$$1/3\ Cr_2O_3(s) + 13/9\ C(s) = 2/9\ Cr_3C_2(s) + CO(g)$$

In her work, the gases were sampled directly over the specimen rather than in the cold part of the apparatus, to try to eliminate errors due to thermal segregation. In order to arrive at values for the free energy of formation for chromium carbide, she used the appropriate values for the free energies of formation of carbon monoxide and chromium gas from Elliott and Gleiser[27] and of Cr_2O_3 from Kelley[34] and Mah[37]; thus the accuracy of the results relies heavily on these previous determinations. In her paper, no temperature dependent expression was given for the free energy of formation although some tabulated results were included. Eremenko and Sidorko[43] evaluated her data to yield the expression:

$$\Delta G^0 = -25900 - 3.9T$$

Bolgar, Fesenko and Gordienko[38] studied the evaporation and thermodynamic properties of chromium carbides in 1966 using tantalum and molybdenum effusion cells. The successive evaporation reactions determined in their work were found to be:

$$1/9\ Cr_{23}C_6(s) = 2/9\ Cr_7C_3(s) + Cr(g)$$

$$2/5\ Cr_7C_3(s) = 3/5\ Cr_3C_2(s) + Cr(g)$$

$$1/3\ Cr_3C_2(s) = 2/3C(s) + Cr(g)$$

Their result for the standard heat of formation of Cr_3C_2 was:

$$\Delta H^0 = -23.4 \pm 3 \text{ Kcal}$$

The first publication of a sufficiently critical review of the carbide systems was in 1967 entitled The Refractory Carbides by Storms[4]. Beginning with Heusler's[39] work in 1926 through to Gleiser's[36] in 1965 (although missing Bolgar et al[38] in 1966), it represented the best discussion of the data thus far. In this work, Storms pointed out the differences in the results of Heusler(1926), Kelley (1944) and Gleiser (1965) all of whom measured the CO pressure over a mixture of the oxide, carbide and graphite. He mentioned that, although the discrepancies could have been due to errors in technique, it was more probable that a carbon monoxide-carbon dioxide mixture was actually being studied in each case. As mentioned earlier in this review, Storms pointed out possible sources of error in the experimental techniques of Fujishiro and Gokcen[28] and Vintaykin [30] both of whom used the Knudsen cell approach to vapour pressure measurements.

Kleykamp[40] was the first to determine the free energy by emf measurements. The cells used were:

$$Pt/Cr, CrF_2/CaF_2/CrF_2, Cr_3C_2, C/Pt$$

and $$Pt/Cr, CrF_2/CaF_2/CrF_2, Cr_7C_3, Cr_3C_2 / Pt$$

yielding free energy expressions of:

$$\Delta G^0 = -7200 - 8.0T \qquad 800\text{-}1110^0K$$

and $$\Delta G^0 = -23750 - 8.5T \qquad 920\text{-}1080^0K$$

for the Cr_3C_2 and Cr_7C_3 systems, respectively.

Kleykamp used a calcium fluoride solid electrolyte sintered for 5 hr at 3500 atm and 900°C in a vacuum of 10^{-5} Torr. As the Cr_3C_2 cell was constructed, the half-cell reactions were:

$$3\,Cr + 6\,F^- = 3CrF_2 + 6e^-$$

and $$3CrF_2 + 2C + 6e^- = Cr_3C_2 + 6F^-$$

for an overall cell reaction of:

$$3Cr + 2C = Cr_3C_2$$

His results were plotted against those of Storms[4], Heusler[38], Kelley et al[14], Gleiser[38], Fujishiro and Gokcen[28], Vintaykin[30] and Wicks and Block[3]. Of these authors, he felt that the data presented by Vintaykin were the most reliable. In plotting Gleiser's results, he has shown a positive temperature dependence for the entropy term which conflicts with the results as originally presented. In order to plot Fujishiro and Gokcen's findings, Kleykamp has apparently used their enthalpy term corrected from the liquid or gaseous state to the metastable solid state and incorporated an unspecified value for the corresponding entropy term. He has plotted their results over the original temperature range studied although claimed to be plotting results for the solid state reaction. This extrapolation to a temperature range where neither chromium nor chromium

carbide exist as solids has little value for comparison and is, at best, only an estimation rather than a presentation of the original data.

Tanaka et al[44] employed the same solid electrolyte as Kleykamp with the exception of using a single crystal rather than a sintered pellet. In a comparison of Tanaka and Kleykamp's results in a paper by Kulkarni and Worrell[41], it was thought that electronic conduction in the sintered polycrystalline electrolyte could have caused the less negative free energy data reported by Kleykamp.

Tanaka's free energy expression for Cr_3C_2 was found to be:

$$\Delta G^0 = -13300 - 4.15T \qquad 885\text{-}1098^0K$$

Mabuchi, Sano and Matsushita[33] also used solid electrolytes to measure the free energy of formation of Cr_3C_2. Their thoria-yttria electrolyte was used in a galvanic cell of the type:

$$Cr_3C_2,\ Cr_2O_3,\ C\ /\ \text{ELECTROLYTE}\ /\ Cr,\ Cr_2O_3$$

so that the overall cell reaction was:

$$4/3Cr + 8/9C(\text{graphite}) = 4/9Cr_3C_2$$

and the free energy was found to be:

$$\Delta G^0 = -10400 - 7.35T$$

Their discussion of previous results pointed out the irreproducibility of Kelley and Gleiser's work with an uncertainty of ±10 Kcal. This was probably due to their failure to establish equilibrium in the system or to carbon monoxide concentration gradients. For this reason, Mabuchi

et al's cell design was such that it enabled them to measure the emf at the solid/electrolyte/solid interface rather than using a technique requiring sampling of the gases away from the specimen. However, in examining their cell design one wonders, despite their claims that the electrolyte was securely sealed with glass, whether the emf measured was not influenced by oxygen leakage along the glass-electrolyte interface.

The free energy expressions and temperature ranges quoted in this paper agree with most original works[30,38,40,44]; however, the free energy equations cited for Kelley[14] and Wicks and Block[3] disagree markedly from those originally presented by these authors.

Kulkarni and Worrell[41] used the torsion-effusion technique to measure the equilibrium carbon monoxide pressure in a mixture of $Cr_{23}C_6$-Cr_2O_3-Cr and of Cr_7C_3-Cr_2O_3-$Cr_{23}C_6$ between 1100° and 1300°K. From the equilibrium data, they were able to calculate the free energy of $Cr_{23}C_6$ and Cr_7C_3. They attempted to obtain thermodynamic data for Cr_3C_2 in two different investigations but neither was successful. The first was an attempt to determine the carbon monoxide pressure in equilibrium with a mixture of Cr_3C_2-Cr_7C_3-Cr_2O_3 but they were unable to obtain a constant CO pressure. The second method tried was the measurement of the chromium pressure in a Cr_3C_2-C mixture but the values obtained were much too high. They attributed these high values to trace amounts of oxygen in the system

reacting with carbon to form carbon monoxide gas.

They used their data for Cr_7C_3 to re-evaluate the equilibrium data of Kelley et al[14] and arrived at the expression for Cr_3C_2:

$$\Delta G^0 = -16400 \pm 700 - 4.4T$$

which is not in agreement with the original expression as presented by Kelley et al themselves.

Chang and Naujock[42] studied the relative stabilities of $Cr_{23}C_6$, Cr_7C_3 and Cr_3C_2 in ternary Cr-Mo-C systems. In order to ascertain the stabilities, they combined the free energy values for the binary phases which they obtained from the calorimetric data of Mah[45] and Kelley[20, 48]

For Cr_3C_2 at 1573°K they obtained a value of:

$$\Delta G^0 = -26760$$

In 1973 Eremenko and Sidorko[43] used the emf method to study the chromium carbides. The electrolyte was an equimolar mixture of potassium and sodium chlorides with an addition of powdered chromium and anhydrous $CrCl_3$. For the reaction:

$$3Cr + 2C = Cr_3C_2$$

they obtained the expression:

$$\Delta G^0 = -20230 - 0.18T$$

They compared the results of numerous other authors[2, 3, 4, 28, 29, 30, 33, 36, 38, 40] and tabulated the temperature ranges over which they were valid.

Also in 1973, Barin and Knacke[13] published Thermochemical Properties of Inorganic Substances which

lists heat capacities, entropies and free energies of formation for a large number of compounds. Although comprehensive in its broad coverage, the data were not as current as they could have been. Barin and Knacke have cited values for the compounds $Cr_{23}C_6$, Cr_7C_3, Cr_3C_2 and Cr_4C quoting Kubaschewski, Evans and Alcock's fourth edition of Metallurgical Thermochemistry as the source for the last compound. It is surprising that, in 1973, they have given data as precise as six significant figures for a compound that was proven to be non-existent in 1930. They have apparently not performed a thorough literature survey on the available data for the carbide compounds since Toth's[5] publication of Transition Metal Carbides in 1971 included detailed phase diagrams, crystal structures, lattice parameters and tabulated thermal functions for the three existing carbides of chromium.

The fifth edition in 1979 of Metallurgical Thermochemistry by Kubaschewski et al[7] bears the same appearance of an incomplete literature search. They obtained their data from Richardson's[2] paper of 1953 who, in turn, used earlier works of Kelley et al and Boericke in 1944. By using only Richardson's data, Kubaschewski has omitted the valuable contributions made by the authors reviewed previously.

A much more complete compilation of equilibrium and thermodynamic data of the carbides was done in 1979 by Shatynski[8]. The results of numerous authors[2, 3, 4, 7, 14, 30, 33, 38, 40, 41, 44] were compared and the comment made that the data of Kulkarni and Worrell[41] were believed to be the most reliable. The free energy values quoted were supposedly taken from Kulkarni and Worrell's work but Shatynski has made some serious errors in presenting the results. He claimed that they studied the reactions:

$$23/6\ Cr + C = 1/6\ Cr_{23}C_6$$

where $\Delta G^0\ (1/6\ Cr_{23}C_6) = -12833 - 3.05T$

and $$7/27\ Cr_{23}C_6 + C = 23/27\ Cr_7C_3$$

where $\Delta G^0(23/27\ Cr_7C_3) = -29985 - 7.41T$

and $$3/5\ Cr_7C_3 + C = 7/5\ Cr_3C_2$$

where $\Delta G^0(7/5\ Cr_3C_2) = -9840 - 2.64T$

when, in fact, the first two reactions should have been:

$$Cr_{23}C_6 + 2\ Cr_2O_3 = 27\ Cr + 6\ CO(g)$$

and $$3\ Cr_7C_3 + Cr_2O_3 = Cr_{23}C_6 + 3\ CO(g)$$

as they measured the CO gas pressures using effusion cells. They made two unsuccessful attempts to study the Cr_3C_2 system so that the third reaction should not have been included at all.

As well, Shatynski has used the free energy expression for the Cr_7C_3 system that resulted from a combination of Kulkarni and Worrell's data with that of Kelley et al[14] not, as he has stated, from their study alone.

For the Cr_3C_2 system, Shatynski quoted the expression

that Kulkarni and Worrell arrived at by recalculating the data of Kelley et al. He has also made a calculation error in wrongly presenting the free energy value when converting the expression given per mole of carbide to the reaction given in his paper. Instead of using the factor 7/5 he has incorporated a 3/5 factor into the expression, i.e., Shatynski converted the free energy values to 3/5 Cr_7C_3 yet cited it for the 7/5 Cr_3C_2 system.

The corrected expression for the second reaction should be:

$$\Delta G^0(23/27\ Cr_7C_3) = -29303 - 7.75T$$

and, if he chose to include their recalculation for the Cr_3C_2 system, the expression should be:

$$\Delta G^0\ (7/5\ Cr_3C_2) = -22960 - 6.16T$$

Finally, in his comments on the agreement between Kulkarni and Worrell's results with those of previous authors, Shatynski stated that their results were in "poor agreement" with those of Kelley et al[14] even though he had already mistakenly incorporated their data into that presented as Kulkarni and Worrell's.

The free energy expressions obtained from the authors discussed in this section are plotted for comparison in Fig. 2.

B. MOLYBDENUM CARBIDE

INTRODUCTION

The molybdenum-carbon system consists only of Mo_2C and MoC_{1-x}, each having two crystal forms as shown on the molybdenum-carbon phase diagram, Fig. 3. According to Storms[4], at temperatures less than 1200°C, only Mo_2C is stable, so that studies within this temperature range are greatly simplified compared to the chromium-carbon system.

The data existing in the literature are less than for the chromium carbides with direct free energy investigations, in particular, being of limited number.

THERMODYNAMIC DATA

Moissan[22], near the turn of the century, was the first to prepare molybdenum carbide. Much later, Schenck, Kurzen and Wesselkock[10] used the same methane gas approach as for chromium to study Mo_2C. Their free energy results were presented in a later review[4] along with that of the other authors who had evaluated the free energy of formation.

Approximately thirty years later, Browning and Emmett[47] used the system Mo_2C-CH_4-MoC-H_2 only modifying it to a dynamic method to avoid thermal segregation. However, they included MoC in their system at temperatures less than 1098°C and therefore the reaction cannot be one of equilibrium since MoC is not stable in that temperature range. Their free energy value of:

$$\Delta G^0 \text{ (at } 950^0K) = -8862$$

for the reaction:

$$2Mo + C = Mo_2C$$

is more consistent with the decomposition of MoC into Mo_2C.

In their work, Browning and Emmett made an arithmetic error as explained by Kempter[48]. He corrected the values at 298°K for the reactions:

$$Mo + C = MoC \text{ from } -3211 \text{ to } -3798 \text{ cal/mole}$$

and for: $MoC + Mo = Mo_2C$ from -5651 to -5064 cal/mole

Storms[4] has included Kempter's correction in his comparison of these two authors' results. He also pointed out the similarity between their free energy values and those for the reaction;

$$2H_2 + C = CH_4$$

The reviews carried out by Kelley[1], Richardson[2] and Wicks and Block[3] discussed previously have included thermodynamic data on the molybdenum carbides; yet the source of their data frequently stems from only a few original papers.

Elliott and Gleiser[27] have presented Browning and Emmett's results in tabular form; yet it doesn't appear that they have taken Kempter's correction into account since no mention of it was made.

Gleiser and Chipman[49] performed a direct investigation on the free energy of formation of Mo_2C by measuring carbon monoxide and carbon dioxide equilibrium partial pressures. In the temperature range 1200° to 1340°K, they gave the expression:

$$\Delta G^0 = -11710 - 1.83T$$

Worrell[50] presented a thermodynamic analysis of the Cr-C-O, Mo-C-O and W-C-O systems discussing previous authors' data. Phase relationships and Pourbaix-Ellingham diagrams are included as well as tabulated Gibbs energy of formation expressions making it a useful reference paper for the Group VIB ternary systems.

The expression given for $Mo_{2.2}C$ was:

$$\Delta G^0 = -12000 - 1.5T$$

with the comment made that "although this equation applies only to the metal-rich side of the Mo_2C phase (designated $Mo_{2.21}C$), it was also used in calculations involving carbon-saturated Mo_2C".[50]

In a subsequent study[51] the heat capacity of Mo_2C was measured. The results were combined with known heats of formation and the entropy at 298°K to obtain values for the heat and free energy of formation from 298°K to 1400°K. The data were presented in tabular form at 100°K increments within the temperature range specified. The comparison was made with previous results[49] and differences were found to be in the order of about 0.1 Kcal/mole.

Solbakken and Emmett[52] reacted molybdenum with methane gas to form Mo_2C and hydrogen to determine the free energy of formation of Mo_2C. Evaluation of an earlier work[47] was made with the comment that the source of error was most probably due to the presence of MoO_2 which would result in water vapour, carbon monoxide and carbon dioxide being present in their methane sample. They performed a series of

tests using cold traps which substantiated their claims of MoO_2 contamination in Browning and Emmett's previous study.

Included in their data presentation were the results of Pankratz et al[51] and Gleiser and Chipman[48] as well as a discussion of the works of two previous authors[1,10]. The results of Gleiser and Chipman were in closest agreement with their data.

As with the chromium system, Storms[4] has included discussions on phase relationships, lattice parameters, structures and thermodynamic properties for the molybdenum system. Comparisions were made of various works[10,47,48,55] with comments on their experimental techniques and results.

The phase diagram presented by Toth[5] is more detailed than Storms but his thermodynamic data were obtained from the latter author so that no discussion is included here.

Chang and Naujock[42] have tabulated four equilibrium reactions for the molybdenum carbides along with their free energy at 1573°K. The results of other authors[48,51,53] were summarized for Mo_2C although no temperature dependent equations were included.

The vaporization of Mo_2C was investigated from 2125° to 2550°K by Fries[54]. In this work, he included a discussion of previous free energy determinations[47,48,49,55] but did not report a free energy expression.

Alekseev and Shvartsman[55] studied the reactions:

$$Mo_2C(s) + 2H_2 = 2Mo(s) + CH_4(g)$$

and

$$C + 2H_2(g) = CH_4(g)$$

They determined the free energy change for the Mo_2C reaction to be:

$$\Delta G^0 = +3800 - 14.84T \qquad 873 - 1123^0K$$

However the formation reaction presented in the paper was:

$$2Mo_3 + C = Mo_2C_3$$

which neither balances nor is the formation reaction for Mo_2C. It is probable that typographical errors were made in printing since Mo_2C was included in the hydrogen-methane equilibrium reaction. The final formation reaction should then be:

$$2Mo(s) + C(s) = Mo_2C(s)$$

In the fifth edition of Metallurgical Thermochemistry, Kubaschewski and Alcock[7] have not included any carbides of molybdenum in their free energy, heats of formation or vapour pressure tables. They have, however, included heat capacity data taken from Pankratz et al[51].

Barin and Knacke[13] cite values for Mo_2C and MoC with Kubaschewski et al[7] and a private communication from Kubaschewski as their sources of data, respectively.

The free energy data obtained from the authors discussed in this section are plotted for comparison in Fig. 4.

C. TUNGSTEN CARBIDE

INTRODUCTION

Moissan[22] was also the first to prepare the tungsten carbides by melting either tungsten or tungsten trioxide together with carbon.

Only two phases, W_2C and WC are to be found for this system although WC undergoes a structure change at high temperatures (T>2450°C) as shown on the phase diagram, Fig. 5.

In this investigation the highest carbide, WC, was used in the galvanic cell since, at temperatures less than 1300°C, it is the only stable carbide[81].

THERMODYNAMIC DATA

As with the chromium carbide and molybdenum carbide compounds, initial investigations on the tungsten carbide compounds reported compounds which were later proven to be non-existent. Schenck et al[10] reported results for the compounds W_5C_2, W_3C, WC and what they thought might possibly be W_2C using equilibrium reactions between tungsten, methane, hydrogen and the tungsten carbides.

Their work was later reviewed by Richardson[2] who maintained that their results were subject to error due to thermal segregation and that W_5C_2 was more probably W_2C. Richardson reported a value of -8400 cal/mole for the standard free energy at 298°K for the carbide formation reaction:

$$W + C = WC$$

Kelley[1] also evaluated the work of Schenck et al but did not correct the W_5C_2 compound to the more probable W_2C. The temperature dependent expression given for the reaction:

$$5W + 2CH_4 = W_5C_2 + 4H_2$$

was $\Delta G^0 = 41000 - 16.1T\log T + 10.16T$

Mention was also made of W_2C, W_3C_2 and WC but no calculations were included for these compounds.

Goldschmidt[18] carried out a review of the available literature on the phase relationships for the tungsten-carbon system in 1948 and confirmed the existence of only two carbides, W_2C and WC. No thermodynamic data were included in this review.

Elliott and Gleiser[27] quoted standard heats and free energies of formation for both W_2C and WC. The data for WC are simply taken from Richardson's earlier work[2] so no temperature dependent expression was given.

Gleiser and Chipman[57] studied the reaction:

$$WC(s) + CO_2(g) = W(s) + 2CO(g)$$

between 1215° and 1266°K. The expression given for the reaction was:

$$\Delta G^0 = 48490 - 41.50T$$

so that by using the formation expressions for both carbon monoxide and carbon dioxide gases, a value of -8340±320 cal/mole was arrived at for the formation of tungsten carbide.

Alekseev and Shvartsman[58] investigated the reactions:

$$W_2C(s) + 2H_2(g) = 2W(s) + CH_4(g)$$

and $2WC(s) + 2H_2(g) = W_2C(s) + CH_4(g)$

The data obtained were used to derive equations for the following reactions:

$2W(s) + C(graphite) = W_2C$

where $\Delta G^0 = -7550 + 1.61T$ 923 - 1173°K

$W_2C(s) + C(graphite) = 2WC$

where $\Delta G^0 = 3700 - 8.9T$ 973 - 1273°K

and $W(s) + C(graphite) = WC(s)$

where $\Delta G^0 = -1950 - 3.9T$ 973 - 1173°K

However, using Gupta's[61] tungsten-carbon phase diagram (one of the few available that extend below 2300°C), it can be seen that only WC is stable below 1300°C so that the above reactions involving W_2C are not strictly valid.

Wicks and Block[3] gave a free energy function of:

$\Delta G^0 = -7860 + 1.86T\ln T - 0.2X10^{-3}T^2 - 1.05X10^5T^{-1} - 12.63T$

for the reaction:

$W + C = WC$

valid within the temperature range 298° to 2000°K.

Along with his evaluation of the stable phases for the W-C-O system and presentation of the Pourbaix-Ellingham diagrams, Worrell[50] has included the Gibbs free energies of formation of all the oxides and carbides of tungsten. For WC(s) the expression given was -9600 + 1.0T and for W_2C it was -6400 - 1.0T.

Toth[5] has summarized the phase relationships, lattice parameters and crystal structures for the tungsten-carbon system in his work. Although he did not include

thermodynamic data, the phase diagrams presented are valuable for their detail and temperature precision.

Kubaschewski et al's[7] fifth edition of Metallurgical Thermochemistry cites an expression of:

$$\Delta G^0 = 9000 - 0.4T$$

for the reaction

$$WC = W + C$$

although no mention was made of their source of data.

Barin and Knacke[13] have tabulated heats and free energies of formation for both W_2C and WC quoting Schick[58] and Ancey-Moret and Deniel[60] as their data sources.

Gupta[61] studied the free energies of formation of WC and W_2C by equilibrating mixtures of tungsten and carbide powder with iron rods in the temperature range 900° to 1375°C. The expression given for the reaction:

$$W + C = WC$$

was $\Delta G^0 = -10020 + 1.17T \pm 100$

and for the reaction:

$$WC + W = W_2C$$

was $\Delta G^0 = -6970 - 0.735T \pm 65$

A discussion of a previous study by Gleiser and Chipman[57] included the comments that the heat of formation of WC implied by their results appeared to be much too low and that their results were questionable due to the possibity of the presence of carbon dioxide in the system. Gupta's evaluation of Orton's[62] results concluded that the values were too low to satisfy established heats of

formation. Orton's x-ray diffraction technique of determining the formation and dissolution of the carbides was also questioned.

Mention was also made of Alekseev and Shvartsman's work[55] where he pointed out that, although they maintained that they were studying two different systems, it was apparent that they were, in fact, examining the same system in both cases, i.e., $WC + 2H_2 = W + CH_4$. This was concluded from the results obtained and by the fact that W_2C is not stable in the temperature range used in their investigation.

A review of Gupta's work was included in Shatynski's report[8] along with the tabulations of Kubaschewski et al[7] and Wicks and Block[3]. Apparently, Shatynski did not carry out as complete a literature survey for this carbide system as for the chromium and molybdenum carbides since a number of authors' results are not included.

The free energy expressions obtained by investigators for this system are plotted for comparison in Fig. 6.

D. SOLID ELECTROLYTES

Solid electrolytes have been known since the turn of the century but it is only in the last two decades that their potential has fully been recognized. During their period of development, many different types of electrolytes have been investigated and documented. For example, in 1921 lithium sulphate was known to exhibit high ionic conductivity. Silver iodide was first used in 1935 leading the way for

related compounds such as Ag_3SI and $RbAg_4I_5$. In the 1950's doped zirconia was developed for possible fuel cell applications. Although this failed initially, valuable information was obtained on this important electrolyte.

The discovery of beta-alumina, with its intermediate temperature range of use, spanned the gap between high temperature materials and low temperature silver compounds. Since then, the field of solid electrolytes has mushroomed to a point where it includes dozens of compounds, both organic and inorganic, as well as various glasses and glass-ceramics.

Obviously, to cover the entire field of solid electrolytes is beyond both the scope and intent of this review. A more complete discussion of solid electrolytes can be found in Volume 21 of Topics in Applied Physics[88]. This particular volume, entitled Solid Electrolytes, has sections on the theoretical aspects, the beta-aluminas, and halogenated and oxide solid electrolytes. This brief introduction was meant only to acquaint the reader with the expansive field that is encompassed by the term "solid electrolytes".

E. OXIDE ELECTROLYTES

The domain of oxide solid electrolytes alone is of such a magnitude that it can only be briefly discussed here. For a more complete review of the phase relationships, electrical properties and transport number determinations for a wide

variety of oxygen ion conductors, the reader is referred to a paper by Etsell and Flengas.[83] An excellent chapter on oxide solid electrolytes has also been written by Worrell in Solid Electrolytes.[68] The discussion of the basic theory, the temperature and pressure dependence of conductivity and the measurement of emf included in later sections is, however, applicable to the general field of oxide electrolytes.

The electrolyte used in this investigation was calcia stabilized zirconia ($ZrO_2(CaO)$) so that emphasis will be given to it although reference will also be made to yttria doped thoria ($ThO_2(Y_2O_3)$) since both electrolytes merit consideration for emf measurements in galvanic cells.

II. THEORY

A. IONIC AND ELECTRONIC CONDUCTIVITY

In order for a material to be used as a solid electrolyte, it must have a high ionic transport number (t_i) in the temperature and pressure region of interest. (Generally $t_i > 0.99$.)

Calcia stabilized zirconia is an anionic conductor since, with its fluorite structure and calcia dopant, the predominant intrinsic ionic defects are doubly ionized oxygen vacancies.

For a pure stoichiometric material, the equilibrium between free electrons in the conduction band and electron holes in the valence band can be written as:

$$[h^{\cdot}] = [e']$$

or, whether stoichiometric or not;

(1) $$NIL = h^{\cdot} + e'$$

or $$K_1 = [h^{\cdot}]\,[e']$$

where $h^{\cdot}$ is an electron hole and e' is an excess electron.

For fully ionized defects, the formation of an ionic Frenkel defect can be written as:

(2) $$[V_O^{\cdot\cdot}]\,[O_i^{''}] = \text{CONSTANT}$$

where $V_O^{\cdot\cdot}$ is a doubly ionized oxygen vacancy, and $O_i^{''}$ is a doubly ionized oxygen intersitial.

For calcia stabilized zirconia the preservation of electroneutrality requires that:

(3) $$2[Ca_{Zr}^{''}] + [e'] = 2[V_O^{\cdot\cdot}] + [h^{\cdot}]$$

which reduces to:

$$[Ca''_{Zr}] = [V_O^{\cdot\cdot}]$$

since: $[e'] \ll [Ca''_{Zr}]$ and $[h] \ll [V_O^{\cdot\cdot}]$

Since, at high oxygen pressures, the predominant defects are oxygen vacancies, the defect reaction can be written as:

(4) $\frac{1}{2}O_2(g) + V_O^{\cdot\cdot} = O_O + 2h^{\cdot}$

where O_O is an oxygen ion on a normal lattice site,

therefore $K_4 = \dfrac{[O_O][h^{\cdot}]^2}{[P_{O_2}]^{\frac{1}{2}}[V_O^{\cdot\cdot}]}$

Since, for calcia stabilized zirconia at high oxygen pressures the concentration of oxygen ion vacancies is large and can be considered constant, reaction (4) can be reduced to:

$$[h]^2 \propto [P_{O_2}]^{\frac{1}{2}}$$

or $$[h] \propto [P_{O_2}]^{\frac{1}{4}}$$

Therefore, the electron hole concentration, and thus p-type conductivity, is proportional to $[P_{O_2}]^{\frac{1}{4}}$ in the region of high oxygen pressure.

Following the same argument at low oxygen pressures, the defect equilibrium between oxygen vacancies and excess electrons is expressed as:

(5) $O_O = \frac{1}{2}O_2(g) + V_O^{\cdot\cdot} + 2e'$

where $K_5 = [V_O^{\cdot\cdot}][e']^2[P_{O_2}]^{\frac{1}{2}}$

Again, for calcia stabilized zirconia at low oxygen pressures, the concentration of oxygen vacancies is large and essentially constant so that reaction (5) reduces to:

$$[e']^2 \propto [P_{O_2}]^{-\frac{1}{2}}$$

or $$[e'] \propto [P_{O_2}]^{-\frac{1}{4}}$$

so that the excess electron concentration, and hence n-type conductivity, is proportional to $[P_{O_2}]^{-\frac{1}{4}}$ at low oxygen pressures.

The variation of conductivity with oxygen pressure can be represented schematically as in Fig. 7 where three distinct regions are evident. At low oxygen pressures the conductivity is due to excess electrons and is therefore proportional to $[P_{O_2}]^{-\frac{1}{4}}$. In the intermediate region the conductivity, being mainly ionic, is independent of oxygen pressure and, in the high pressure region, the conductivity due to electron holes is proportional to $[P_{O_2}]^{\frac{1}{4}}$. There are, as well, two regions of mixed conduction where there are both ionic and electronic contributions to the overall conductivity. Figure 8 is a schematic representation of the region over which calcia stabilized zirconia acts as a solid electrolyte (i.e., $t_i > 0.99$).

For an ionic crystal, Schmalzried[84] introduced the parameters $P_{\oplus}$, where $\sigma_{\oplus} = \sigma_i$ and $P_{\ominus}$, where $\sigma_{\ominus} = \sigma_i$. As shown in Fig. 9, the transference number for electronic charge carriers becomes 0.5 at $P_{\oplus}$ and $P_{\ominus}$. Generally, $P_{\oplus}$ and $P_{\ominus}$ represent the ultimate limiting values for the use of the compound as a solid electrolyte.

For an solid oxide electrolyte, $P_{\oplus}$ and $P_{\ominus}$ correspond to the oxygen partial pressures where $t_i = 0.5$ as illustrated in Fig. 7.

B. CONDUCTION DOMAINS

In order to ensure that either zirconia-calcia or thoria-yttria are operating in their solid electrolyte region, an accurate determination of their conduction domains is required. Patterson[85] plotted the conduction domains for these two electrolytes as well as for several halide electrolytes. The pertinent part of his plot of log P_{X_2} vs 1/T is included in Fig. 10. In considering all the previous studies included in his evaluation of the electrolytic domains, he plotted very liberal domain boundaries so that virtually all reported emf studies fell within them. He noted in this work, however, that for calcia stabilized zirconia, evidence of electrolytic behavior at much lower oxygen pressures was becoming evident.

For $ThO_2(Y_2O_3)$, as with $ZrO_2(CaO)$, the low electrolytic boundary was the subject of controversy. For that reason, the low boundary was not extended above 1100°C in his report.

In 1972 Etsell and Flengas[86] reported their findings on the n-type conductivity of calcia stabilized zirconia between 600° and 1400°C. For comparison, previous results for thoria-yttria were included as well. Their coulometric titration results were:

$$\text{Log } P_{\theta} = -[(54.5 \times 10^3) / T] + 14.0$$

Swinkels[87] presented a method for the rapid determination of the electronic conductivity limits for

solid electrolytes. Although mention was made of both zirconia-calcia and zirconia-yttria, results were included only for the latter electrolyte.

For this study, the conduction domains proposed by Etsell will be used since the evidence for electrolytic behavior at lower oxygen pressures has increased since Patterson's original work. By staying within this region, one is assured of virtually pure ionic conduction.

C. THERMODYNAMIC MEASUREMENTS

The measurement of the emf in a galvanic cell is a very accurate method of obtaining thermodynamic data for the associated chemical reaction.

If the galvanic cell is designed in such a way that:

- the solid electrolyte and its mode of ionic conduction are matched to the two electrochemical reactions occurring at the electrodes,
- a single identifiable electrode process occurs reversibly at each electrode,
- the equilibrium pressures of the conducting species generated by the two half-cells falls within the ionic conduction domain for that electrolyte in the temperature region of interest,
- the total pressure of all species in the half-cells is capable of being withstood by the particular solid electrolyte and cell design,

then the emf measured can be related to the appropriate

thermodynamic functions.

For this study, the manner in which these criteria are met can be best described by concentrating on each system individually; however, a general cell reaction can be written to illustrate the method of obtaining the Gibbs free energy of formation for the metal carbide from emf measurements.

Consider the system of a metal (M), the metal oxide (MO), its carbide (MC) and graphite (C). In a cell represented schematicaly as:

(-) M,MO/ELECTROLYTE/C,MO,MC (+)

the electrode reactions would be:

at the anode:

(1) $M + O^{=} = MO + 2e^{-}$

at the cathode:

(2) $MO + C + 2e^{-} = MC + O^{=}$

for an overall cell reaction of:

(3) $M + C = MC$

When the two half-cells are separated by the solid electrolyte, equilibrium oxygen pressures will be established: at the anode, P_{O_2}' and at the cathode, P_{O_2}'' where $P_{O_2}'' > P_{O_2}'$. The free energy change for (3) will be:

$$\Delta G^{0} = -RT \ln (P_{O_2}'' / P_{O_2}')$$

Using the Nernst equation:

$$\Delta G^{0} = -nEF$$

and substituting into the previous free energy expression results in:

$$E = RT/nF \ln (P_{O_2}'' / P_{O_2}')$$

Thus the emf for the cell will depend on the difference in the values of the anodic and cathodic equilibrium oxygen partial pressures and, at any specific temperature, a corresponding Gibbs free energy value can be obtained. By measuring the emf over an appropriate temperature range (to ensure strictly ionic conductivity), a plot of the Gibbs free energy of formation of the carbide versus temperature can be made.

D. CELL REACTIONS

CHROMIUM CARBIDE

The cell can be represented schematically as:

$$(-)\ Cr, Cr_2O_3 / ELECTROLYTE / C, Cr_2O_3, Cr_3C_2\ (+)$$

the electrode reactions would then be:

at the anode:

$$4/3Cr + 2O^{=} = 2/3Cr_2O_3 + 4e^{-}$$

at the cathode:

$$2/3Cr_2O_3 + 8/9C + 4e^{-} = 4/9Cr_3C_2 + 2O^{=}$$

for a resulting cell reaction of:

$$4/3Cr + 8/9C = 4/9Cr_3C_2$$

The free energy change for the reaction as written would be:

$$\Delta G = 4/9\, \Delta G^{0}$$

where ΔG^{0} is the standard free energy of formation of Cr_3C_2. Using the Nernst equation and a value of 4 for n yields: $E = - \Delta G^{0}/9F$

MOLYBDENUM CARBIDE

The cell was arranged similar to the chromium system:

$$(-)\ Mo, MoO_2 / ELECTROLYTE / C, MoO_2, Mo_2C\ (+)$$

where the electrode reactions are:

at the anode:

$$2Mo + 4O^{=} = 2MoO_2 + 8e^{-}$$

at the cathode:

$$2MoO_2 + C + 8e^{-} = Mo_2C + 4O^{=}$$

For an overall cell reaction of:

$$2Mo + C = Mo_2C$$

And the free energy for the reaction is:

$$\Delta G = \Delta G^{\circ}$$

where ΔG° is the standard free energy of formation of Mo_2C. Again, substituting the Nernst equation and a value of 8 for n into the above equation yields:

$$E = -\Delta G^{\circ}/8F$$

TUNGSTEN CARBIDE

The cell arrangement was as follows:

(-) W, WO_2 /ELECTROLYTE/C, WO_2, WC (+)

where the electrode reactions are:

at the anode:

$$W + 2O^{=} = WO_2 + 4e^{-}$$

at the cathode:

$$WO_2 + C + 4e^{-} = WC + 2O^{=}$$

for an overall cell reaction of:

$$W + C = WC$$

And the free energy change would be:

$$\Delta G = \Delta G^{0}$$

where ΔG^{0} is the standard free energy of formation of tungsten carbide.

Using a value of 4 for n and substituting the Nernst equation yields:

$$E = - \Delta G^{0}/4F$$

III. EXPERIMENTAL

A. MOLYBDENUM RESISTANCE FURNACE

DESIGN AND CONSTRUCTION

The resistance furnace was originally designed such that it would:

- have a large thermal mass to minimize temperature fluctuations
- have a high maximum operating temperature
- be of sufficient physical dimensions to accept the cell design
- enable gases to be passed over each side of the cell
- be able to withstand high temperatures for weeks at a time.

Molybdenum wire (0.127 cm (0.050 in.) diameter) was chosen for the winding because of its high melting point (2617°C) and its low cost compared to more common windings such as platinum. The use of molybdenum necessitated a hydrogen environment in the furnace shell to prevent catastrophic oxidation at high temperatures. A mixture of 15% hydrogen and 85% nitrogen was used for this purpose to minimize the explosion hazard yet maintain a sufficient amount of hydrogen for oxygen scavenging.

The molybdenum wire was wound over an alumina tube (5.7 cm (2.25 in.) O.D.) with the spacing between successive turns closer at each end than in the middle to try to maintain a longer constant temperature zone. The windings

were secured to the alumina tube with a 1.25 cm coating of high temperature cement (Aremco Products, Inc., Ossining, New York). Double lengths of molybdenum wire were used from the ceramic insulating feed-throughs to the winding to minimize overheating of the wire in the insulation of the furnace.

The furnace contained two types of insulation: a 15 cm core of alumina bubbles surrounded the windings and furnace tube since it could withstand higher temperatures than the Fiberfrax (Caborundum Corporation) used as the outer layer.

The furnace shell was constructed of 16 gauge (1.58 mm) stainless steel and the 10 cm diameter end holes were covered by water cooled brass end caps sealed with high temperature rubber gaskets.

The furnace was held in a stand that allowed it to be operated in any position from horizontal to vertical.

The controlling thermocouple (Pt-6%Rh / Pt-30%Rh) was housed in an alumina sheath that butted against the furnace cement on the windings. The furnace was controlled by a LeMont Eurotherm Power Supply (LeMont Scientific, State College, Penn.) rated at 208 V, 25 A maximum output. Figure 11 is a schematic drawing of the furnace and the furnace and controller are shown in Photograph 1.

TEMPERATURE PROFILE

A temperature profile was taken when the furnace was operated in the vertical position to determine the extent of the temperature gradients at various temperature settings.

This is shown in Fig. 12.

B. CELL DESIGNS

ARGON FLOW CELLS

Initially, the chromium carbide cell was set up using an inert argon atmosphere surrounding the two half-cell mixtures. It was thought that a gas flow rate independent region could be attained which would allow the equilibrium oxygen pressure to be maintained.

Prepurified argon was further treated by passing it through two drying stages (magnesium perchlorate and phosphorous pentoxide) and two stages to remove any traces of oxygen (copper turnings at 500°C and titanium gettering chips in a copper boat at 850°C) as shown in Photograph 2.

The argon gas was introduced through quartz tubes extending to within 2.5 cm of the powders and a common gas exit was used. A calcia stabilized zirconia tube (zirconia plus 10 mole % calcia from the Zirconium Corporation of America) was used as the solid electrolyte separating the two half-cells. A mixture of chromium carbide, chromium oxide and graphite (1:1:1 weight ratio) was placed in the zirconia tube over a platinum gauze electrode such that its height in the tube was less than 1.25 cm. The outer bottom surface of the closed-end zirconia tube was covered with platinum gauze and connected to a Pt / Pt-13%Rh thermocouple.

The zirconia tube was then placed in an alumina

crucible containing the chromium, chromium oxide mixture (3:1 weight ratio). The height of the powder in the crucible was limited to 1.25 cm so that the overall cell height was only 2.5 cm in total. By limiting the dimensions to this height, the cell could be operated in the constant temperature zone of the furnace. If the overall dimensions were to be reduced further, it was thought that one of the components might be totally consumed in the reaction to reach equilibrium or that possible traces of oxygen in the argon would fully oxidize either the carbon in the inner cell or the chromium in the outer cell.

The zirconia tube and alumina crucible were placed in a larger alumina tube and the top glass section of the cell installed. A stainless steel spring was incorporated into the design to exert pressure on the zirconia tube and ensure good contact between it and the outer cell powder. DeKhotinsky cement (Central Scientific Company) and high temperature o-rings were used to seal the components together. Before placing the cell in the furnace, the section of the outer alumina tube around the cell was covered with platinum foil and subsequently grounded to eliminate possible electrical interferences from the furnace windings or from stray signals in the immediate environment (fluorescent lights, other electrical instrumentation, etc.).

The platinum-rhodium thermocouple was connected via temperature compensating wire to a digital thermometer

(Fluke, Model 2100A). The platinum electrode from the inner cell and the platinum side of the measuring thermocouple were connected via shielded cable to a Keithley Model 616 digital electrometer (Keithley Instruments, Inc., Cleveland, Ohio) whose input impedance was sufficiently high (greater than 2×10^{14} ohms) to ensure that the current passed through the cell while measurements were being taken was at a minimum. The thermocouple and cell outputs were initially monitored using a Leeds and Northrup Speedomax two pen recorder so that any drift in the readings could be easily detected.

This initial flow cell was operated for approximately two weeks during which time the temperature was cycled from 700° to 1200°C and the argon flow rate was varied from 0 to 500 cc/min. Emf readings were taken as a function of the argon flow rate at 100°C increments over the above temperature range with no success in achieving stable, flow rate independent values.

Since this cell failed to provide stable emf readings, a second argon flow cell was designed and constructed. It was felt that the two cell compartments should be totally isolated from each other even though a positive gas flow was maintained in the first cell design.

In the second cell, the same argon environment was maintained over the reference electrode mixture but the inner electrode compartment containing the carbide mixture was purged, evacuated and sealed rather than being

maintained in a separate gas environment. This was done because the inner diameter of the zirconia tube would make introduction and separate withdrawal of the argon gas difficult. A brass end cap containing ports for argon flow, thermocouple wires and the zirconia tube was used to seal the outer alumina tube. All other features previously described (i.e., cell components, electrode materials and platinum grounding foil) were maintained as before except that Apiezon wax (Shell International Chemical Company Ltd., London, England) was substituted for the DeKhotinsky cement. This was deemed necessary since polymerization had apparently taken place in the wax joints of the first cell. When this happens, the wax-like sealing properties are lost and gas transfer through the cement may occur. The polymerization may have been caused by overheating during initial application or simply because the cement suffers degradation when stored for extended periods of time. Regardless of the cause, it was felt that Apiezon wax would be more suitable for this application.

The second cell is shown in Photographs 3 and 4.

EVACUATED CELLS

The second flow cell also failed to provide stable, argon flow rate independent readings, so it was decided to construct a third cell with both sides evacuated. A Pyrex glass top was constructed such that both electrode compartments could be isolated using Apiezon wax but purging and evacuating could be carried out simultaneously to

prevent the "piston-like" action that would otherwise occur.[88] After evacuation, both sides were isolated by flame sealing the Pyrex tubing. The Pyrex top was sealed into a quartz tube which held the alumina crucible and cell components. Due to the possibility of damage caused by thermal expansion, a layer of alumina bubbles was placed between the quartz tube and the alumina crucible so that adequate pressure could be maintained between the two half-cells but excessive pressure would be taken up by the collapse of the alumina bubbles.

The quartz cell seemed to work initially but when the temperature was raised to 1200°C the readings became erratic. Subsequent checking of the outer cell compartment with a Tesla coil indicated that the vacuum had been lost. When the cell was dismantled, the quartz tube was highly devitrified near the "hot zone" of the cell. The quartz had collapsed and cracked because of the high temperature and vacuum in the cell.

A second evacuated cell was designed using an alumina bottom and Pyrex top. A brass collar containing Apiezon wax was used to join the two sections together. A quartz baffle was placed between the upper and lower parts to prevent any wax from dripping into the lower cell during assembly and to act as a radiation baffle to keep the glass top cool. Two fans were also used to cool the glass top since the Apiezon wax softened at approximately 120°C.

This final design was used for all subsequent runs for

the chromium, molybdenum and tungsten systems. A close-up of the cell top is shown in Photograph 5.

C. CELL COMPONENT MIXTURES

The chromium cell was initially set up limiting the volume of powder in order to keep the cell within the constant temperature zone of the furnace. Since a thermocouple was required as near the cell center as possible, it had to be located in the outer cell compartment (i.e., alumina crucible) due to the limited size of the inner diameter of the zirconia tube. According to the carbon-platinum phase diagram and other literature sources[70,71], there is limited solubility of carbon in platinum at high temperatures which could have affected the thermocouple emf over the extended high temperature runs that were planned. Thus the final arrangement of the cell components was with the chromium oxide, chromium carbide and graphite inside the zirconia tube ("inner cell") and the chromium metal and chromium oxide mixture in the alumina crucible ("outer cell").

D. CHEMICAL REAGENTS

All reagents used as cell components were purchased from companies which could supply the purest form available. The source and purity are listed below for each system.

CHROMIUM

Chromium Metal

Ventron-Alfa Inorganics, Beverly, Mass.

-140 mesh, 99.9% pure

Chromium Oxide

Electronic Space Products, Inc., Los Angeles, Calif.

99.999% pure

Chromium Carbide (Cr_3C_2)

Cerac/Pure, Menomonee Falls, Wisc.

-325 mesh, typically 99% pure

MOLYBDENUM

Molybdenum Metal

Apache Chemicals, Rockford, Ill.

100 mesh, 99.8% pure

Molybdenum Dioxide

Research Organic/Inorganic Chemical Corp., Sun Valley, Calif.

99.9% pure

Molybdenum Carbide (Mo_2C)

Ventron-Alfa Products, Beverly, Mass.

99.8% pure

TUNGSTEN

Tungsten Metal

Cerac/Pure Incorporated, Menomonee Falls, Wisc.

-100 mesh, typically 99.8% pure

Tungsten Dioxide

Cerac/Pure Incorporated, Menomonee Falls, Wisc.

-100 mesh, typically 99.9% pure

Tungsten Carbide (WC)

Ventron-Alfa Products, Beverly, Mass.

99.9% pure

CARBON

Graphite Powder

Apache Chemicals, Rockford, Ill.

325 mesh, 99.999+% pure

ARGON

Matheson of Canada, Whitby, Ontario

Ultra High Purity, typically 99.999% pure

Typical Impurities (less than 10 ppm total)

Oxygen ... 1 - 2 ppm

Nitrogen ... 3 - 4 ppm

Carbon Dioxide ... less than 1 ppm

Hydrocarbons (as methane) ... less than 1 ppm

IV. RESULTS AND DISCUSSION

A. CHROMIUM CARBIDE

FLOW CELLS

The first argon flow cell failed to produce any consistent, meaningful results. This could have been due, in part, to the mixing of the anode and cathode cell gases even though positive flows were maintained. Since a common exit was incorporated into the cell design, interdiffusion of the gases could have occurred. Further reasons for the lack of consistent readings could be that the equilibrium oxygen partial pressures were not established due to:

(1) the oxygen activity in the argon gas being higher than theoretically predicted by the titanium-titanium dioxide free energy values due to the kinetics of the gettering reaction.

(2) oxygen in traces of carbon monoxide, carbon dioxide or water vapour not removed from the argon. (phosphorous pentoxide used as the drying agent may form channels allowing unreacted water through this drying stage and no provision was made for the removal of traces of carbon monoxide or carbon dioxide).

(3) oxygen in desorbed water on the cell components (i.e., chemical reagents or cell apparatus).

(4) oxygen diffusion through the tygon tubing or leakage around the o-rings.

Assuming that these factors did not contribute to higher than equilibrium oxygen partial pressures, it may have been that the kinetics of the chromium-chromium oxide or the graphite-chromium carbide-chromium oxide reactions were not sufficiently rapid to counteract removal of oxygen by the flowing argon gas. Thus the oxygen partial pressures would always be lower than the equilibrium values.

One additional effect of using the argon gas could have been cooling of the reaction zone of the cell when the cell temperature was appreciably higher than the operating temperature of the titanium purification furnace. Also, at low argon flow rates, the temperature of the gas would have dropped from 850°C due to cooling in the tygon inlet lines.

As explained in the experimental section, the second flow cell was constructed with the inner cell evacuated and the outer cell maintained in argon gas. It was felt that the main reason for the lack of reliable results in the first flow cell was the mixing of the gas environments rather than excessive oxygen contamination in the system.

The results obtained for this cell were more consistent than for the first, but the scatter in the readings was thought to be too great to be of value. Also, altering the argon flow rate produced variations in the emf readings and a flow rate independent region was not found where stable readings could be obtained. When the argon was shut off completely, the emf rose in value indicating that perhaps oxygen was being added to the cell by the argon. Readings

were taken throughout the run varying the argon flow rates as well as when the gas was shut off completely. By taking only the points where the argon had been shut off (in most cases, it was off overnight and "equilibrium" was allowed to be established), a data set was obtained that was more consistent with literature values.

These readings are presented in a plot of emf versus temperature in Fig. 13.

EVACUATED QUARTZ CELL

The third chromium cell using an evacuated Pyrex top and quartz bottom gave reasonable readings until a temperature of 1200°C was reached.

At a set point of 1200°C the emf dropped until it became negative and, even though the furnace was reset to lower temperatures, the readings never returned to their previous values indicating a total malfunction of the cell. Unfortunately, the cell was not first cycled in the lower temperature range to reproduce the readings that were obtained. Examination of the dismantled cell revealed that the outer compartment had cracked so that the equilibrium oxygen partial pressure could no longer be maintained.

Figure 14 is a plot of the emf readings obtained from the quartz cell before the vacuum had been lost.

EVACUATED ALUMINA CELLS

This type of chromium cell used an alumina outer tube and Pyrex top which enabled it to be taken to much higher temperatures without damage. However, as in the previous cells, the high resistance of the zirconia electrolyte or the sluggishness of the cell reactions prevented the cell from operating properly in the low temperature region even though the equilibrium oxygen partial pressures in each half-cell fell within the theoretical bounds for the solid electrolyte.

When the cell was cycled towards the higher temperatures (near 1200°C), the emf values consistently fell off the expected linear relationship. When the cell was returned to the lower temperatures, the readings returned to their previous values but each attempt to obtain readings above 1200°C resulted in values lower than predicted by an extrapolation of the linear portion of the low temperature results.

After cycling the cell through the productive temperature range, it was taken apart and the cell components analyzed by x-ray diffraction. The outer cell components showed peaks for both constituents of the same order of magnitude as on a previous scan taken before use in the cell. However, analysis of the inner cell showed only a trace of chromium oxide compared to its original peak before use.

The disappearance of one of the components could

account for the drop off in the readings at high temperatures since, with chromium oxide no longer present, the oxygen partial pressure would be less than its theoretical equilibrium value. Since the emf depends on the difference in the anodic and cathodic oxygen partial pressures, the inability of the cathode compartment to reach its equilibrium value, while the anode compartment functioned normally, would decrease this partial pressure difference and the emf would be lower than its expected value.

The reason for the trace of chromium oxide present in the x-ray diffraction analysis could be that when the cell was cooled slowly back to room temperature, it was reformed to some extent by the reaction between the oxygen and chromium carbide. Due to the low cell temperature, this recombination would only be slight.

The emf results obtained from this cell and the corresponding free energy values are plotted in Fig. 15 and 16 respectively.

The chromium cell was set up again using the same configuration as before but changing the inner cell component mixture. A ratio of 1:1:1.5 for the graphite, chromium carbide and chromium oxide was used to try to eliminate the total decomposition of the chromium oxide. Indeed, at the elevated temperatures in this run, the emf stayed at higher values than before but if the cell was raised to even greater temperatures, the same decrease in

the readings was noted.

This cell was cycled over the temperature range bounded by slow reaction kinetics and/or high electrolyte resistivity at the low end and the non-linear response at the high temperatures.

Subsequent dismantling of the cell and analysis of the components by x-ray diffraction indicated the presence of all phases but, as mentioned for the previous cell, this does not prove that all of the components were present at the higher temperatures since recombination could have occurred as the cell cooled. Quenching the components from the high temperatures may have substantiated the disappearance of one of the constituents, but this was not possible since it would have resulted in the total destruction of the ceramic tubes which, in turn, would have led to questionable recovery of the chemicals from the quenching medium.

Before analyzing the cell components by x-ray diffraction, examination of the outer cell compartment and the zirconia electrolyte was carried out to ensure that good contact had been maintained between the constituents, electrode and electrolyte. The high operating temperature of the cell sintered the chromium-chromium oxide mixture onto the platinum gauze used as the outer electrode often making the removal of the sintered powder from the thermocouple and platinum gauze impossible.

Photograph 6 shows the outer cell with the alumina

crucible removed. The thermocouple used to measure the cell temperature is embedded in the chromium-chromium oxide powder and is located in the "heart" of the cell at the bottom of the closed-end zirconia tube. This thermocouple arrangement minimized the error in the temperature determination due to thermal gradients in the furnace since it is located as near as physically possible to the area of oxygen transfer through the electrolyte.

Photograph 7 shows the cell with the thermocouple and the majority of the powder removed to illustrate the intimate contact between the powder and electrolyte surface. The powder had sintered onto the surface to the extent that it had to be ground from the electrolyte surface. The inner powder (not able to be shown in a photograph) had also sintered into a coherent mass but did not bond as readily to the electrolyte.

The zirconia tube was progressively discoloured from dark grey at the closed-end to light grey approximately 10 cm from the reaction zone as shown after sectioning in Photograph 8. In order to ascertain whether the electrolyte composition had been adversly altered by reaction with the cell constituents, it was sectioned and analyzed both using x-ray diffraction and a scanning electron microscope coupled with an energy dispersive x-ray analyzer. The purpose of the analysis was to determine whether the discolouration was due to graphite diffusion out from the inner cathode compartment or to chromium diffusion through the electrolyte from the

outer anode compartment. This would not present a problem unless enough of the material had diffused through to totally remove one of the reactants in the other half-cell. A problem might arise if sufficient chromium had diffused into the electrolyte to alter its electrolytic properties by acting as a source of free electrons and thus increase the electronic portion of the overall conductivity.

Both methods of analysis confirmed that only the proper cell components were present in each cell compartment.

The flat end of the zirconia tube was then sectioned and polished on a diamond wheel to determine the extent of the discoloration through the electrolyte wall. The end thickness of the tube was reduced in this way to approximately one half of its original dimension with no change in the colour as shown in Photographs 9 and 10. X-ray diffraction analysis of the new surface failed to show anything but the presence of calcia stabilized zirconia. Subsequent treatments of the tube in solutions of mineral acids ranging from nitric, hydrochloric, sulphuric and aqua regia through to hydrofluoric acid failed to remove the discolouration although the latter did start to attack the surface of the electrolyte. The discolouration was probably due to the solid-solid interdiffusion of the cell constituents and the zirconia electrolyte which would be expected when the cell was operated at high temperatures for extended periods of time. Although the extent of the discolouration seems severe, it should be pointed out that

this can result from only trace quantities of transition metal contaminants as borne out by the x-ray diffraction and S.E.M. analyses of the electrolyte surface.

Very little information is available on the metal content needed to substantially alter the electrolytic properties of this electrolyte, but it was felt that the electronic conductivity due to these impurities was well within acceptable limits since successive runs for this system produced similar emf values. If the diffusion of the chromium into the zirconia had affected the electronic portion of the conductivity, its contribution would increase as a function of time and temperature, and measurements taken at the end of the run would be lower than those at the beginning. This was not found to be the case.

The emf and free energy results obtained from this cell are plotted in Fig. 17 and 18 respectively.

B. MOLYBDENUM CARBIDE

The first molybdenum cell was set up using the final evacuated cell design as previously described. The cathode compartment contained the components in a 1:1:1 weight ratio while the anode compartment had a 3:1 weight ratio for the molybdenum and molybdenum oxide.

On initial heating, condensation was noticed on the inside of the Pyrex glass top but this disappeared after a few hours of operation. Similarly to the chromium system, the emf values were frequently erratic at temperatures below

700°C. The slow reaction kinetics for the molybdenum system could have been the cause; however, there was some evidence to the contrary in that the cell was frequently left for periods of 12 - 14 hr at the 700° temperature with no success in achieving stable, meaningful results. This is further substantiated by the fact that when the cell temperature was raised approximately 200°, the emf rose gradually and reached a stable value when left for similar periods of time. The high resistivity of the electrolyte may have contributed to the erratic readings at the low temperatures; however, calcia stabilized zirconia has been used before as an electrolyte at low temperatures.

The results obtained were scattered and reproducibility between cycles was not as good as expected. Since this was the first run for the molybdenum system, it was not performed for an extended length of time in order to dismantle the cell and examine the components for any anomalies. X-ray diffraction analysis of anode components showed both phases present but the top layer of the powder had developed a different colour from the rest. Comparative x-ray diffraction scans of both coloured layers indicated that the lower layer was richer in molybdenum dioxide than the top but this does not present a problem since both phases were present at the electrolyte surface.

Analysis of the cathode components indicated very little graphite present so that its ratio was doubled when the next cell was set up.

The emf results for this cell are shown in Fig. 19.

Before the second molybdenum cell was put together the anode and cathode chemicals, the alumina tube, crucible and bubbles, the zirconia tube and the Pyrex glass top were dried at 80°C for 2 hr to eliminate the problem of adsorbed moisture being released on initial heating.

This cell also required a minimum temperature to function properly although it appeared to be able to be taken to slightly lower temperatures than the first cell. During temperature cycling it was found that at temperatures over 1220°C the readings dropped off from the expected values much the same as for the chromium system. Returning to the lower temperatures re-established their previous values so that successive cycles could be made between 900° and 1200°C. After numerous temperature cycles a final run was tried where the temperature was raised from 900° to over 1250°C while continuously monitoring the emf using a digital electrometer. The results increased linearly until the temperature exceeded 1200°C where the same drop off occurred. The cell was cooled to room temperature and testing of both cell compartments with a Tesla coil confirmed that a good vacuum was present in each. The vacuum had been maintained to the extent that implosion occurred when the Pyrex top was heated to remove it from the brass collar. Sintering of the cell powders had taken place similar to the chromium mixtures and good electrode/powder/electrolyte contact was evident as shown in

Photograph 11. X-ray diffraction analysis indicated that both the anode and cathode mixtures were low in molybdenum dioxide compared to scans taken before use in the cell. For this reason, the component ratios were altered for the next cell to:

2:1:1.5 for $C:Mo_2C:MoO_2$

and 2.5:1 for $Mo:MoO_2$

The emf and free energy results obtained for the second molybdenum cell are plotted in Fig. 20 and 21 respectively.

Before assembling the third cell, the chemicals and apparatus were again dried at 80°C for 2 hr as this treatment was found to be effective in eliminating the condensation inside the glass top. When initial heating was carried out, the cell blew up before it reached 1000°C. The explosion took place only at the top section enclosing the cathode compartment while the anode compartment remained intact. X-ray diffraction analysis of the recovered cathode mixture showed an almost complete disappearance of the molybdenum dioxide whereas one might have expected the graphite and molybdenum carbide to be completely oxidized since it had contacted the atmosphere at this temperature.

On start up, the cell was heated fairly rapidly up to the 1000°C mark which could have resulted in non-equilibrium conditions in the cathode compartment. Since the molybdenum dioxide was no longer present after the explosion, one might suspect that the rate of the reaction with it and either graphite or molybdenum carbide to be greater than their

being reformed by recombination of the products. On rapid heating excessive pressures could have developed due to the formation of carbon dioxide or carbon monoxide gas. For the next cell the initial heating was carried out at a slower rate to allow equilibrium conditions to be established.

The fourth molybdenum cell used the same component ratios as the third and the chemicals and apparatus were again dried before assembling the cell. Initial heat up of the cell was carried out over a period of 24 hr before attempting to cycle the temperature towards the high end. The values obtained were very similar to those of the first and second cells but this cell could be taken to higher temperatures before the results fell below the expected linear relationship.. The high temperature emf and free energy values obtained are shown in Fig. 22 and 23 respectively.

C. TUNGSTEN CARBIDE

The first tungsten cell was set up using the same component ratio as for the last molybdenum cell. Drying of the components was also carried out as before. The initial heating was performed slowly to lessen the possibility of explosion. After approximately 24 hr, temperature cycling was carried out extending the upper and lower limits to the point where either the results dropped off or became erratic at the two respective extremes. The cell was dismantled after approximately two weeks of operation and the anode and

cathode compartments examined. Sintering of the powders had occurred with evidence of good electode/powder/electrolyte contact. X-ray diffraction analysis confirmed the presence of the proper phases in each half-cell. The high temperature results for this cell are plotted in Fig. 24 and 25.

The second tungsten cell was constructed identically to the previous cell. Initial heating and subsequent temperature cycling were also carried out in a similar manner. The same drop off in the readings was experienced at high temperatures as well as the inability of the cell to function properly at temperatures below 900°C. The cell was operated for ten days and then dismantled for examination. As with all of the previous evacuated cells, this system had maintained excellent vacuum as indicated by testing with a high voltage coil and implosion on heating the Pyrex top.

The high temperature emf and free energy results from this cell are plotted in Fig. 26 and 27 respectively.

D. HIGH TEMPERATURE QUENCH TESTS

To try to determine whether the drop off in the high temperature readings was caused by the disappearance of one or more of the constituents or, possibly, the formation of a new phase, a quartz ampule was constructed that would allow quenching of the cell constituents from 1250° to 0°C in a matter of a few seconds (the dimensions of the ampule (8 cm long by 1.25 cm I.D.) were kept small to facilitate rapid heat transfer on quenching). It was hoped that this would

prevent reformation of the compound that was being consumed or else preserve the new phase, if present.

A series of ampules were constructed using the following conditions:

(1) graphite, molybdenum carbide and molybdenum dioxide (2:1:1 weight ratio) contained in a platinum boat (to prevent any reaction with the quartz glass) and fire sealed at atmospheric pressure.

(2) the same components as in (1), except that this ampule was evacuated down to approximately 10^{-3} Torr before fire sealing.

(3) the same components as in (1) and (2), again evacuated and fire sealed, but the rate of heating was carried out in 50°C increments over a period of 24 hr to allow equilibrium to be established.

(4) graphite, tungsten carbide and tungsten dioxide (2:1:1.5 weight ratio), evacuated, sealed and slowly heated.

(5) the same components as for (4), but the constituents were dried at 80°C for 2 hr to simulate the treatment that was carried out for the cells. Initial heating was performed over a period of four days using four increments of 50°C per day. On the fifth day, the temperature was set to 1250°C.

All of these efforts to reach 1250°C resulted in violent explosions which completely shattered the ampule and dispersed the powders so that x-ray diffraction analysis was not possible.

Further attempts to quench the powders were abandoned

since not only would a temperature of 1250°C have to be reached, but it would also have to be maintained for a sufficient length of time to allow the phenomenon causing the drop off in the emf values to occur.

E. EQUILIBRIUM PRESSURE CALCULATIONS

In order to explain the violent explosions that occurred when the quartz ampules were heated, the equilibrium partial pressures of oxygen, carbon monoxide and carbon dioxide were calculated for each system. Using the chromium system as an example, it can be seen that the partial pressures can be obtained by using the appropriate combinations of the following reactions:

(1) $2\ CO + O_2 = 2\ CO_2$

where $\Delta G^0_1 = -135000 + 41.50\ T$

(2) $C + CO_2 = 2\ CO$

where $\Delta G^0_2 = 40800 - 41.7\ T$

(3) $C + O_2 = CO_2$ (combination of (1) + (2))

where $\Delta G^0_3 = -94200 - 0.20\ T$

(4) $2\ C + O_2 = 2\ CO$ (combination of (1) + 2(2))

where $\Delta G^0_4 = -53400 - 41.90\ T$

(5) $Cr_2O_3 = 2\ Cr + 3/2\ O_2$

where $\Delta G^0_5 = 267750 - 62.1\ T$

(6) $3\ Cr + 2\ C = Cr_3C_2$

where $\Delta G^0_6 = -14800 - 3.42\ T$

Using reactions 3, 5 and 6 the following reaction can be obtained:

(7) $3\ Cr_2O_3 + 17/2\ C = 2\ Cr_3C_2 + 9/2\ CO_2$

where $\Delta G^0 = 349750 - 194.04\ T$

Reactions (1), (2) and (7) are the three independent reactions that can be written for a six component, three specie system.

Using the equation $\Delta G^0 = - RT \ln K$

where $\ln K = 9/2 \ln P(CO_2)$

yields $\ln P(CO_2) = -39111.4/T + 21.70$

Similarly, in reaction (2), it is seen that the equilibrium constant is:

$$\ln K = 2 \ln P(CO) - \ln P(CO_2)$$

and therefore

$$\ln P(CO) = -29821.4/T + 21.34$$

Now, using reaction (1) where:

$$\ln K = 2 \ln P(CO_2) - \ln P(O_2) - 2 \ln P(CO)$$

and substituting the expressions for the free energy and partial pressures of CO and CO_2 gives:

$$\ln P(O_2)\ (cathode) = -86514.8/T + 21.6$$

Similarly, the anodic oxygen pressure can be calculated using only reaction (5), so that:

$$\ln P(O_2)\ (anode) = -89824.9/T + 20.83$$

The calculated equilibrium partial pressures for the chromium, molybdenum and tungsten systems are plotted as a function of temperature in Fig. 28, 29 and 30, respectively.

Using the appropriate partial pressures and the cathode compartment volume, the minimum amount of each constituent required to fulfill the equilibrium conditions can now be

calculated.

As an example, for the chromium system at 1000°K:

$P(CO_2) = 2.75 \times 10^{-8}$ atm

$P(CO) = 2.07 \times 10^{-4}$ atm

$P(O_2) = 1.09 \times 10^{-30}$ atm

Now, using the ideal gas law, $P V = n R T$

where $P = P(CO_2)$

$V = 0.0418$ liters

$R = 0.082$ l atm / °K mole

$T = 1000$°K

yields $n(CO_2) = 1.40 \times 10^{-11}$ moles

or the weight of carbon dioxide is 6.16×10^{-10} g

so that the weight of oxygen is 4.48×10^{-10} g

and the weight of carbon is 1.68×10^{-10} g

For carbon monoxide, using the same values for V, R and T yields:

$n(CO) = 1.06 \times 10^{-7}$ moles

or the weight of carbon monoxide is 2.96×10^{-6} g

and the weight of oxygen is 1.69×10^{-6} g

and the weight of carbon is 1.27×10^{-6} g

The amount of oxygen, although small, can be calculated as:

$n(O_2) = 5.56 \times 10^{-34}$ g

Therefore the weight of oxygen is 1.78×10^{-32} g

Combining these weights gives:

total oxygen = 1.69×10^{-6} g

total carbon = 1.27×10^{-6} g

Since the oxygen can come only from the chromium oxide, the minimum weight required would be 5.35×10^{-8} g.

The carbon could be supplied either by the chromium carbide or by the graphite itself. If it is assumed that both contribute equally, then the weights of each would be 6.35×10^{-7} g for graphite and 9.52×10^{-8} g for chromium carbide.

Partial pressure calculations were carried out for each system as well as the calculation of the total pressure in the cathode compartment and the results are plotted in Fig. 31, 32 and 33 for the chromium, molybdenum and tungsten systems, respectively.

Using these plots, the necessary weight of each component as well as the equilibrium cell pressure can be readily found as a function of the cell temperature. Conversely, when the individual cell constituent weights are known, the maximum temperature to which the results are valid can be obtained. Also, using this approach, the internal cell pressure can be predicted so that explosions of the nature experienced in these experiments may be prevented providing that equilibrium conditions exist.

Determination of the maximum safe operating pressure and related temperature for the evacuated alumina cell design was difficult, since it was dependent on the Pyrex glass as well as the extent and nature of the Apiezon wax seal at the anode/cathode junction. The glass blower associated with the construction of the Pyrex top did not

recommend exceeding pressures greater than 10 atm (10.33 Kg/cm^2). He also pointed out that this fracture pressure could be greatly influenced by the time of exposure to the pressure, the area of glass exposed, inclusions, microcracks as well as the age of the glass used in the construction.

For the chromium system, as can be seen in Fig. 31, a temperature of approximately 1800°K is required to produce a cathode compartment pressure of 10 atm. It can also be seen on this figure that to reach this temperature and pressure, less than 0.2 g of each of the cell constituents is required. Since, during the experimental runs for this system that temperature was never reached, it can be concluded that there was, at all times, sufficient amounts of each constituent to satisfy the equilibrium conditions. Thus the drop off in the readings at high temperatures (>1200°C) could not have been caused by the disappearance of one or more of the cathode compounds providing that equilibrium conditions had been maintained.

Thus, the reason for the presence of chromium oxide in the x-ray diffraction scan taken after dismantling the first evacuated cell was not due to reformation of the reaction products on cooling, but rather because it was always present.

The molybdenum and tungsten cells are not as straightforward as the chromium cell. For the first two molybdenum cells, one gram of molybdenum dioxide and

molybdenum carbide was used which, according to Fig. 32, limits the temperature to 1100°K before the molybdenum dioxide or carbide would be consumed under equilibrium conditions. At this temperature, the cathode pressure would have been approximately 25 atm so that the recommended safe operating pressure had been greatly exceeded. The third cell, using increased amounts of graphite and molybdenum dioxide, exploded due to either higher pressures or to the possible presence of flaws in the glass mentioned previously.

At the low temperatures, due to the sluggishness of the system, the cell required periods of 12 - 14 hr to reach stable values. In addition to the problem created by the sluggish reaction kinetics was the extremely restrictive temperature range over which the cell functioned properly. At temperatures less than 800°C the time required to reach equilibrium was excessive and, at temperatures greater than 850°C, the pressure in the cathode compartment would become too great to be contained in the cell if sufficient oxide had been present to fulfil equilibrium conditions. Thus the temperature range where the carbide formation reaction was controlling the cell emf and where reliable data could be obtained was too narrow to arrive at an expression for the free energy of formation by regression analysis of the data. However, the data points that were able to be acquired within this range are in reasonable agreement with established literature values.

The change in slope of the emf values occurred at approximately 1120° - 1125°K which corresponds to the point in Fig. 32 where the oxide was consumed. This high temperature linear response exhibiting a stronger temperature dependence was caused by the change from the carbide formation reaction controlling the cell emf to that of the Boudouard reaction. By combining the expression for the Boudouard reaction with that for the molybdenum reference electrode, an entropy term was arrived at which was on the same order of magnitude as that for the molybdenum cell at high temperatures.

In the tungsten system, due to the reaction kinetics being even more sluggish than for either the chromium or molybdenum systems, it was felt that it would be more productive to operate in the intermediate to high temperature range. However, subsequent analyses and calculations showed that even at the lowest of the temperatures examined in the runs, the cathodic oxygen partial pressure was being controlled by the Boudouard reaction due to the disappearance of the oxide phase. This is confirmed by the expression obtained when the free energy expressions for the tungsten reference electrode and the Boudouard reaction were combined yielding an entropy term similar to that found for the tungsten cell at high temperatures.

V. CONCLUSIONS

The initial flow cells developed in this investigation were proven to be ineffective for measuring the free energy of formation for two reasons. Firstly, if the argon gas could be purified with respect to oxygen to a point where its partial pressure was less than the cell equilibrium partial pressures, then it is very likely that the oxygen formed by the cell constituents would be swept from the cell due to the sluggishness of the reaction kinetics. Secondly, and more probable, is that even using a titanium gettering system, the oxygen content in the purified argon was higher than the equilibrium values so that it was continually being added to the cell by the flowing gas.

The evacuated cell design subsequently developed had the advantage that if any oxygen remained after purging and evacuation, it would be consumed by reaction with the carbide or graphite in the cathode compartment and by the metal in the anode compartment so that after a period of operation, the true equilibrium oxygen partial pressures would be established.

The technique of using emf measurements for this investigation appears to be limited in the low temperature region by the sluggish cell reactions. At the higher temperatures, in the molybdenum and tungsten systems, it is limited by the pressures developed by carbon monoxide and carbon dioxide. In the chromium system, the high temperatures result in lower pressures in the cathode

compartment; however, the anodic oxygen pressure becomes significantly less than that required to ensure strictly ionic conductivity in the calcia stabilized zirconia electrolyte so that the increased electronic portion of the conductivity would result in a lowering of the emf values at high temperatures.

Since the chromium cell was able to be operated over a wider temperature range, regression analysis was carried out on the combined data for the evacuated cells yielding the following expression:

$$\Delta G^{\circ} = -15000 + 6.1T \text{ for } Cr_3C_2$$

This is less negative than the literature values, but when compared to previous emf studies,[33,40,44] it is in closer agreement, since the emf technique consistently produced values higher than the other methods.

Typical low temperature results for the molybdenum system (-17500 cal/mole at 816°C, -15500 cal/mole at 857°C) are again less negative than the literature values but since the emf technique was not used in previous investigations for this system, a comparison similar to that for the chromium system was not possible.

VI. RECOMMENDATIONS FOR FUTURE WORK

The limitations of the cell developed during this study preclude its use for temperatures outside the range of 800° to 850°C. At the lower temperatures, the electrolyte or more probably the nature of the system itself prevent emf stability or the establishment of equilibrium conditions so that very little can be done to affect a reduction in the useful temperature range; however, extremely long equilibration times could be tried to reduce the lower temperature limit.

In the high temperature region, two modifications could be made which might increase the temperature range.

The first, applying mainly to the chromium system, is the use of yttria doped thoria as the solid electrolyte. Its n-type conductivity boundary is lower than that for calcia stabilized zirconia (see Fig. 10) so that the onset of electronic conductivity would be shifted to a higher temperature. However, as Patterson[55] stated, the placement of the n-type boundary at high temperatures was in question due to the paucity of concurring information so that uncertainty exists in determining the temperature to which the electrolyte may be used.

The second modification would be the construction of a cell which could withstand pressures in excess of 100 atm. This would extend the high temperature range providing that the electrolyte tube itself could withstand these pressures. In order to overcome the problem of the electrolyte tube

weakness, a thick disc of the solid electrolyte could be incorporated into a cell built to withstand high pressures. The main problem using this approach is that the seal around the disc would have to be capable of withstanding high temperatures and pressures as well as being totally impervious to gas leakage or transfer from the cathode to the anode compartment. Further problems in this design would be the possibility of reaction between the anode or cathode constituents and the material used in the cell construction.

To extend the upper temperature range then, a high temperature, high pressure, inert container would be required which incorporated a sealed electrolyte disc capable of withstanding the same stringent conditions.

FIGURES

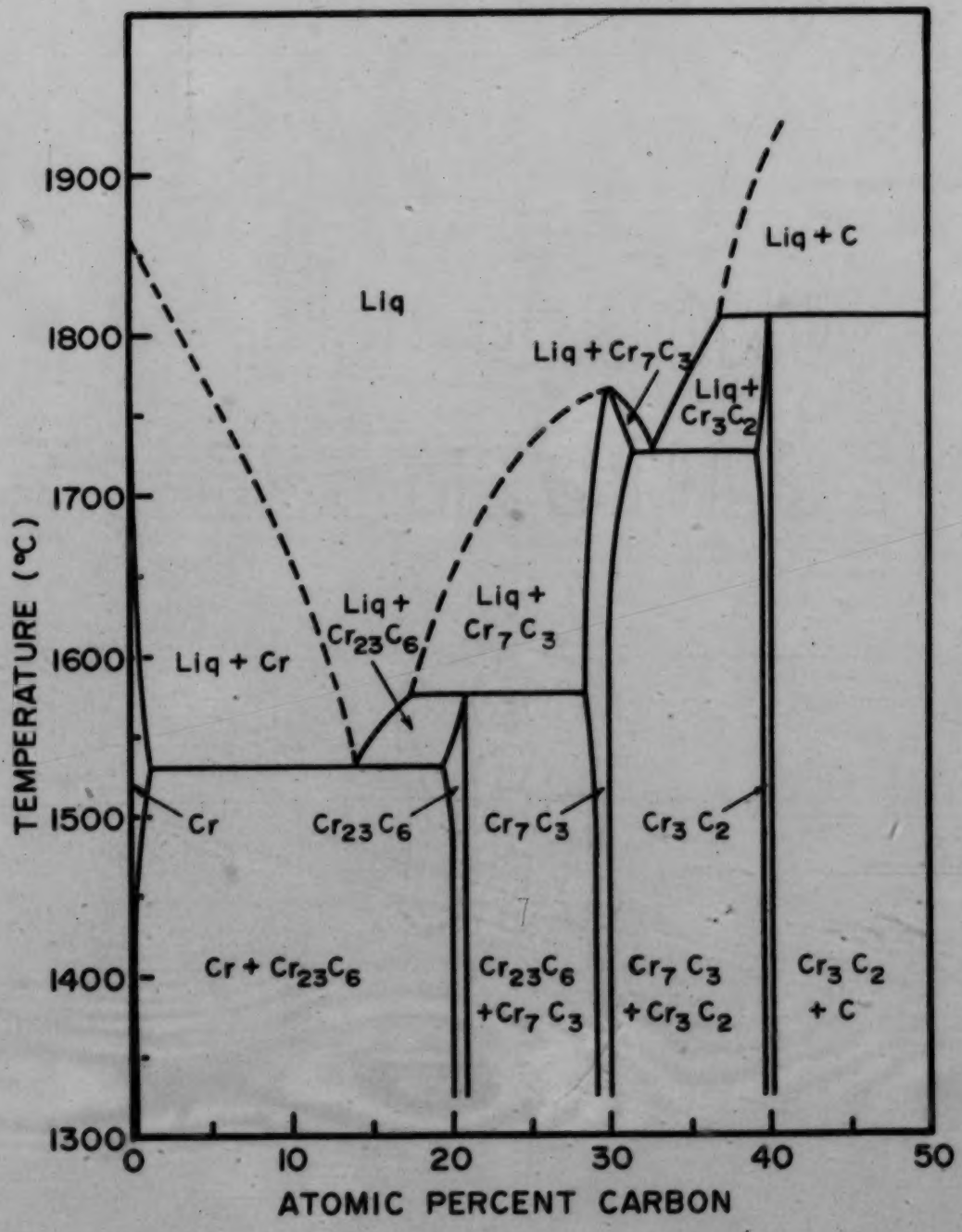

FIGURE 1: CHROMIUM-CARBON PHASE DIAGRAM [4]

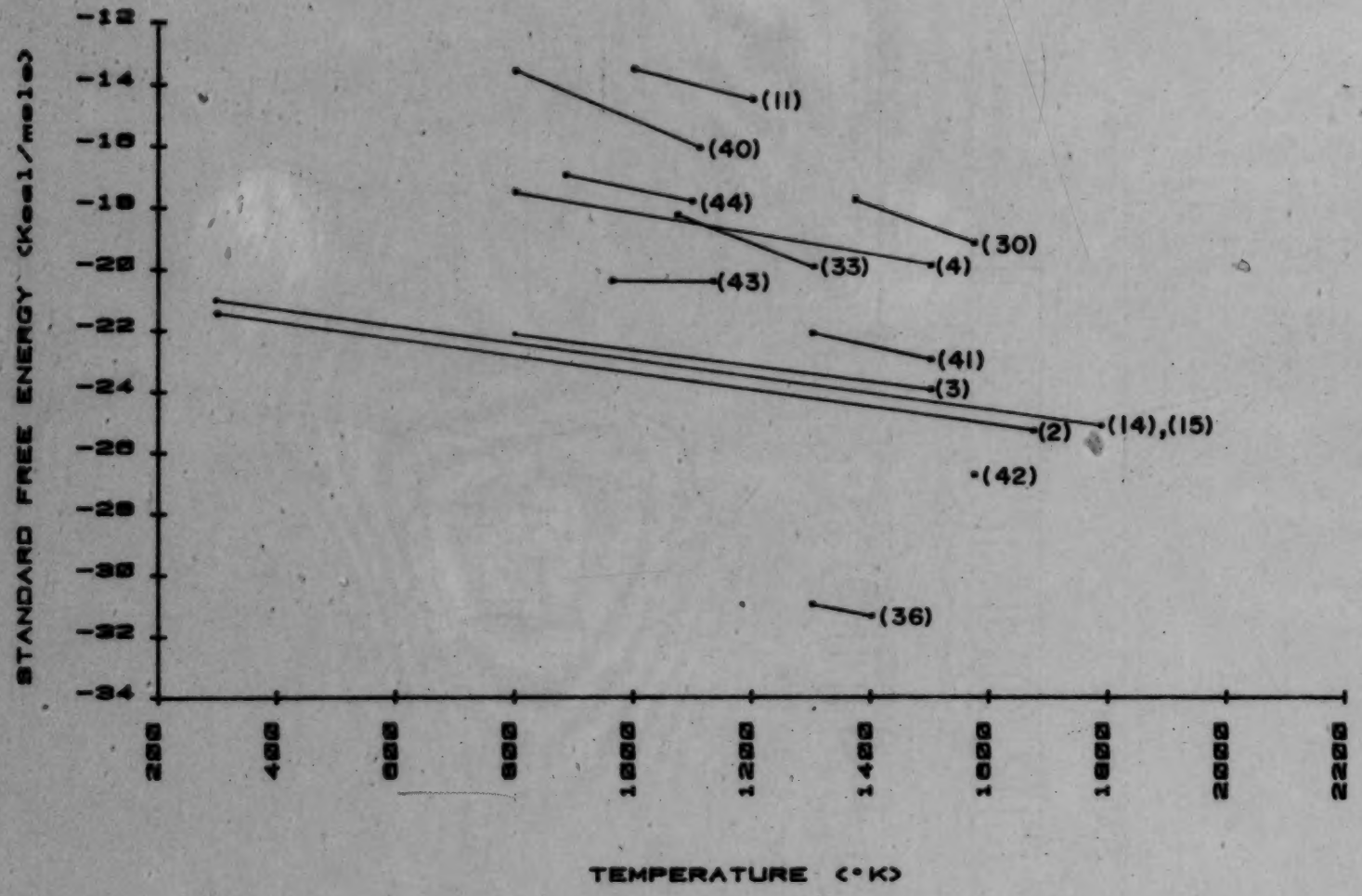

FIGURE 2: CHROMIUM CARBIDE: STANDARD FREE ENERGY COMPILATION

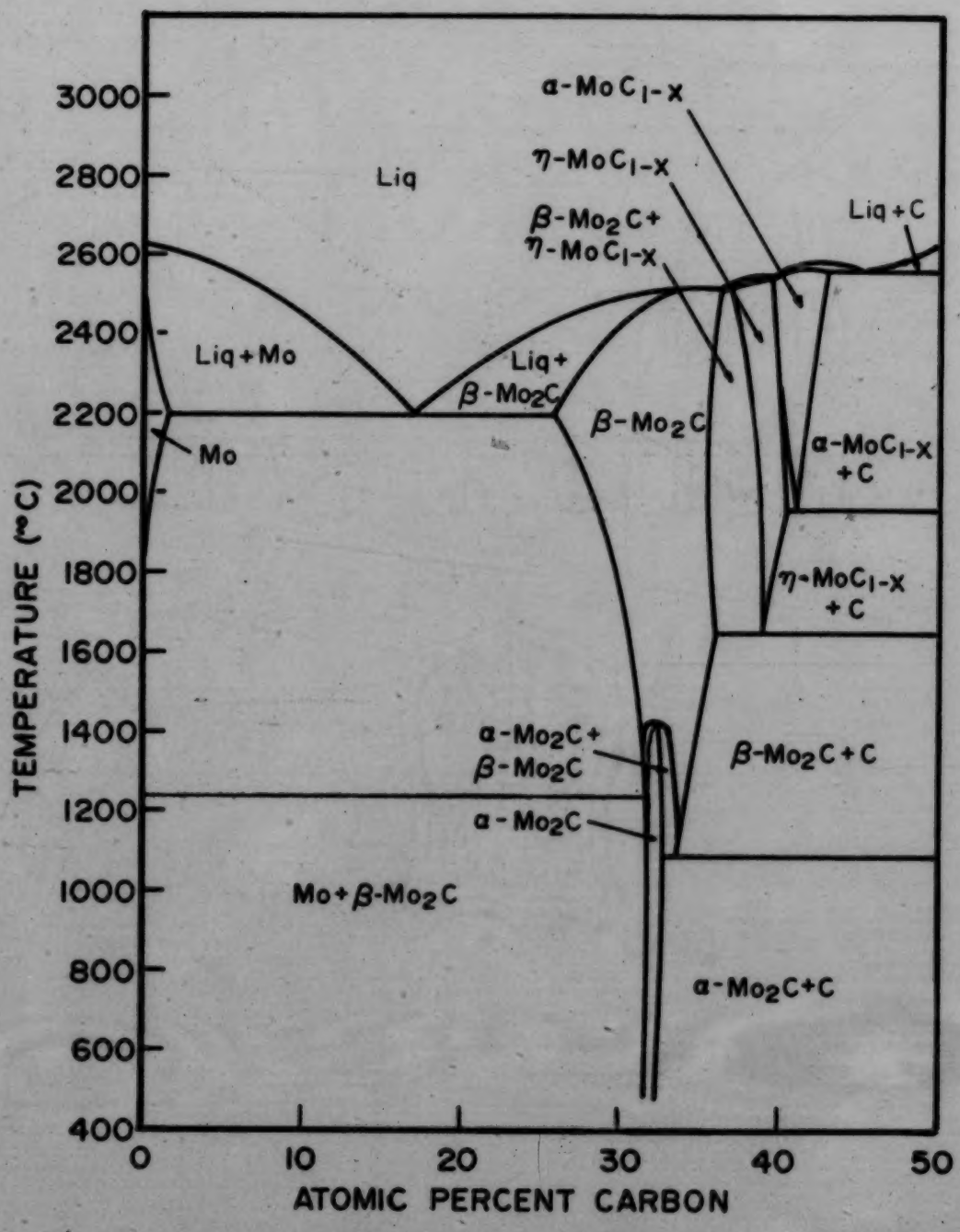

FIGURE 3: MOLYBDENUM–CARBON PHASE DIAGRAM [4]

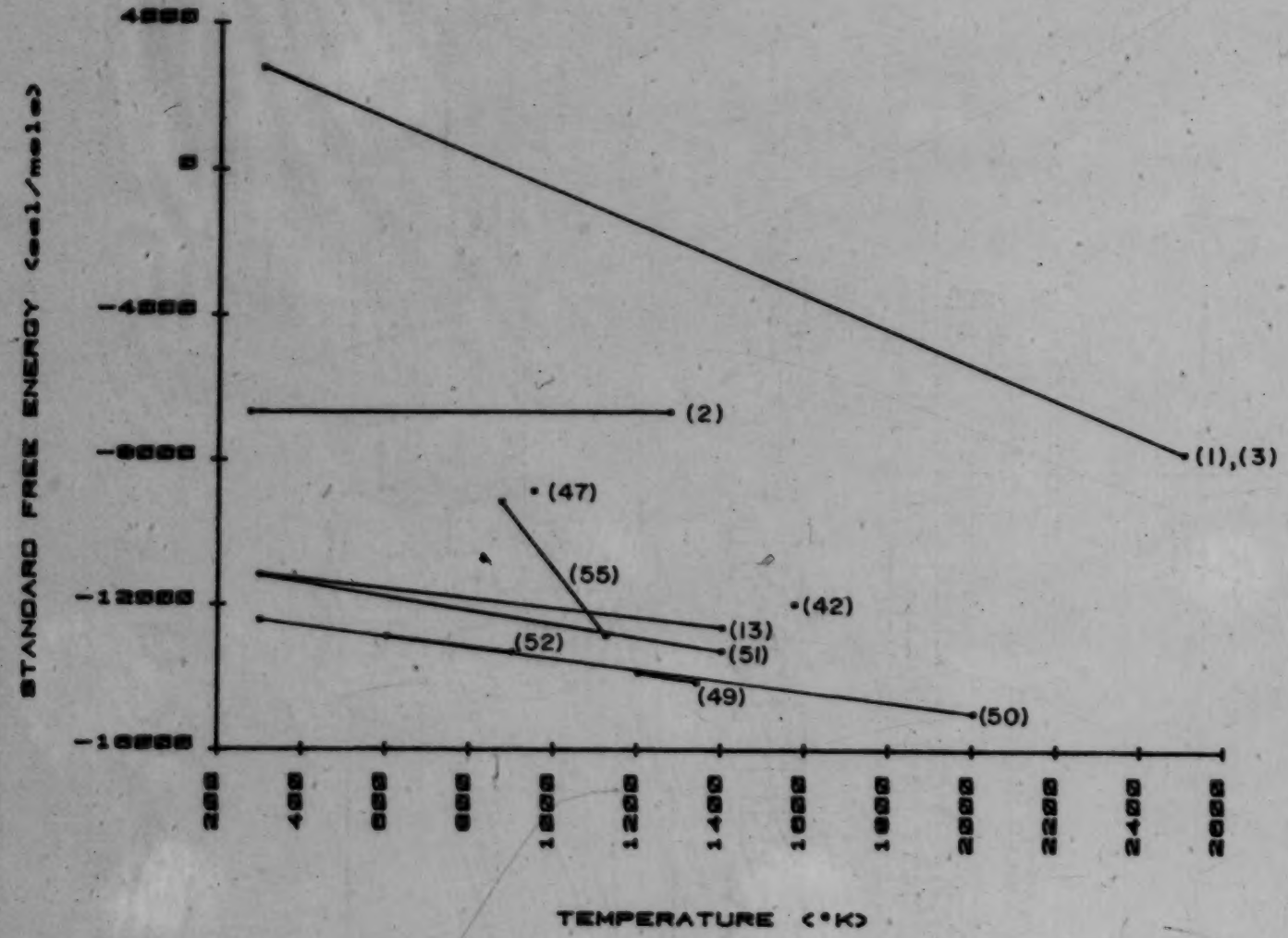

FIGURE 4 : MOLYBDENUM CARBIDE - STANDARD FREE ENERGY COMPILATION

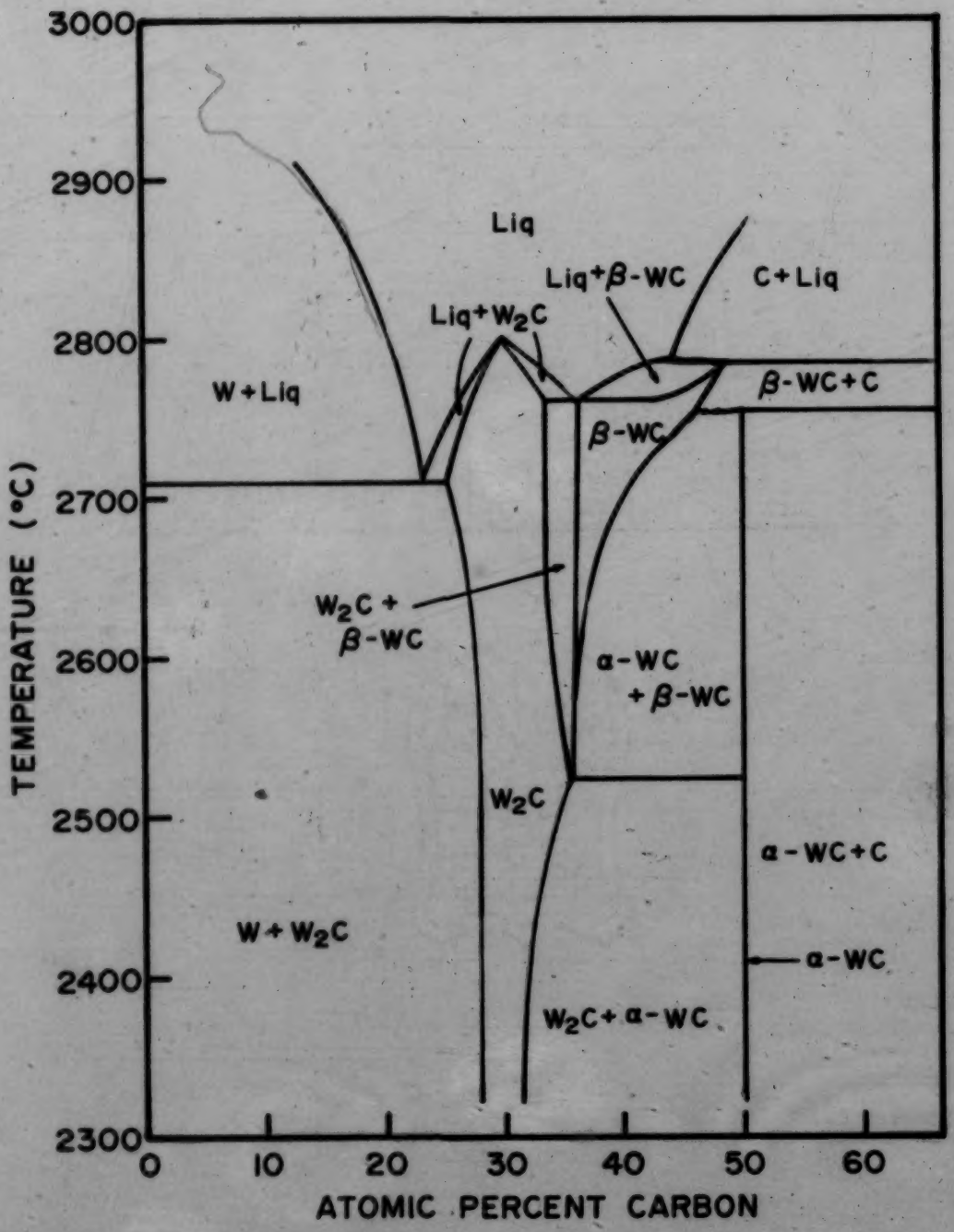

FIGURE 5: TUNGSTEN–CARBON PHASE DIAGRAM [4]

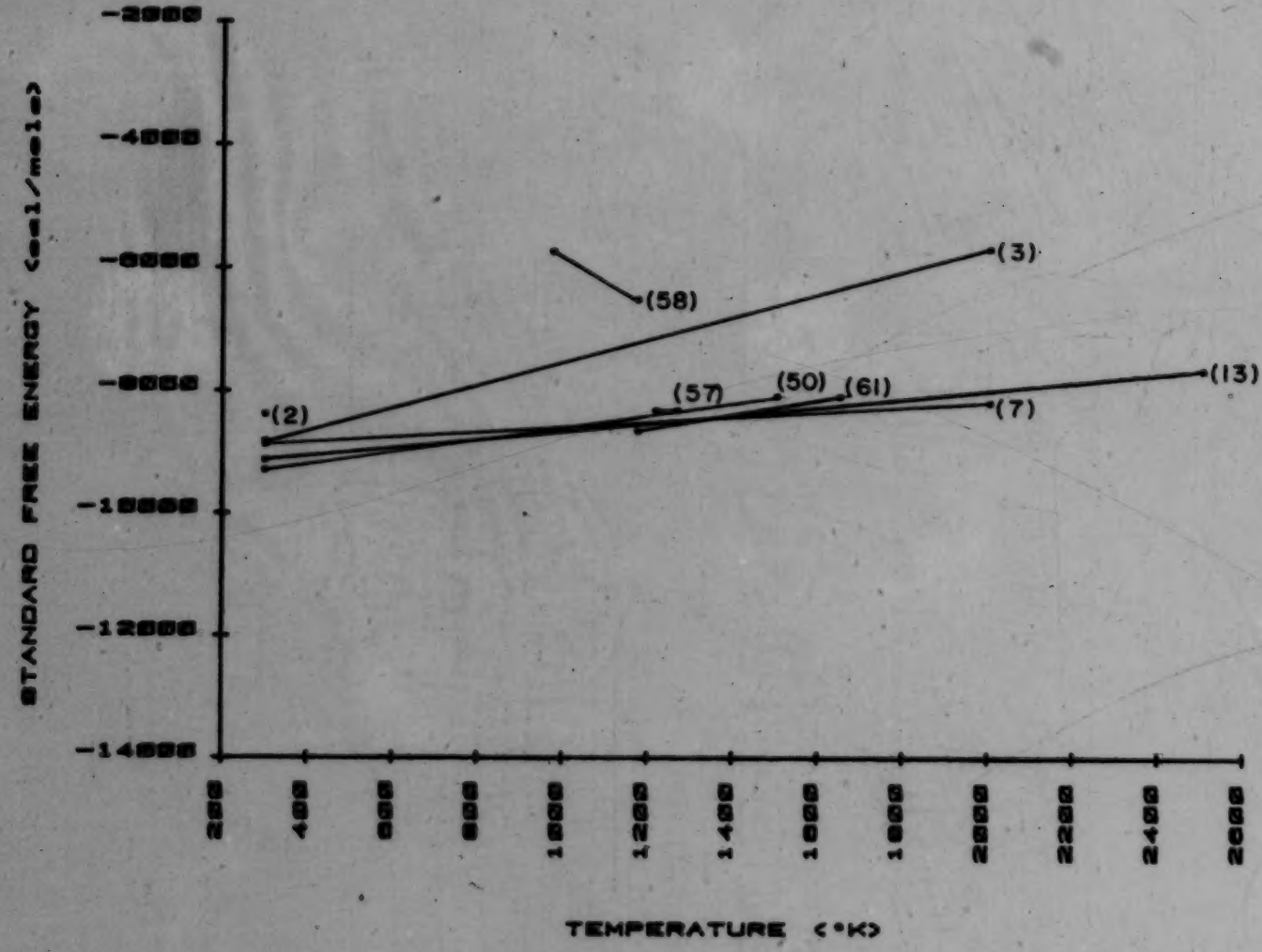

FIGURE 8 : TUNGSTEN CARBIDE - STANDARD FREE ENERGY COMPILATION

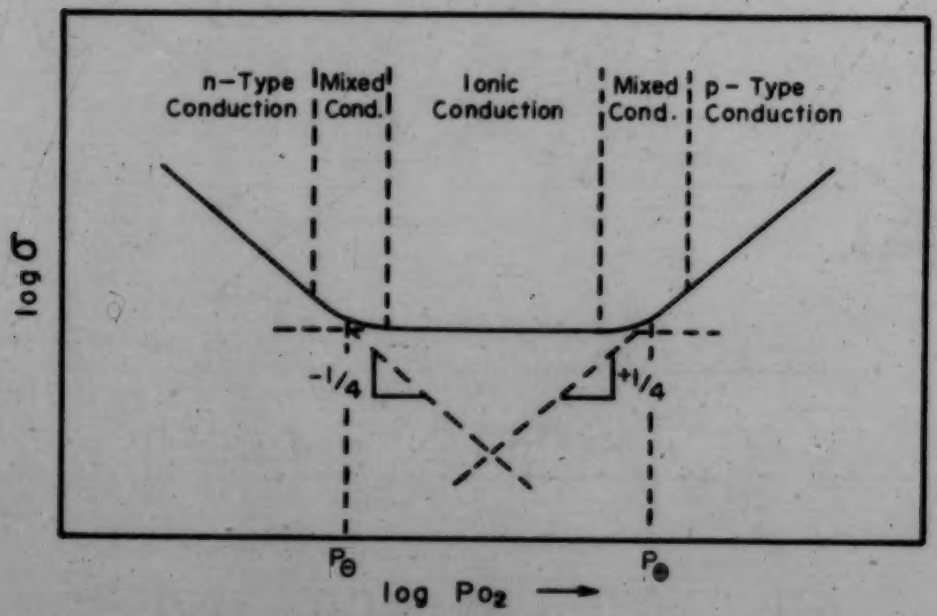

FIGURE 7: SCHEMATIC REPRESENTATION OF PARTIAL IONIC AND ELECTRONIC CONDUCTIVITIES

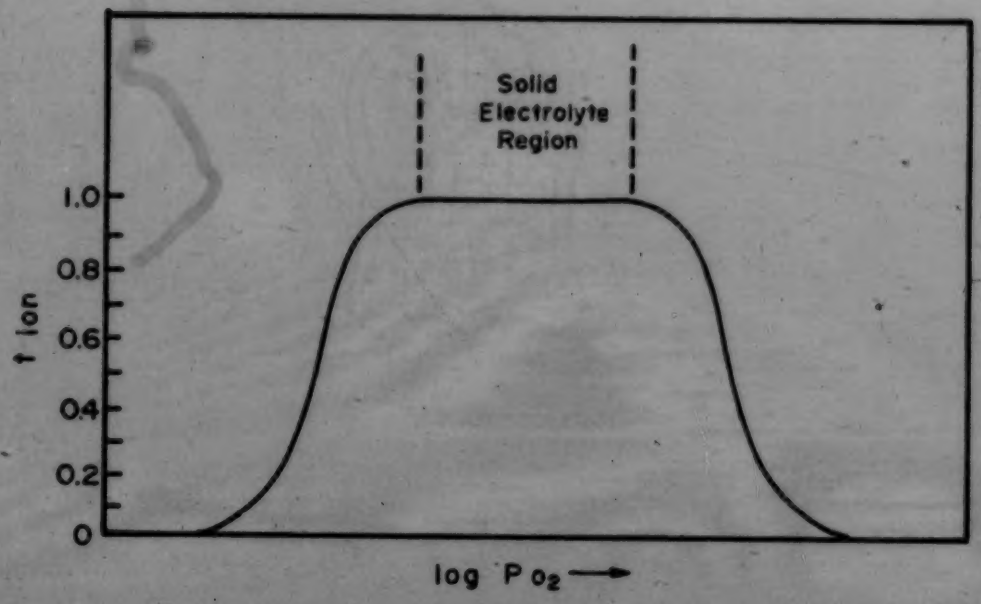

FIGURE 8: SCHEMATIC REPRESENTATION OF THE ELECTROLYTIC REGION WHERE $t_{ion} > 0.99$

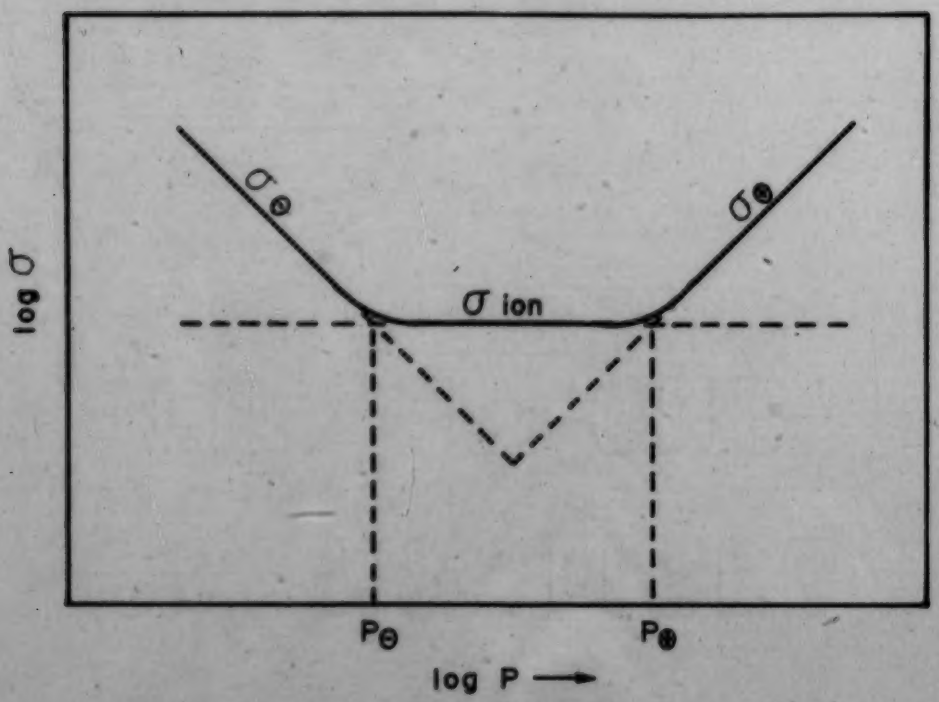

FIGURE 9: PARTIAL CONDUCTIVITIES AS A FUNCTION OF THE COMPONENT PARTIAL PRESSURE

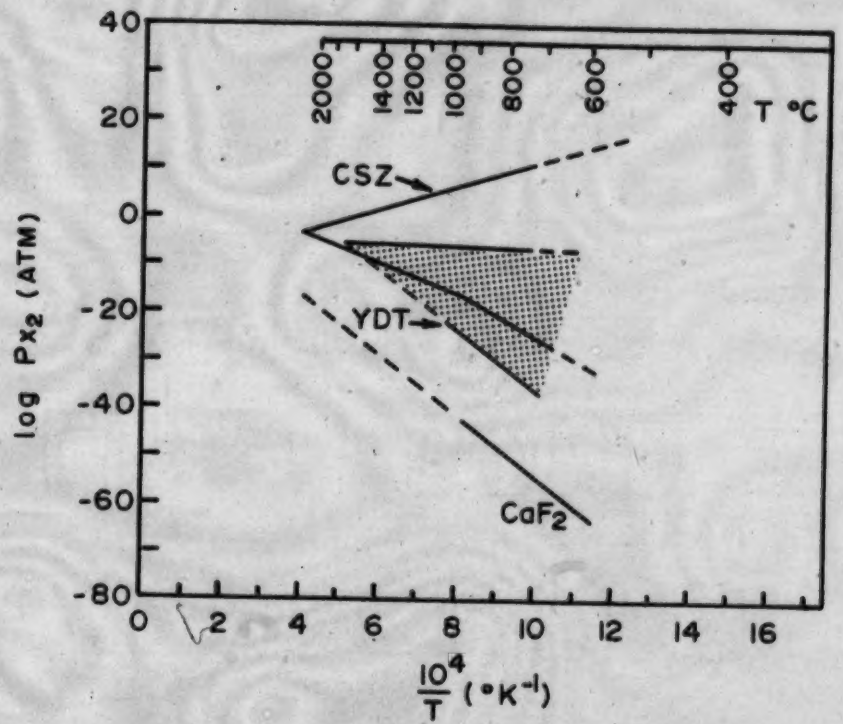

FIGURE 10: ELECTROLYTIC DOMAINS OF CALCIA STABILIZED ZIRCONIA AND YTTRIA DOPED THORIA

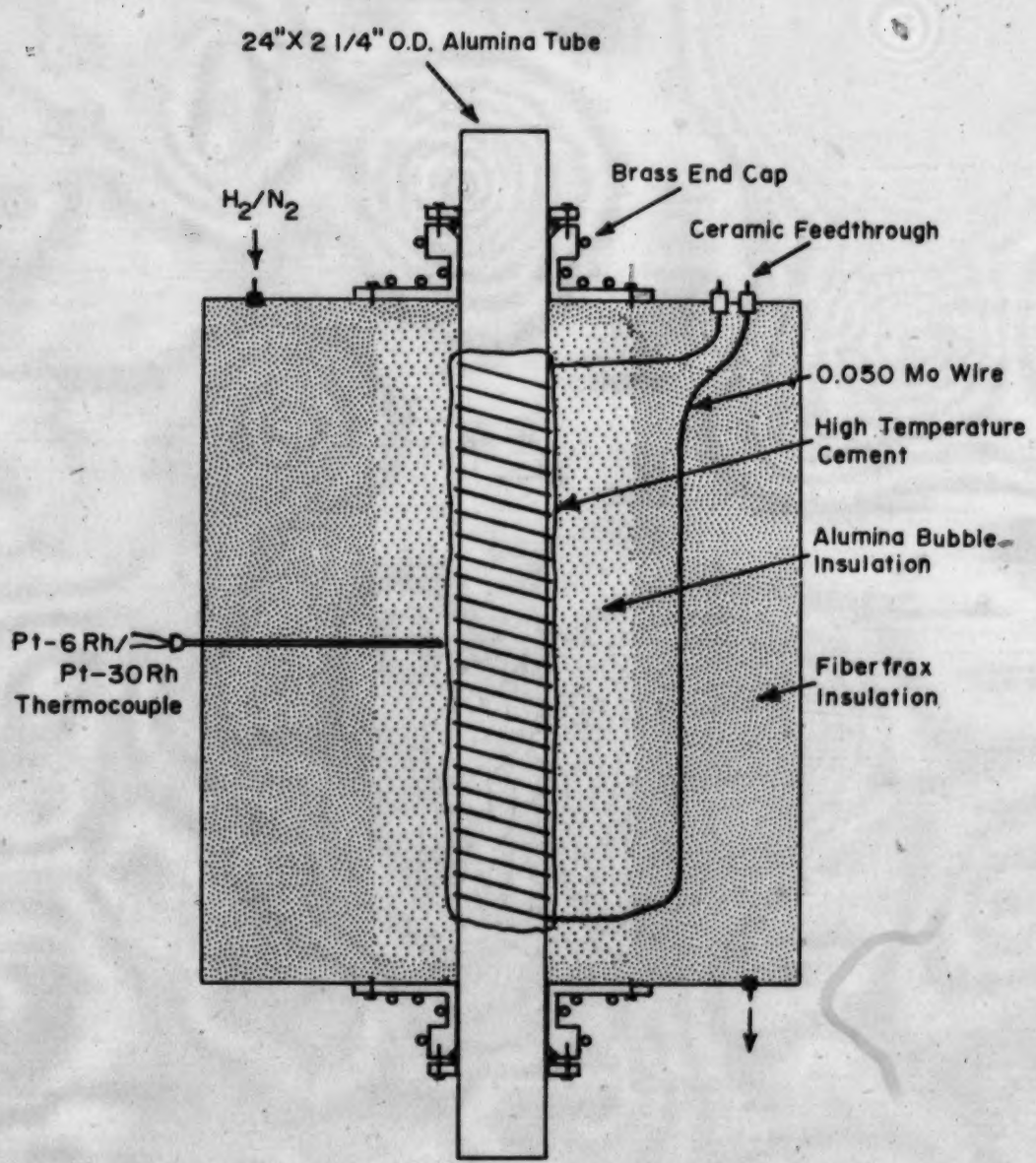

FIGURE 11: FURNACE SCHEMATIC

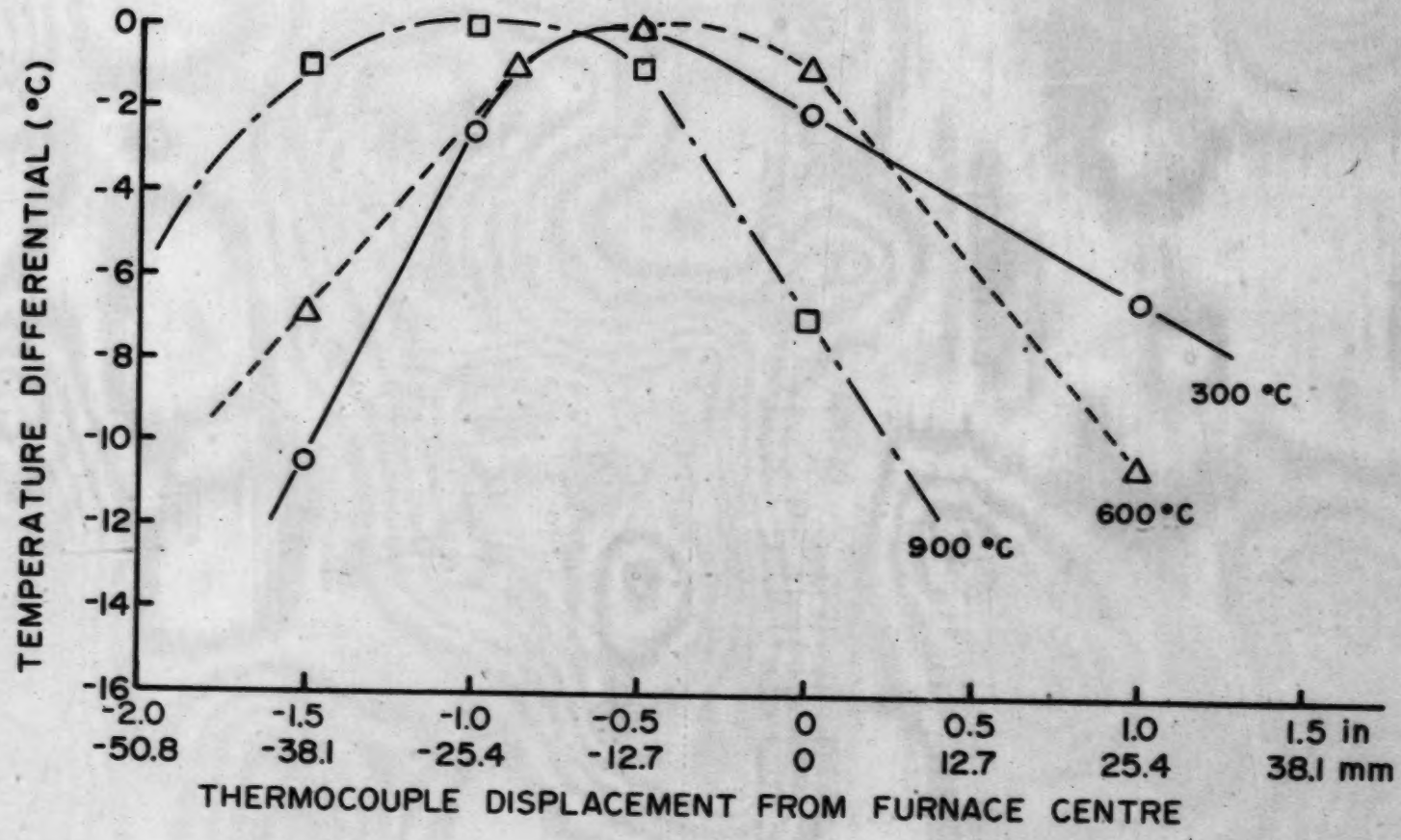

FIGURE 12: FURNACE TEMPERATURE PROFILE (VERTICAL POSITION)

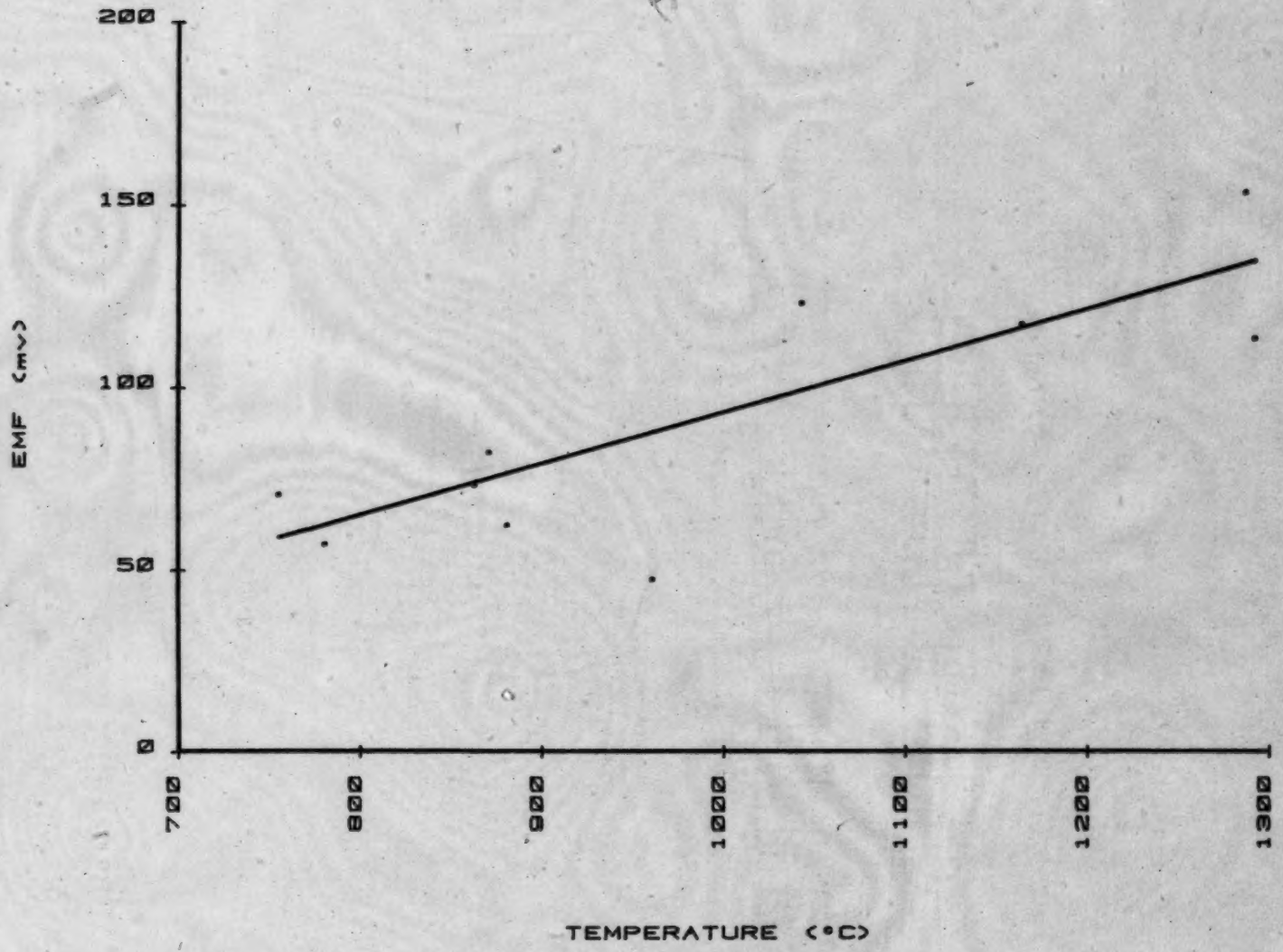

FIGURE 13 : SECOND ARGON FLOW CELL - CHROMIUM SYSTEM

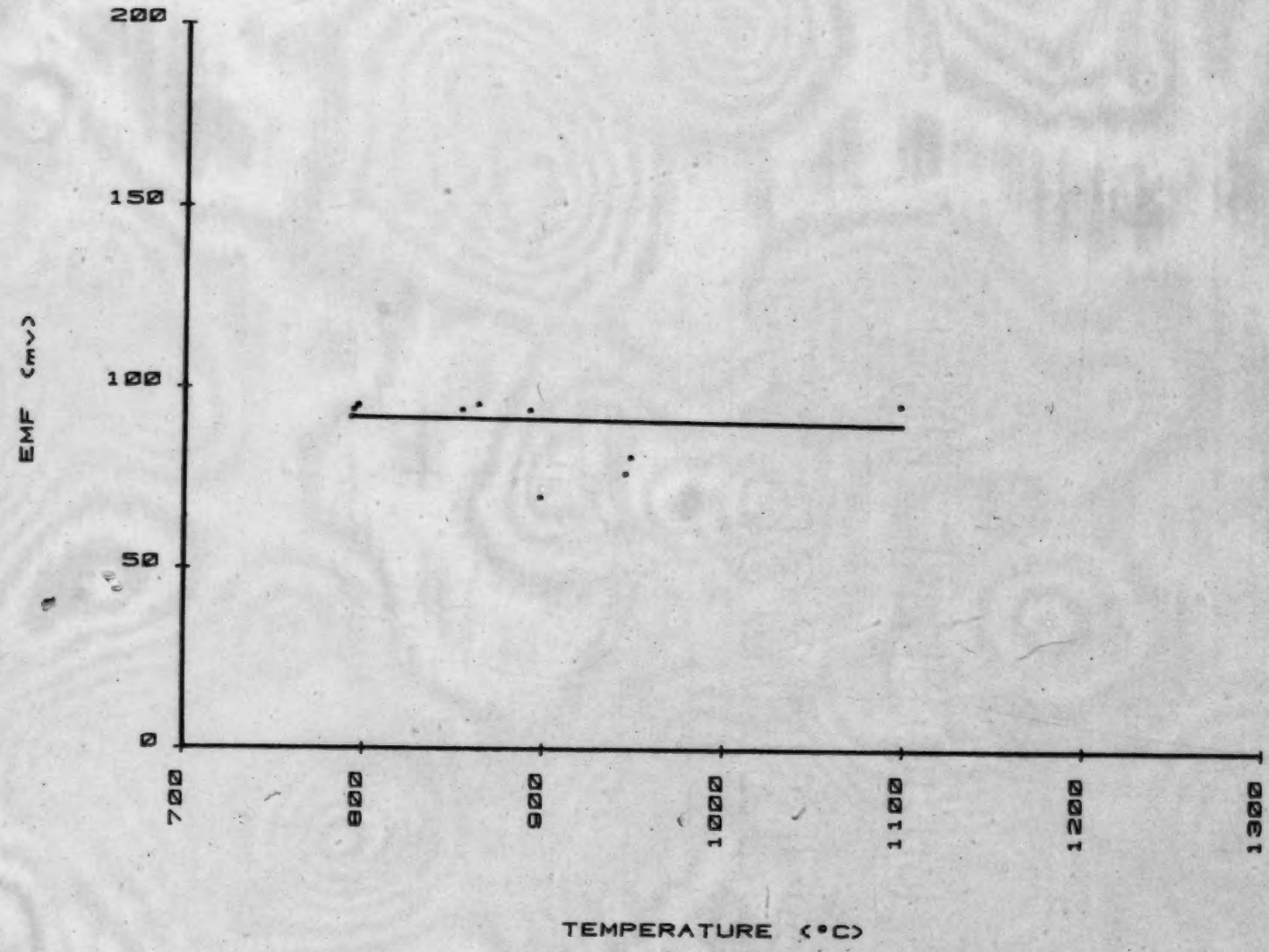

FIGURE 14: EVACUATED QUARTZ CELL - CHROMIUM SYSTEM

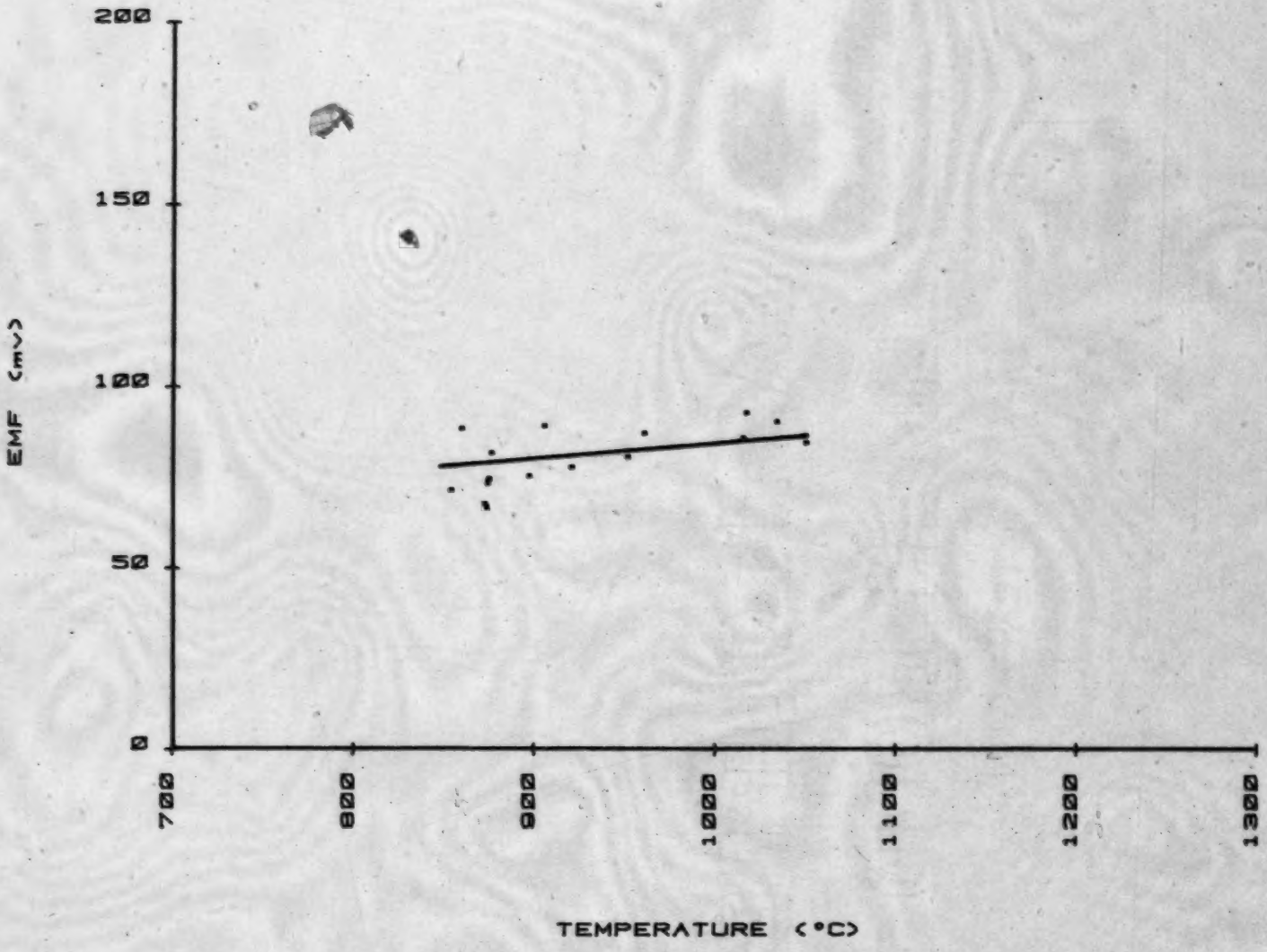

FIGURE 15 : FIRST EVACUATED ALUMINA CELL - CHROMIUM SYSTEM

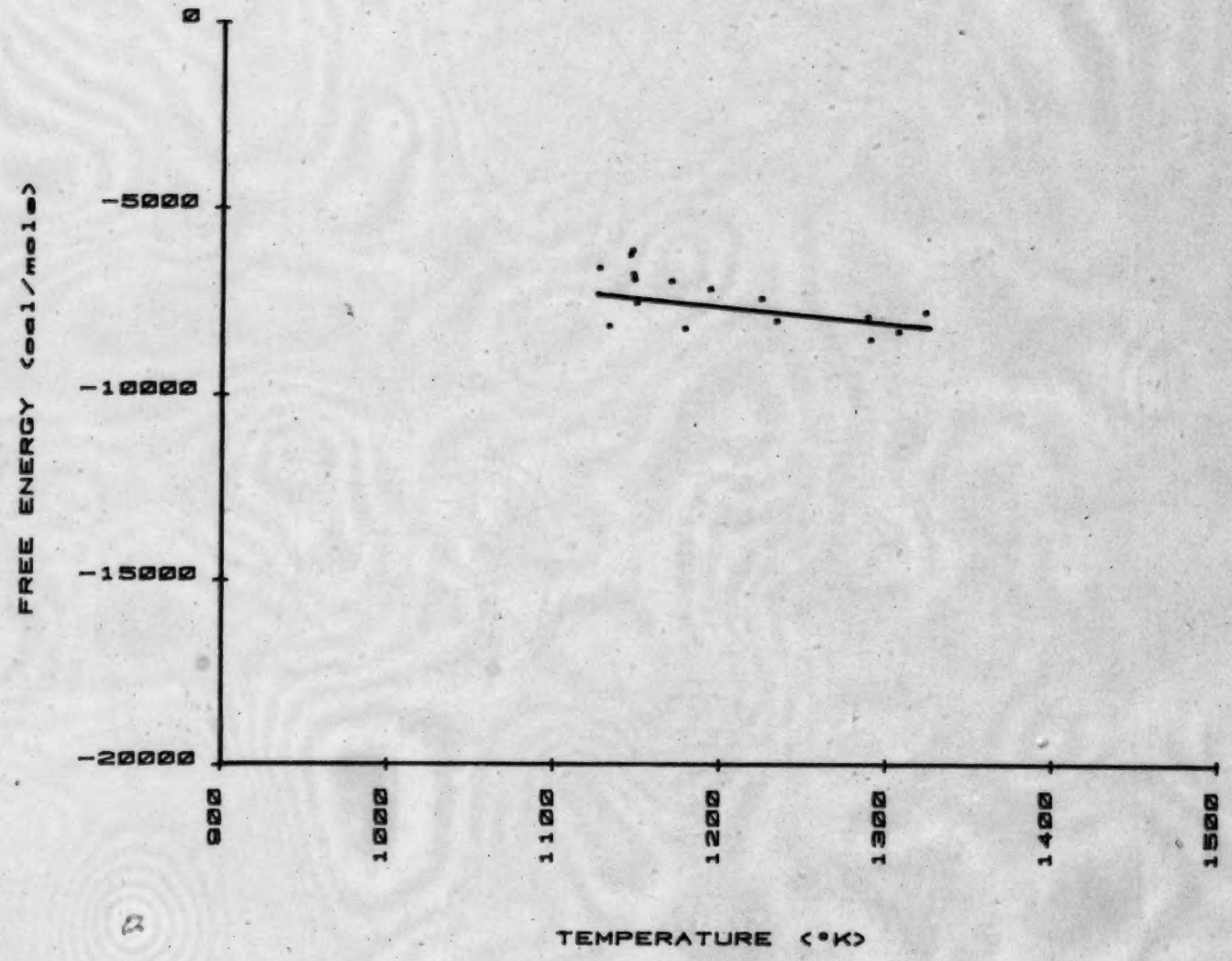

FIGURE 16 : FIRST EVACUATED ALUMINA CELL - CHROMIUM SYSTEM

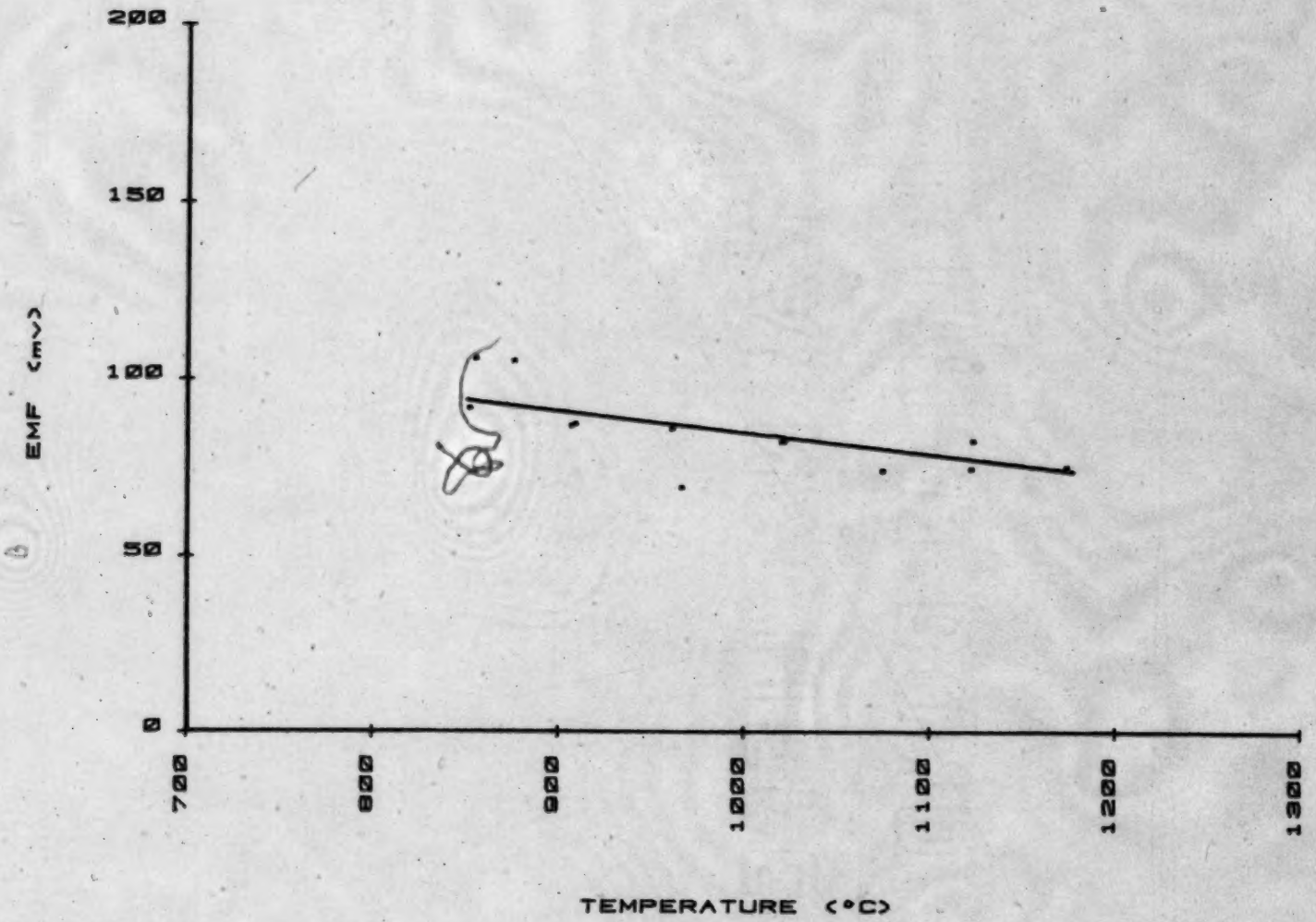

FIGURE 17 : SECOND EVACUATED ALUMINA CELL - CHROMIUM SYSTEM

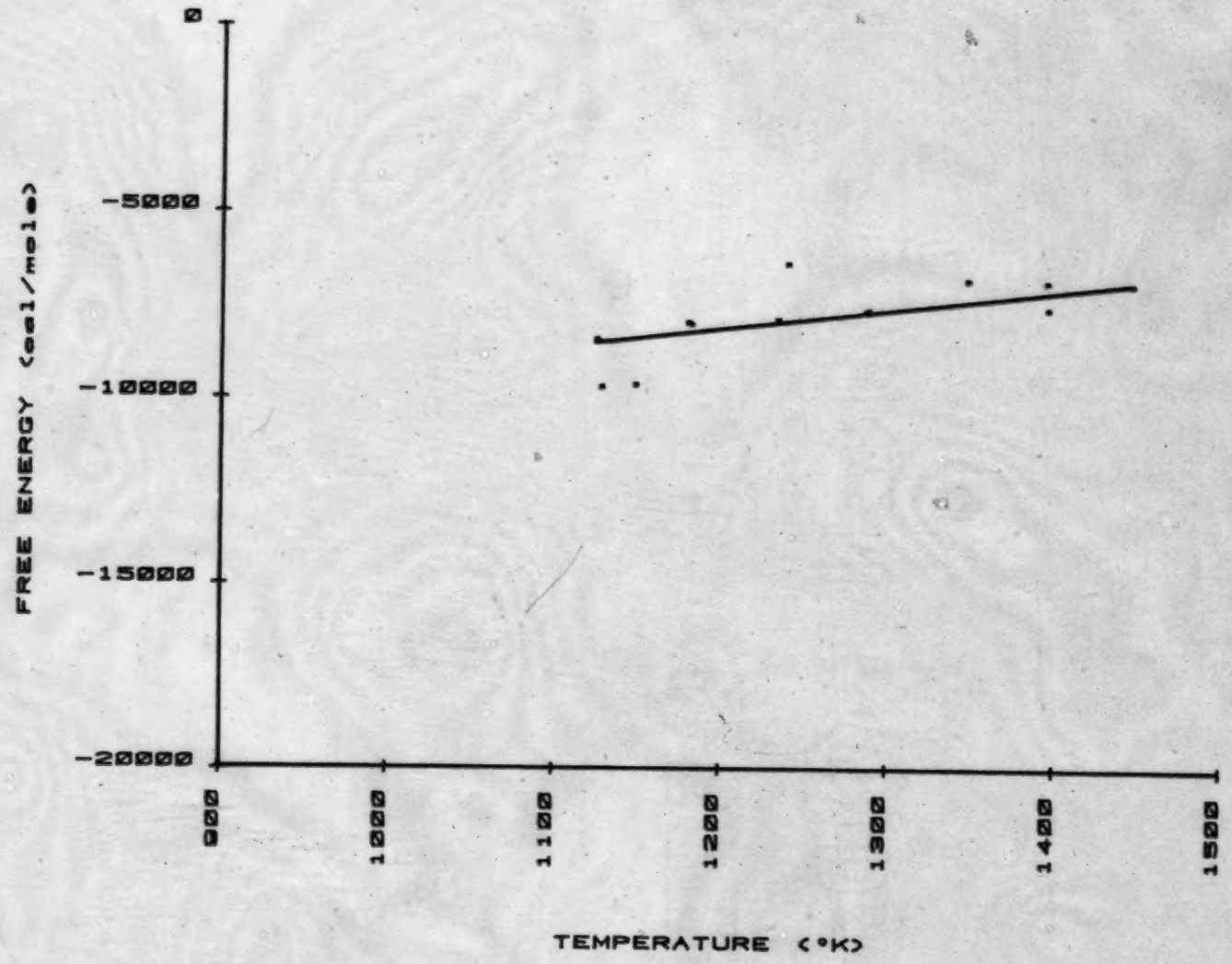

FIGURE 18 : SECOND EVACUATED ALUMINA CELL - CHROMIUM SYSTEM

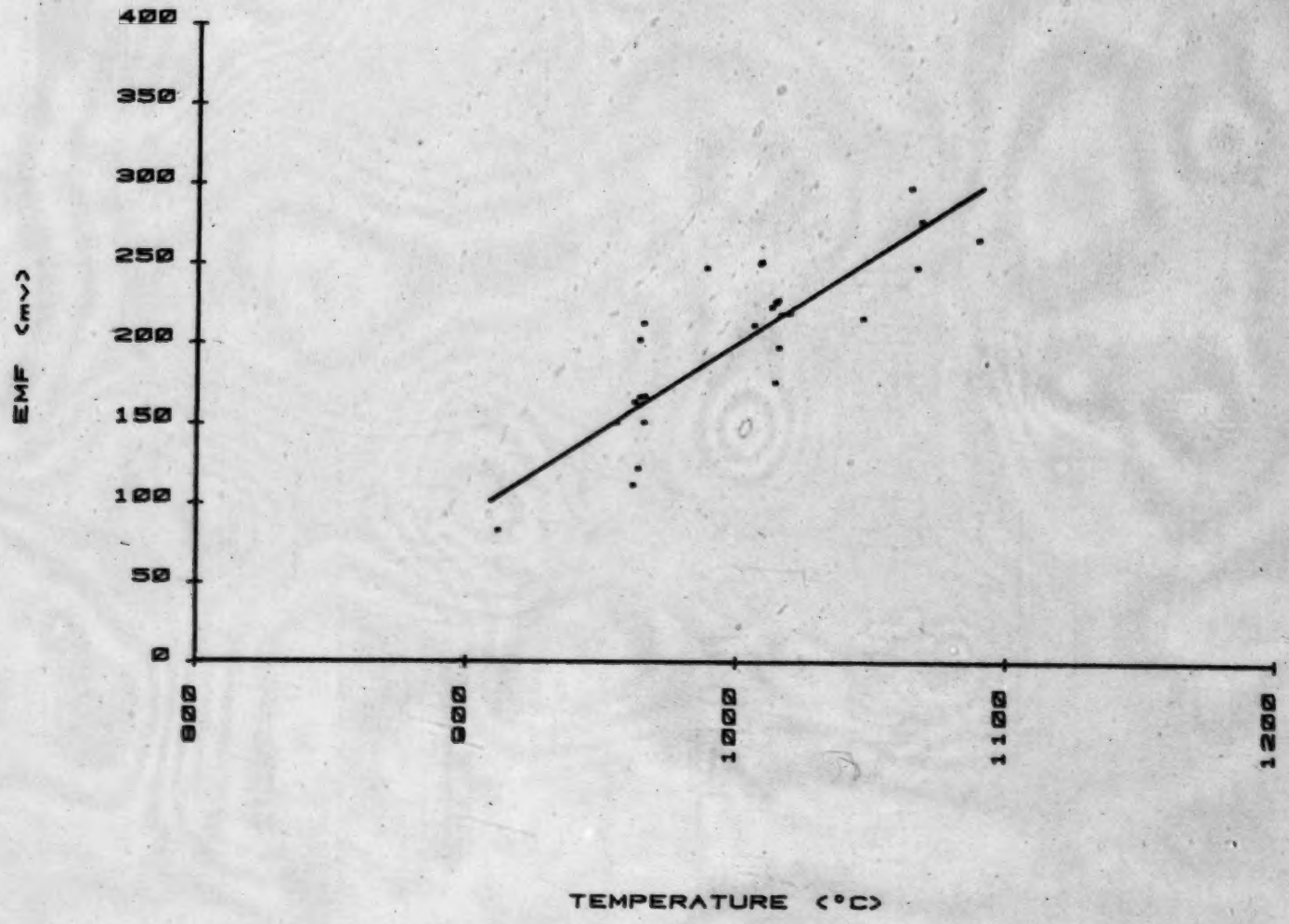

FIGURE 19 : FIRST EVACUATED ALUMINA CELL - MOLYBDENUM SYSTEM

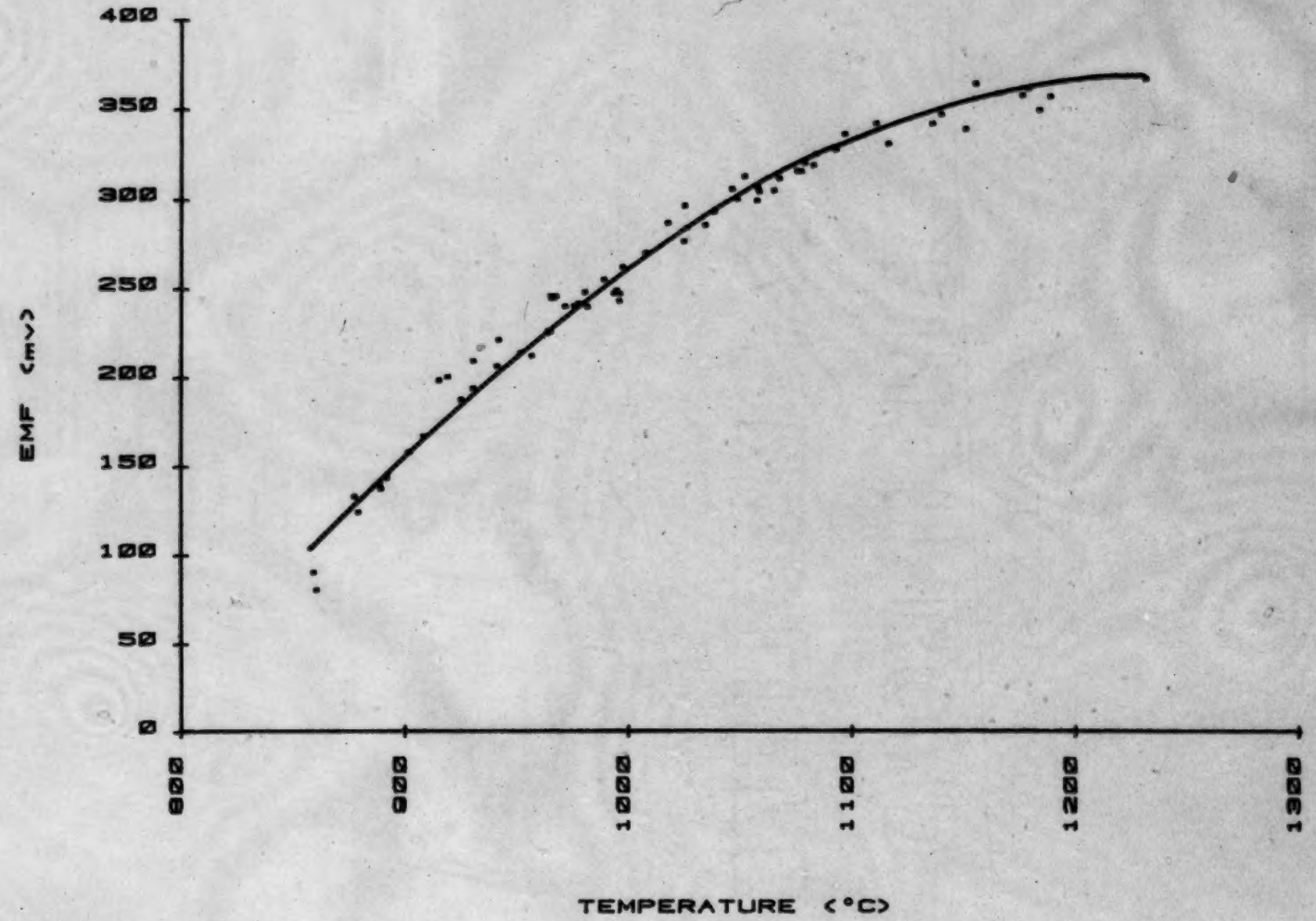

FIGURE 20 : SECOND EVACUATED ALUMINA CELL - MOLYBDENUM SYSTEM

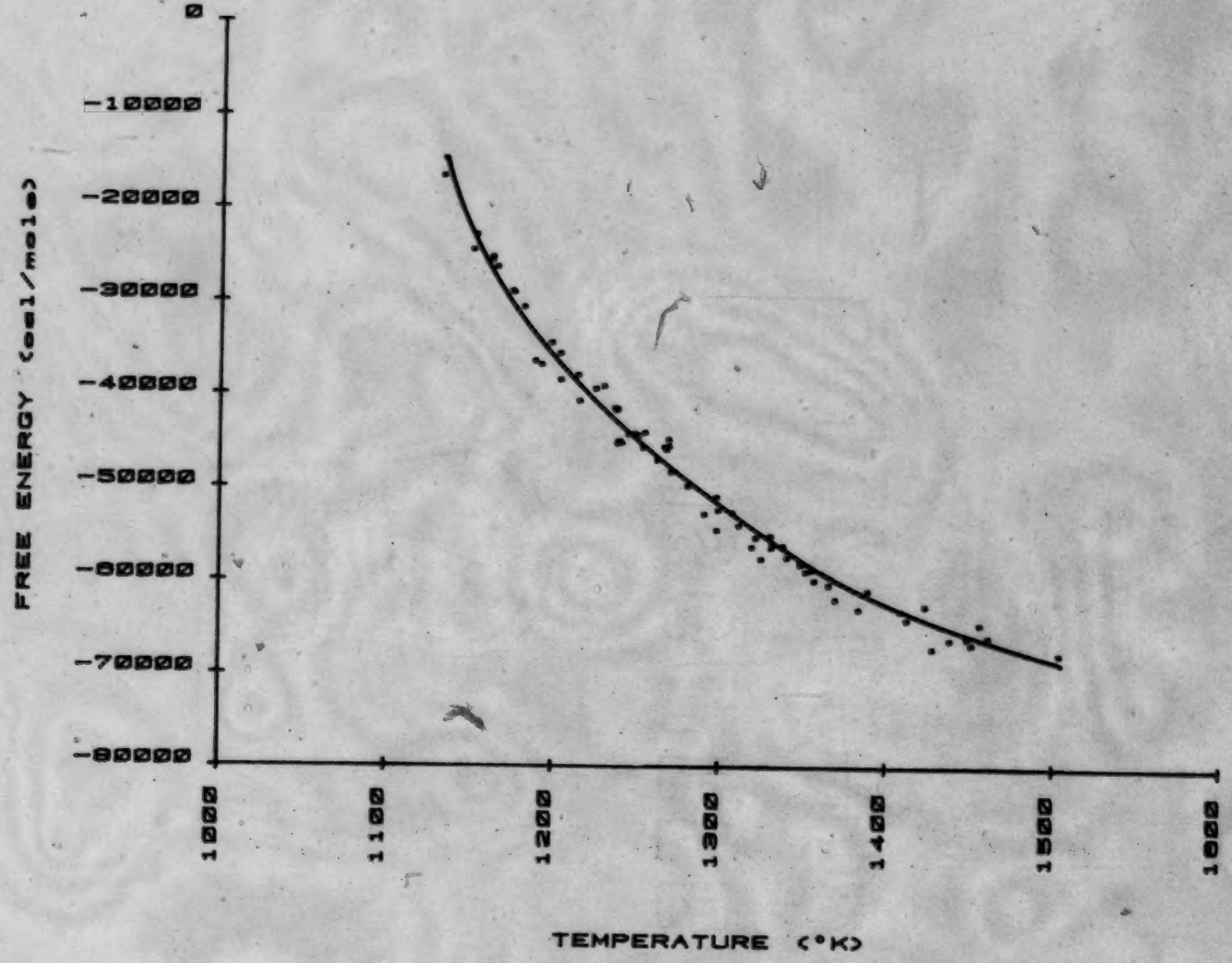

FIGURE 21 : SECOND EVACUATED ALUMINA CELL - MOLYBDENUM SYSTEM

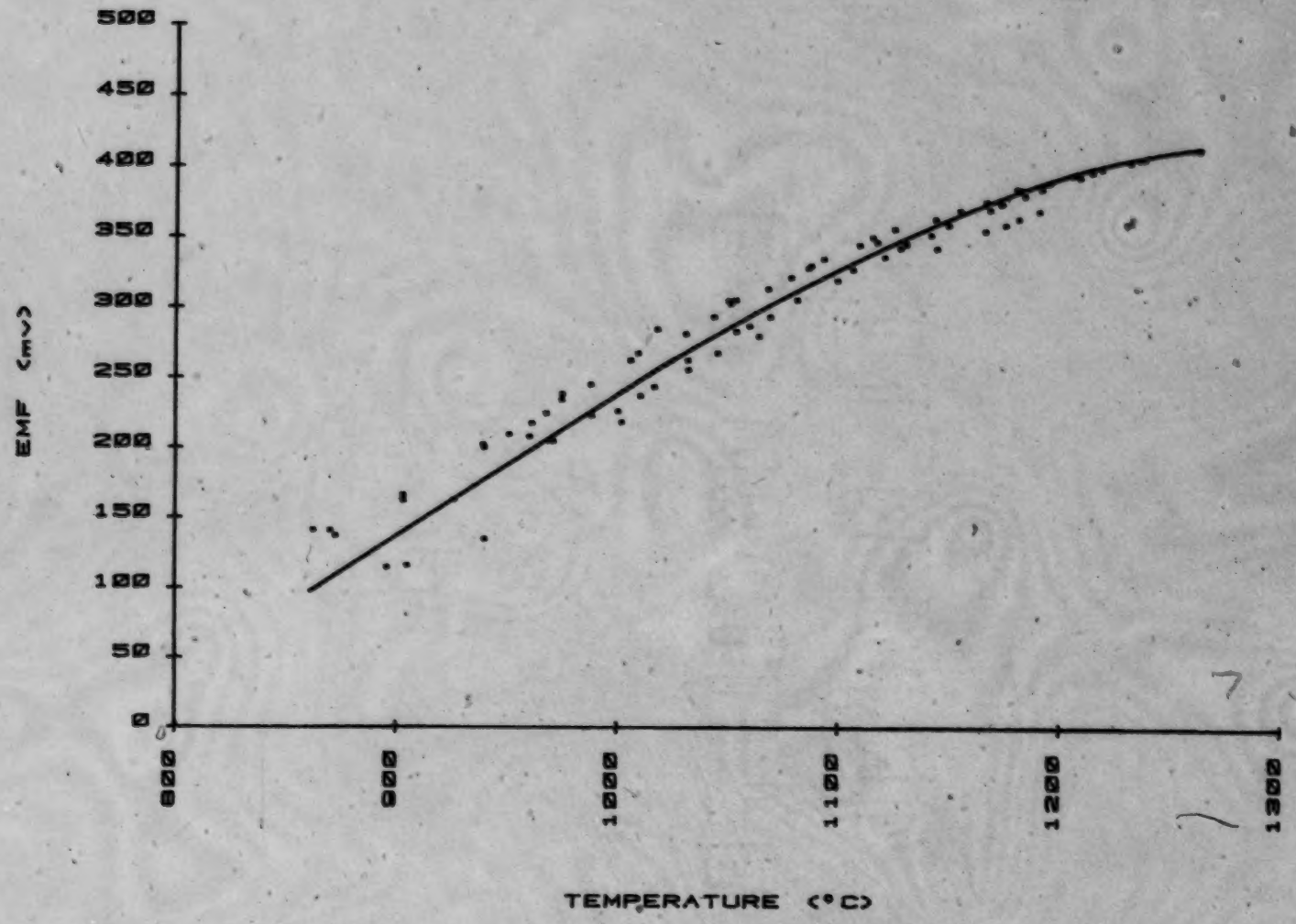

FIGURE 22 : FOURTH EVACUATED ALUMINA CELL - MOLYBDENUM SYSTEM

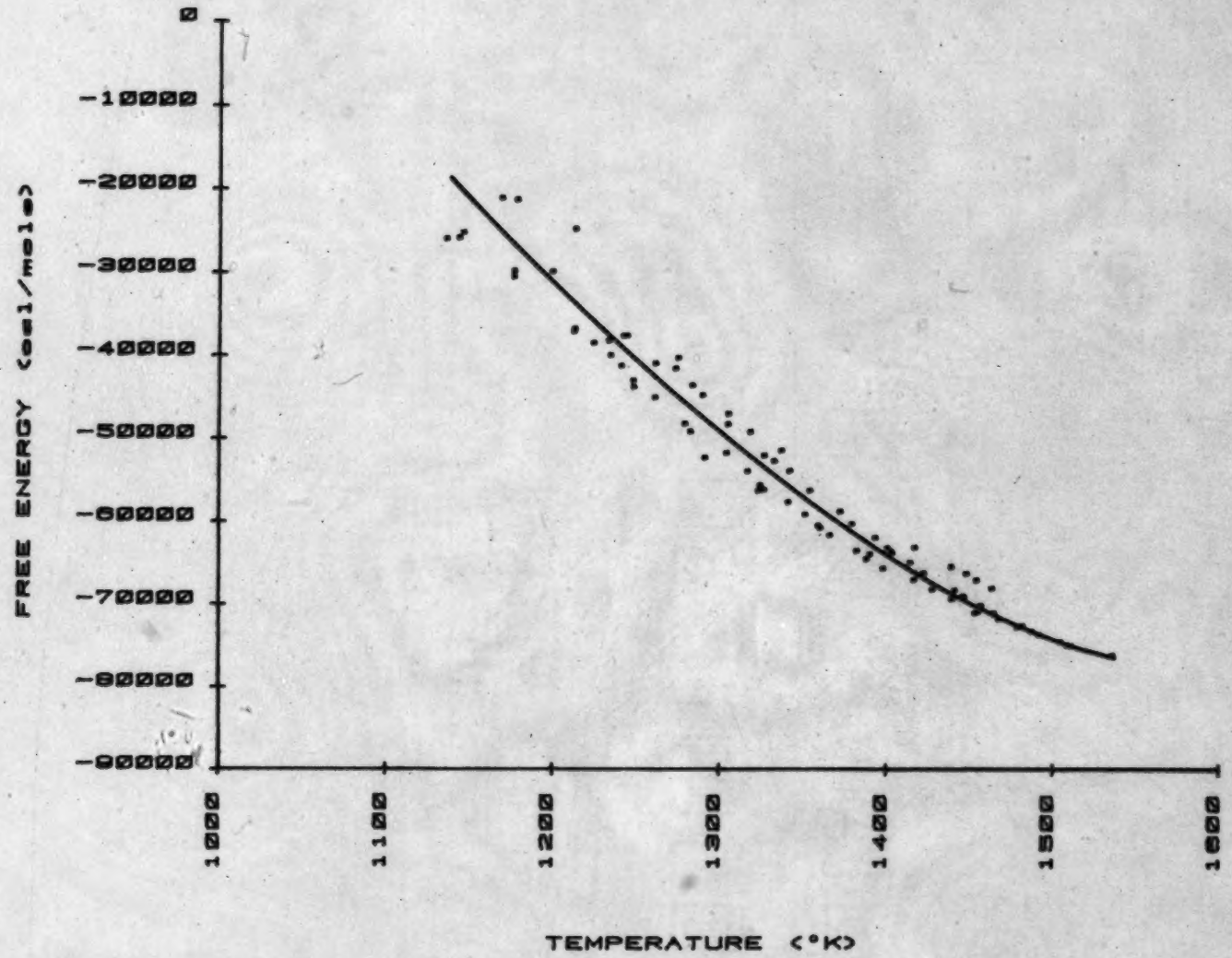

FIGURE 23 : FOURTH EVACUATED ALUMINA CELL - MOLYBDENUM SYSTEM

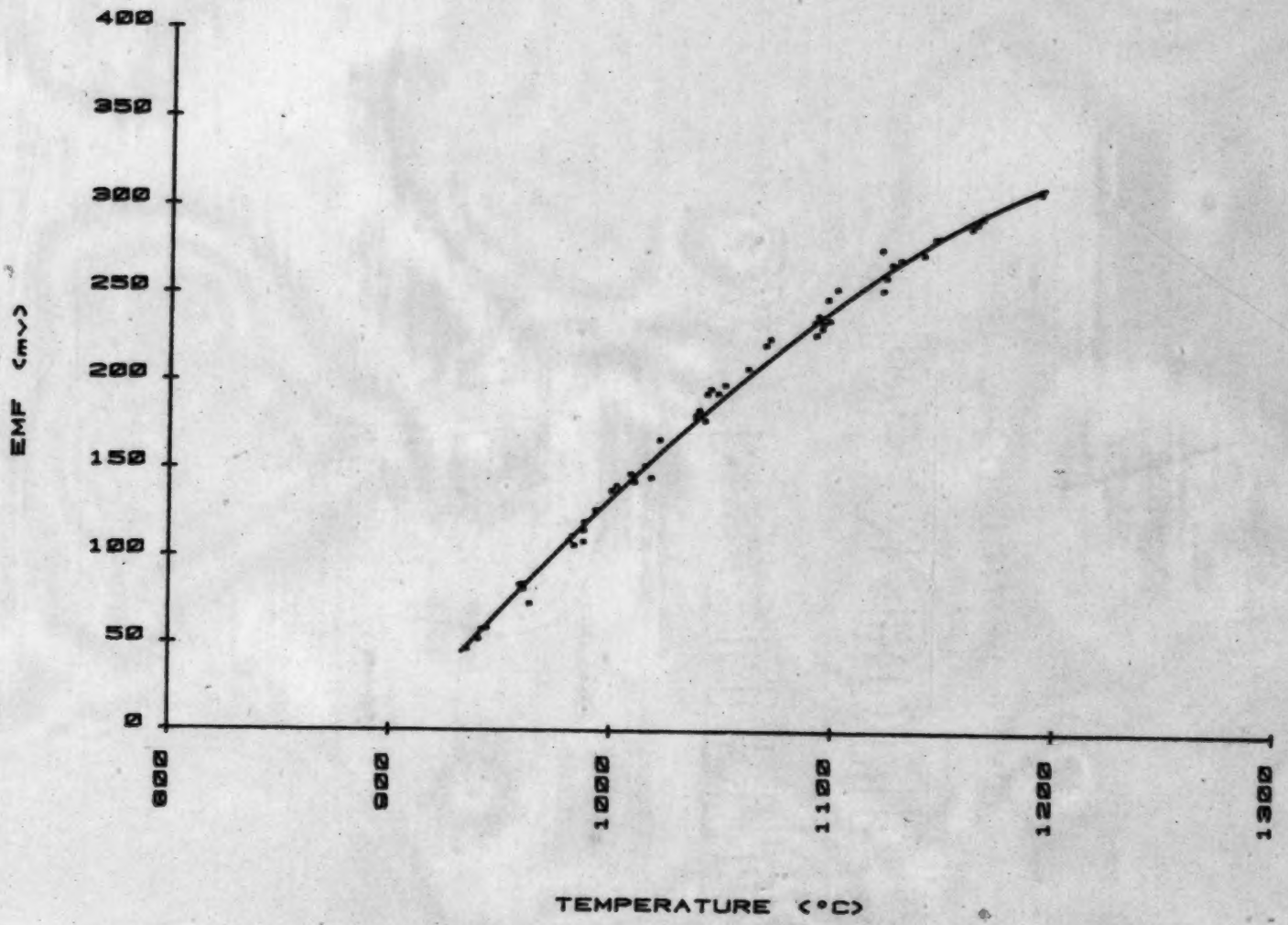

FIGURE 24 : FIRST EVACUATED ALUMINA CELL - TUNGSTEN SYSTEM

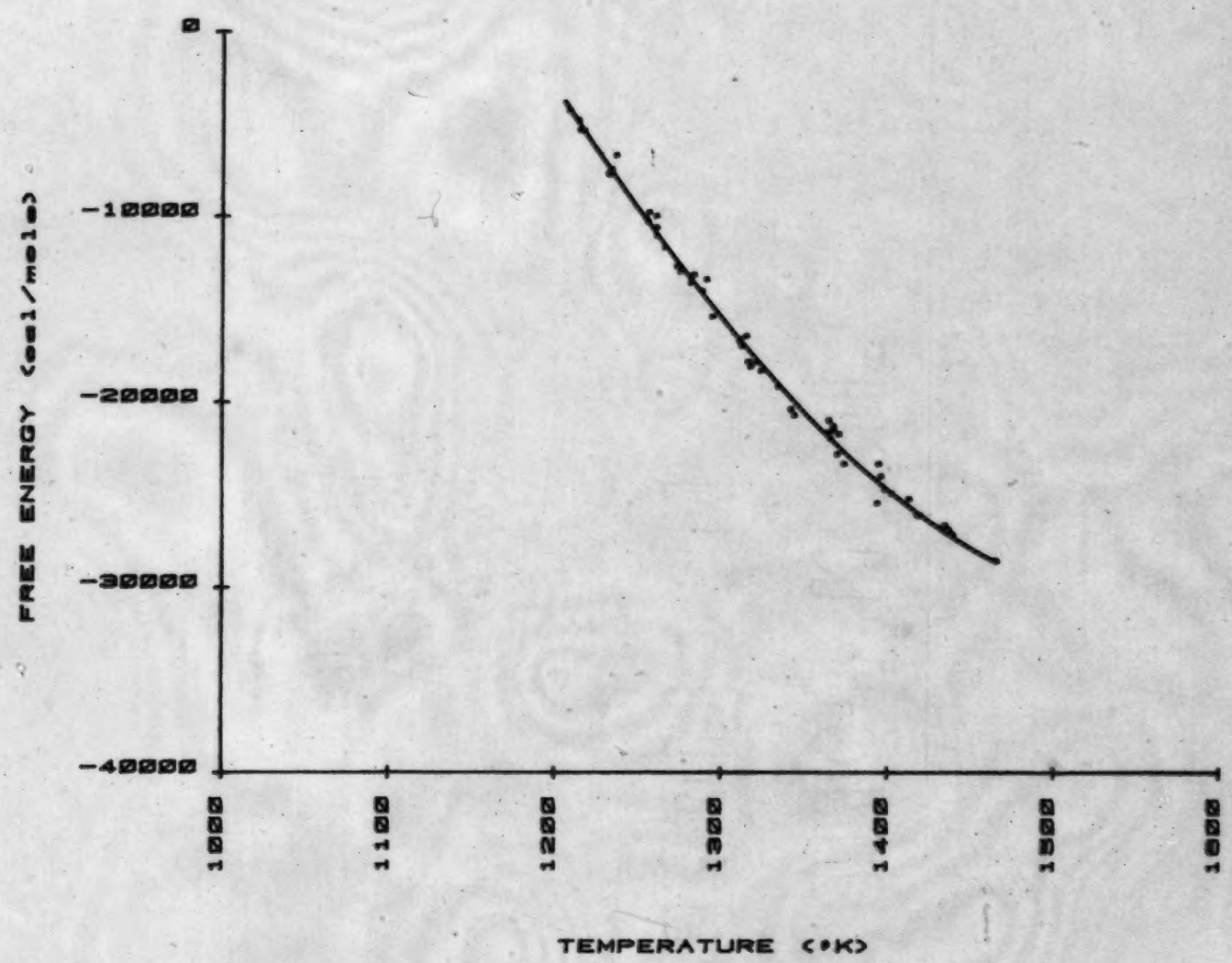

FIGURE 25 : FIRST EVACUATED ALUMINA CELL - TUNGSTEN SYSTEM

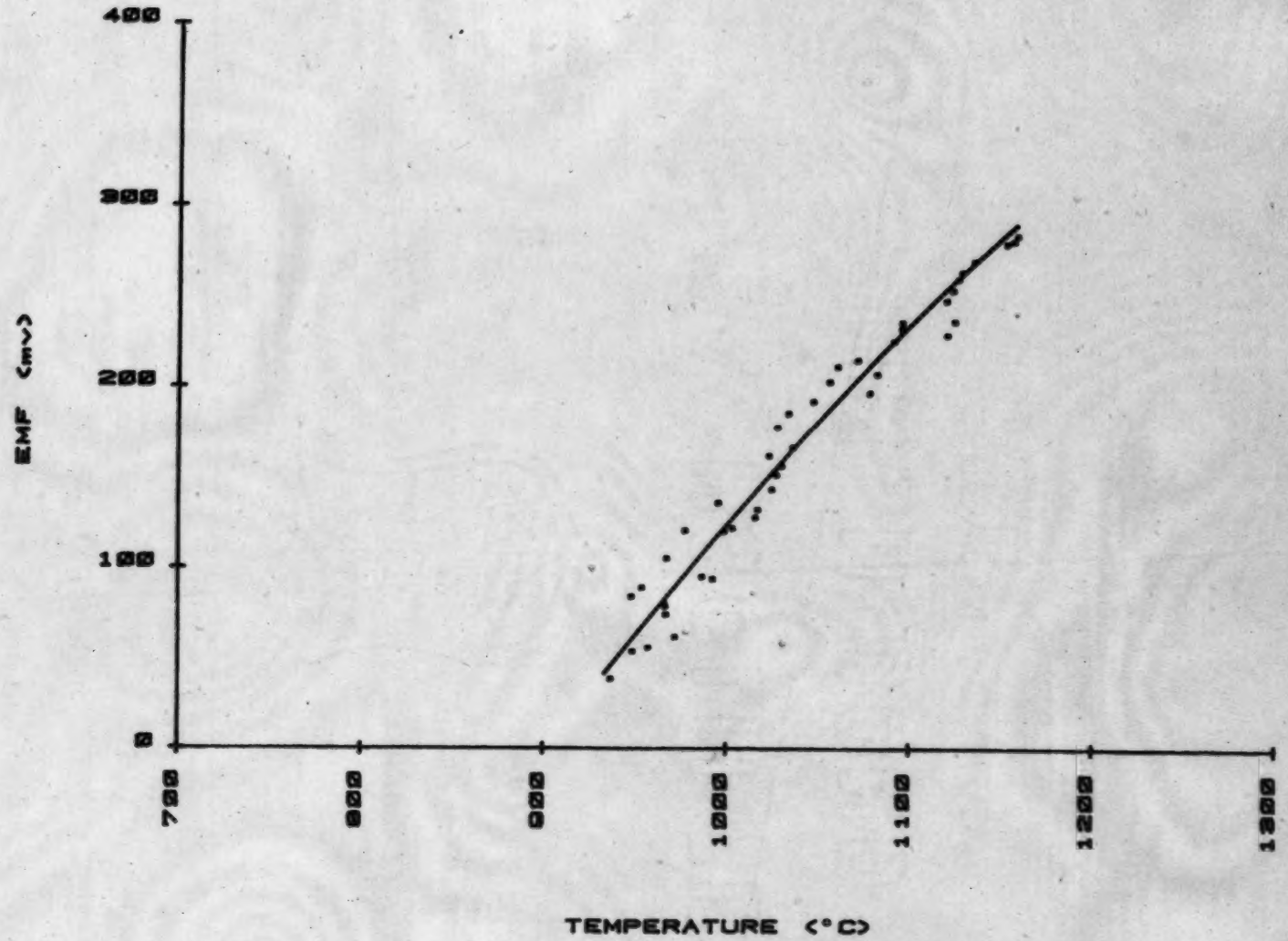

FIGURE 28 : SECOND EVACUATED ALUMINA CELL - TUNGSTEN SYSTEM

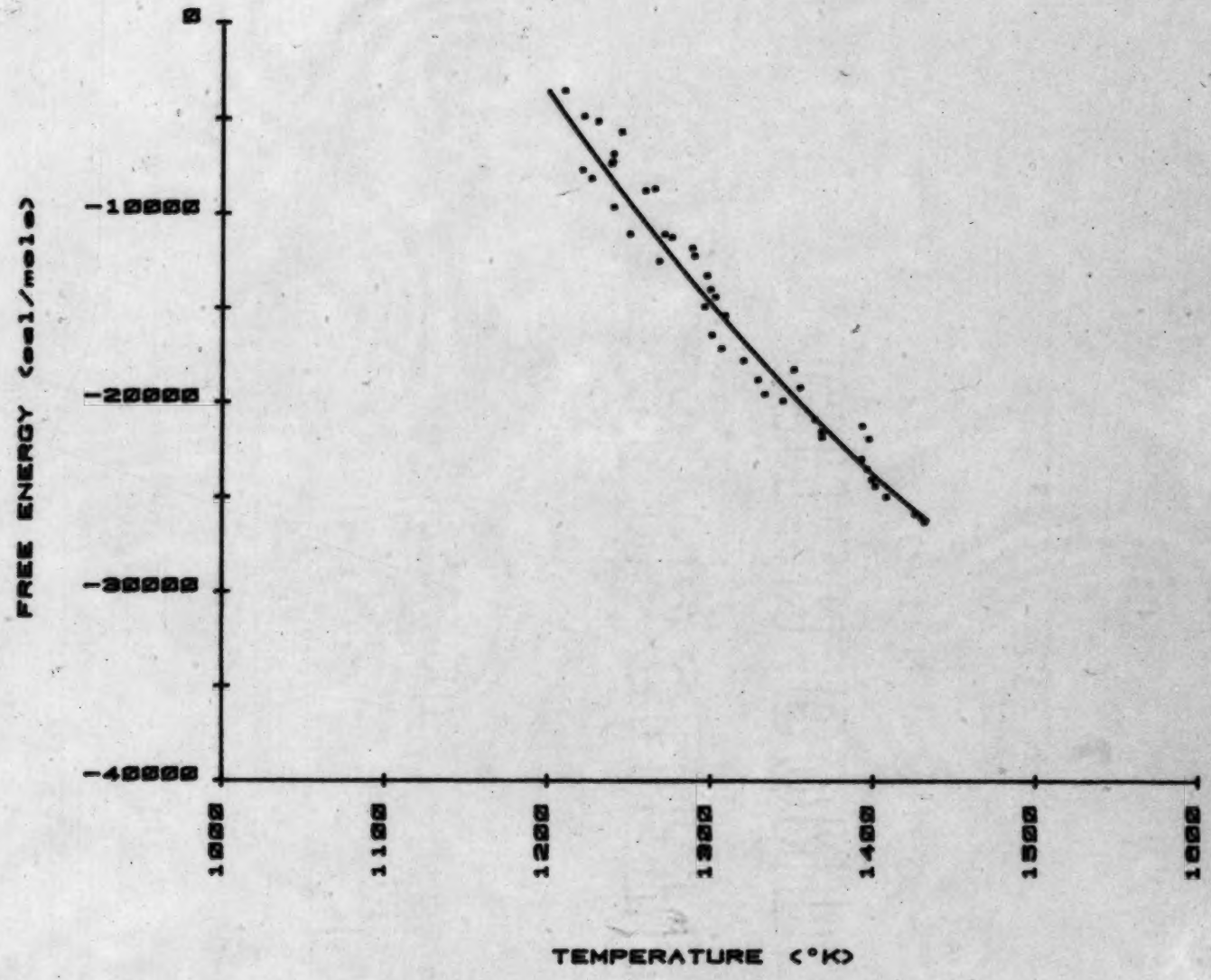

FIGURE 27 : SECOND EVACUATED ALUMINA CELL - TUNGSTEN SYSTEM

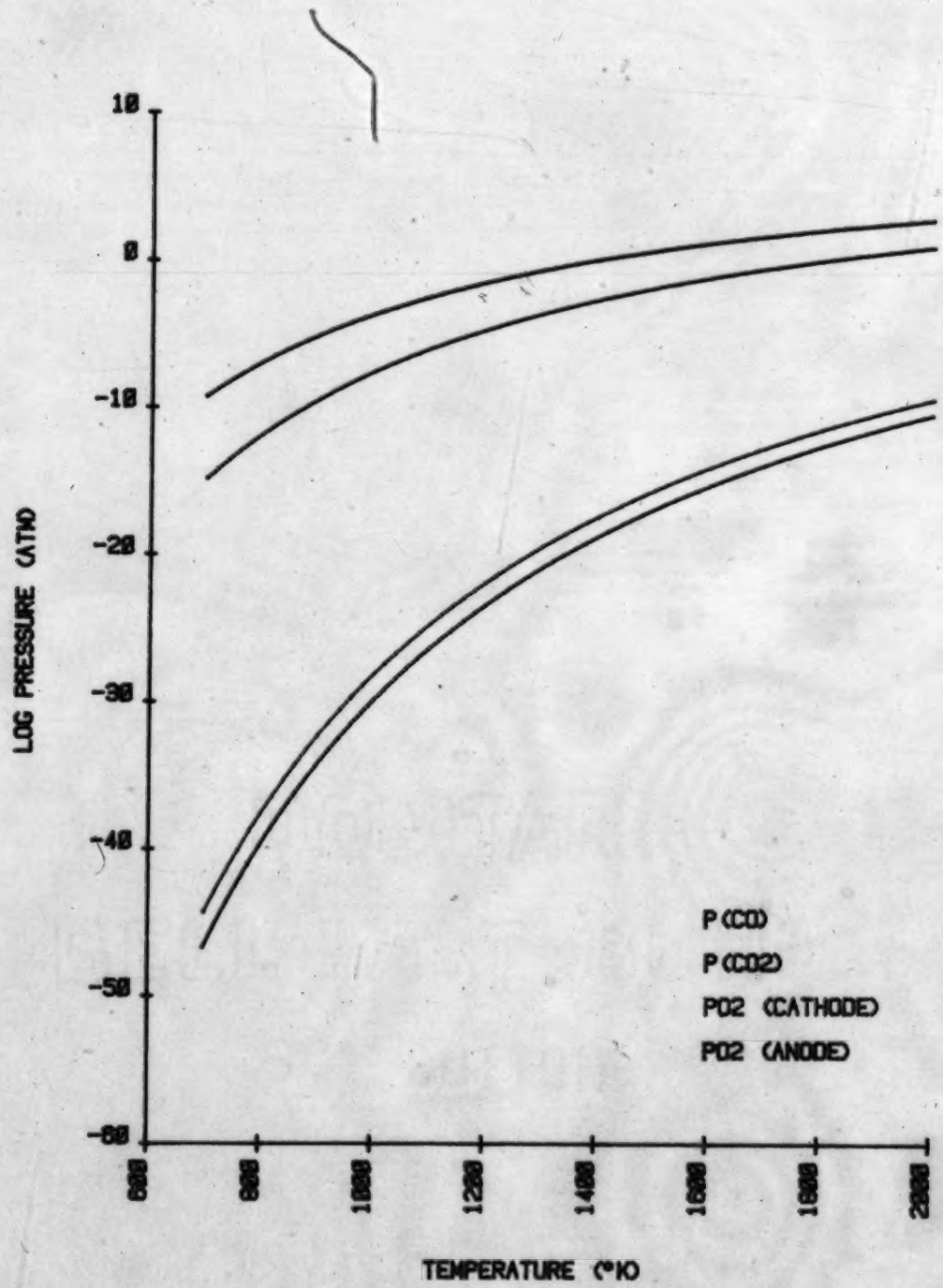

FIGURE 28: THEORETICAL PARTIAL PRESSURES - CHROMIUM SYSTEM

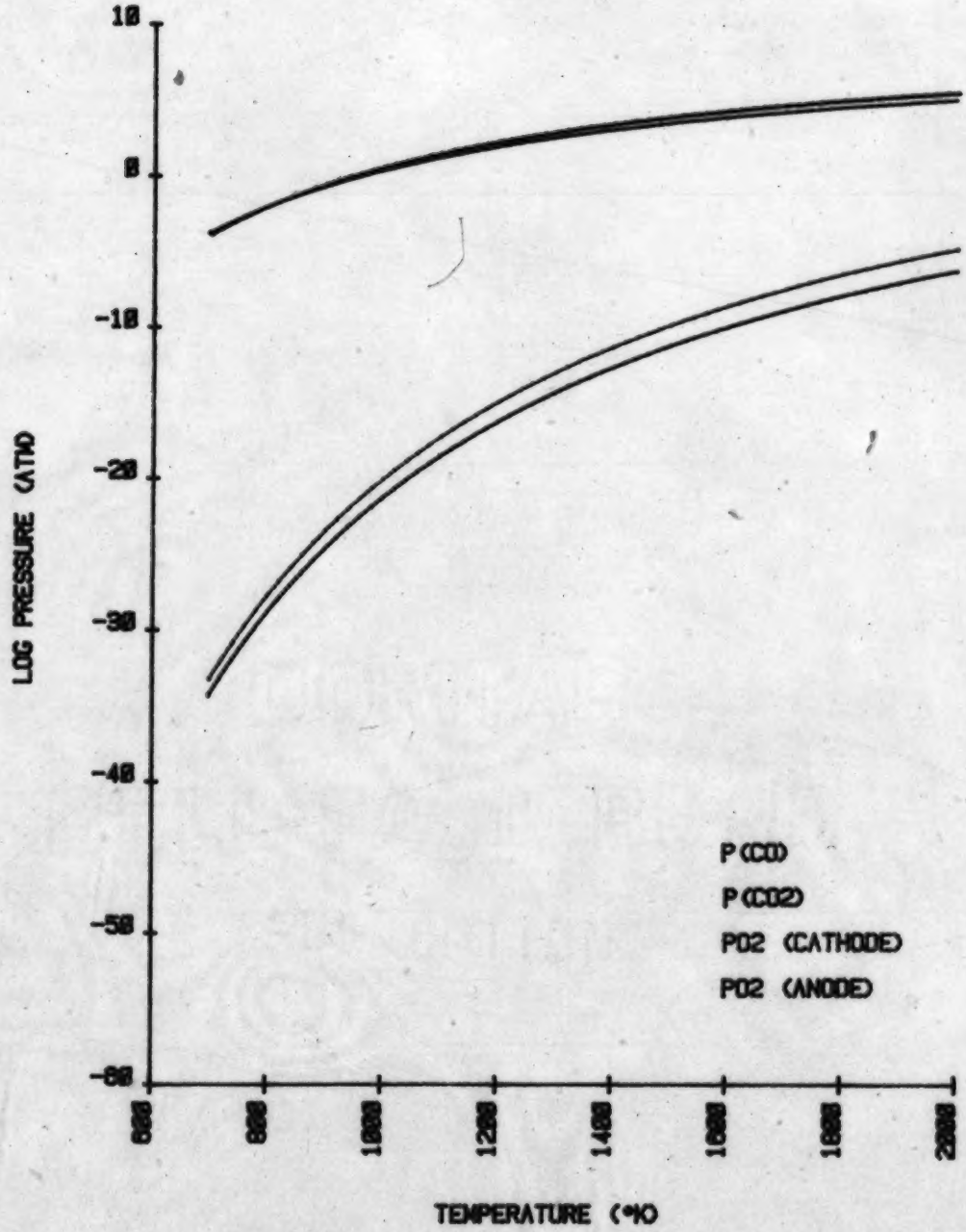

FIGURE 29. THEORETICAL PARTIAL PRESSURES - MOLYBDENUM SYSTEM

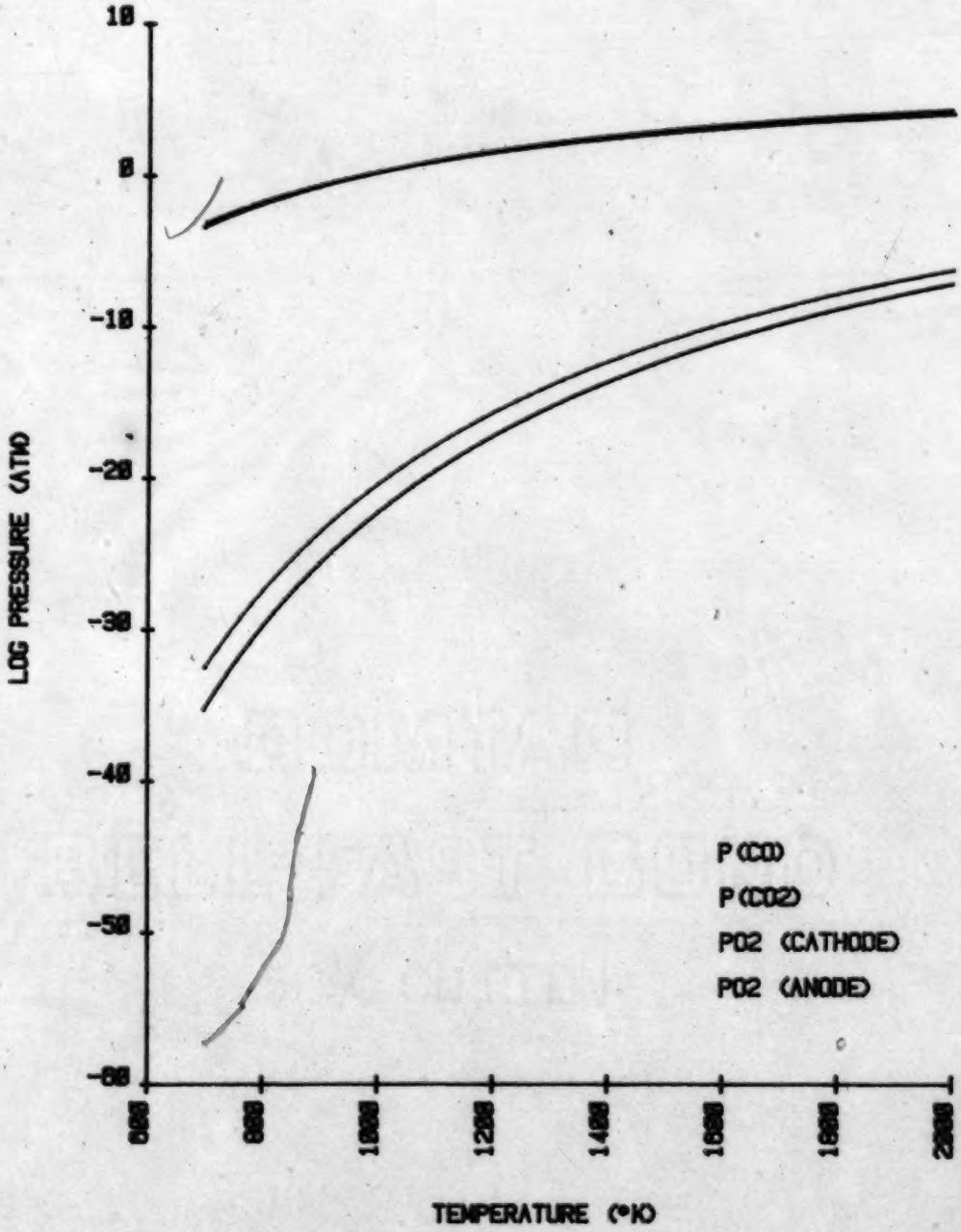

FIGURE 30. THEORETICAL PARTIAL PRESSURES - TUNGSTEN SYSTEM

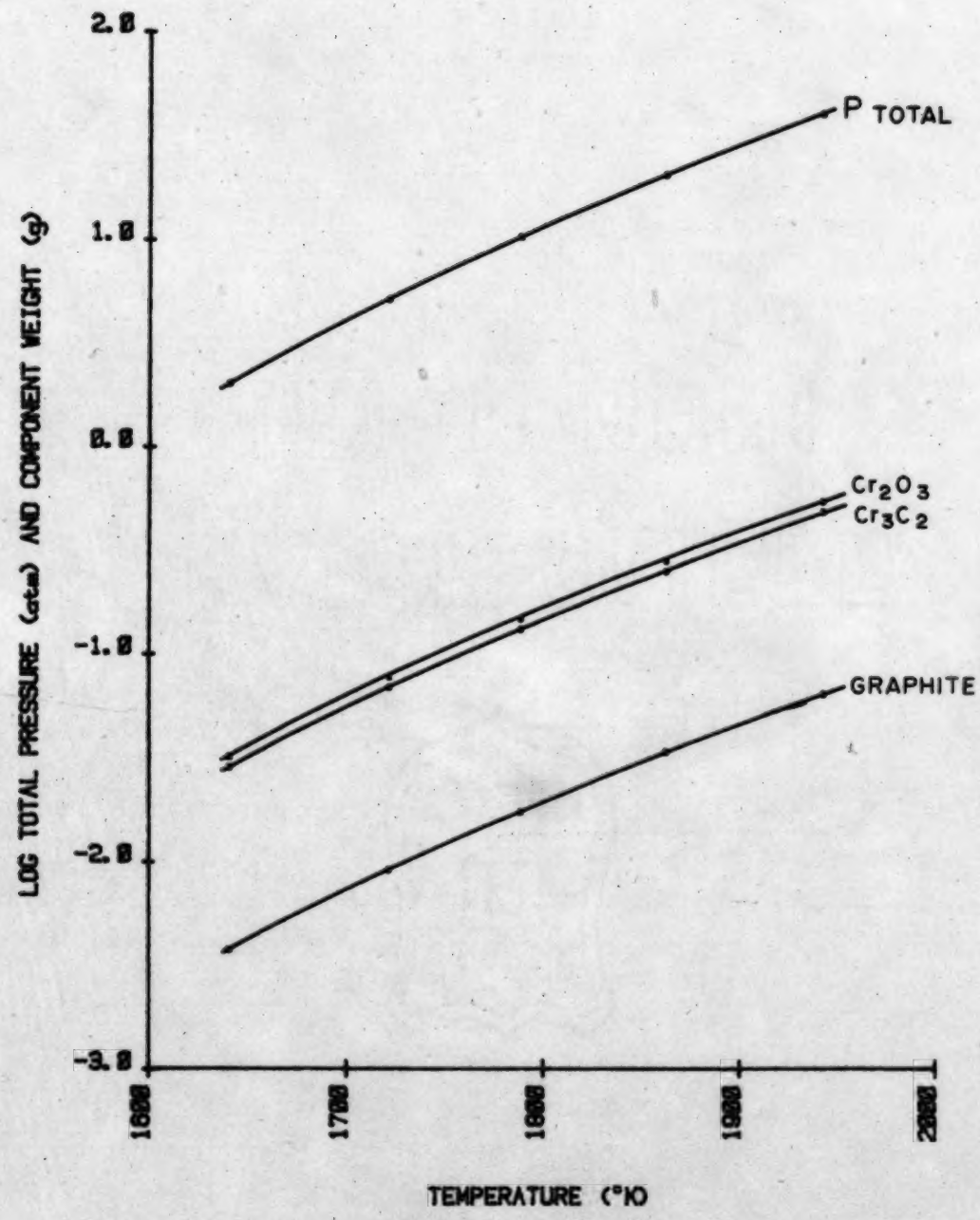

FIGURE 31: CATHODE COMPARTMENT - CHROMIUM SYSTEM
THEORETICAL TOTAL PRESSURE AND COMPONENT WEIGHT

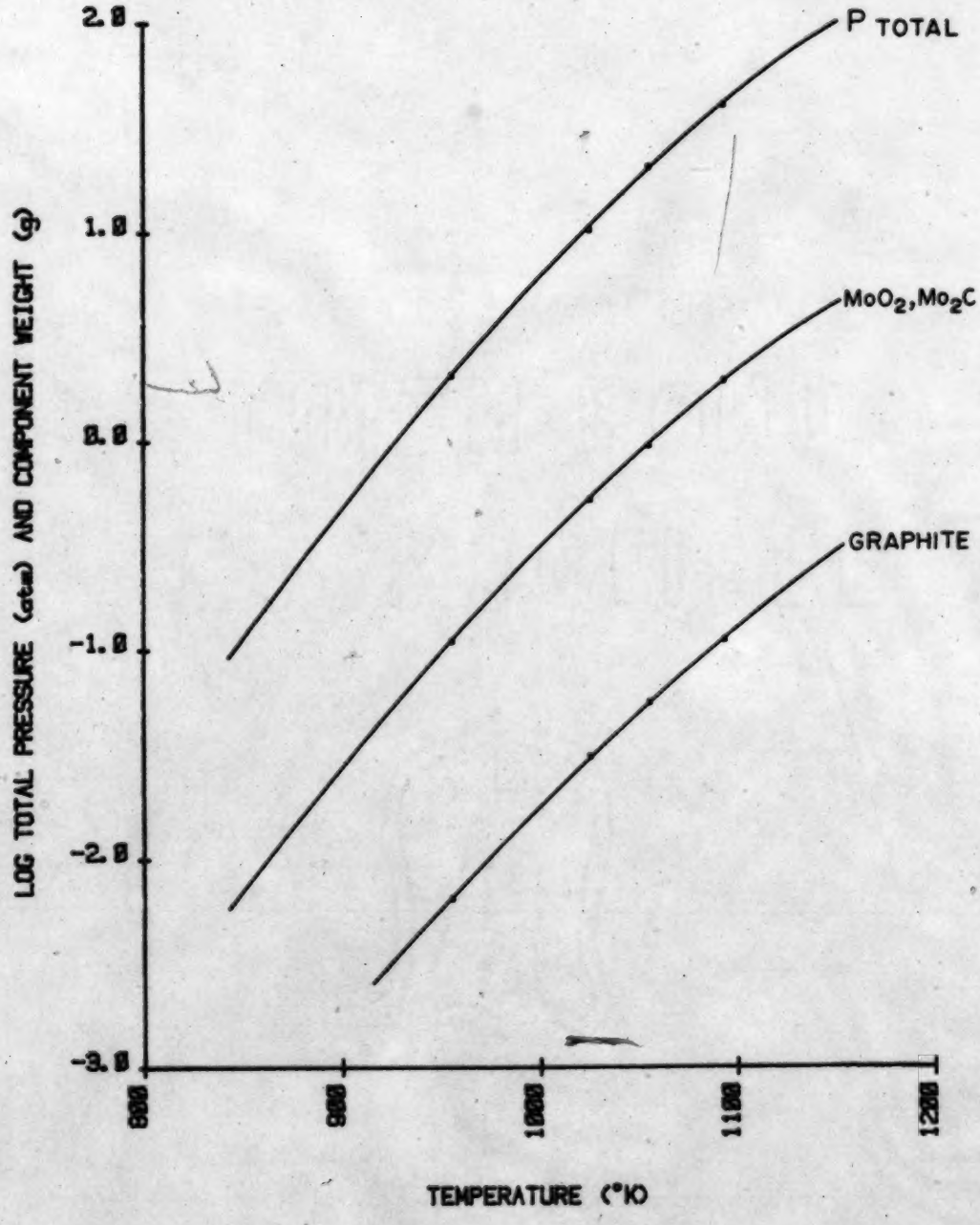

FIGURE 32: CATHODE COMPARTMENT - MOLYBDENUM SYSTEM
THEORETICAL TOTAL PRESSURE AND COMPONENT WEIGHT

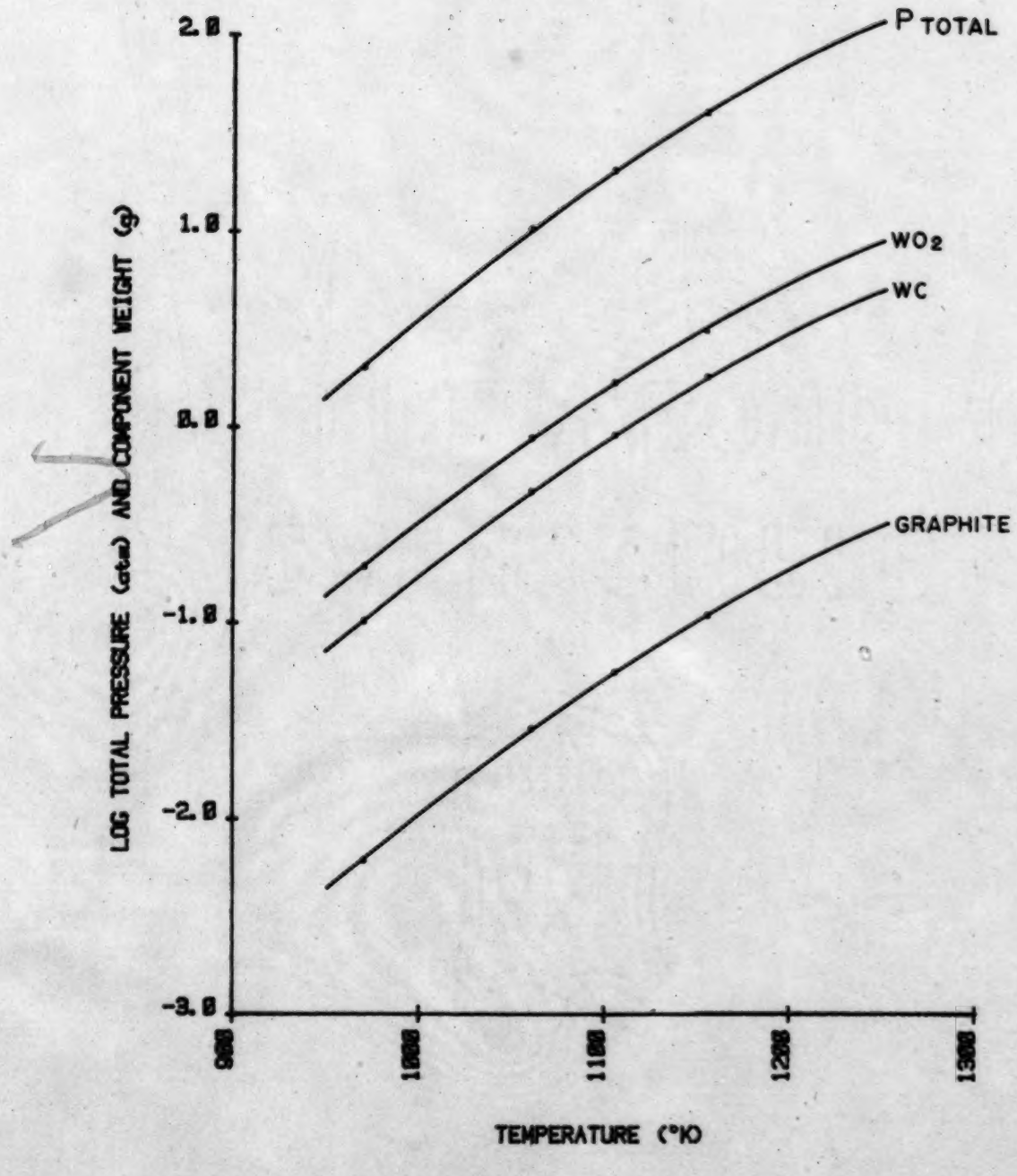

FIGURE 33: CATHODE COMPARTMENT - TUNGSTEN SYSTEM
THEORETICAL TOTAL PRESSURE AND COMPONENT WEIGHT

PHOTOGRAPHS

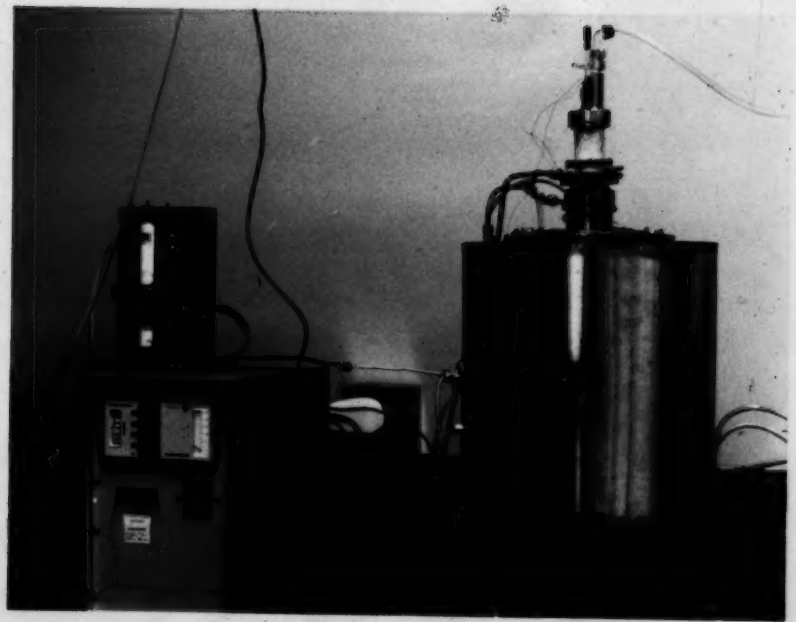

Photograph 1: Molybdenum resistance furnace and controller.

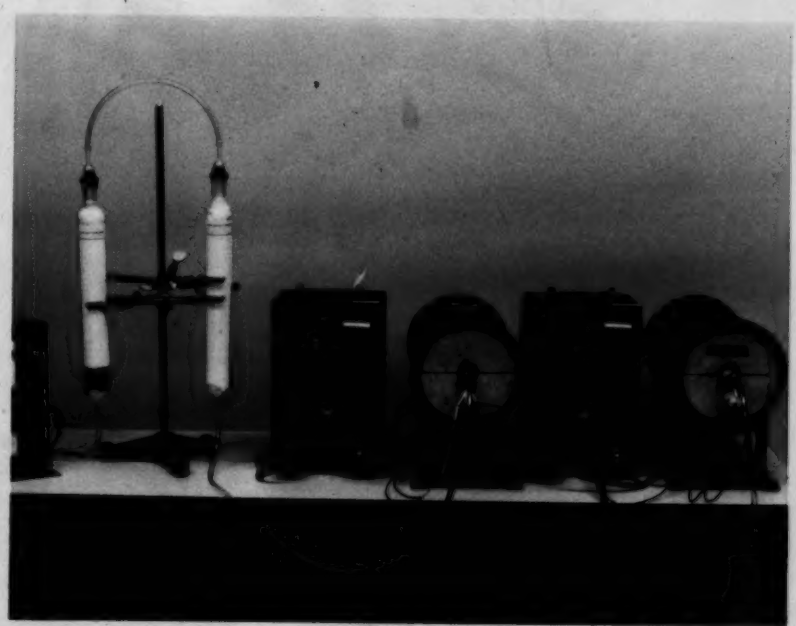

Photograph 2: Argon purification train.

Photograph 3: Argon flow cell.

Photograph 4: Argon flow cell (assembled).

Photograph 5: Evacuated cell - close-up of cell top.

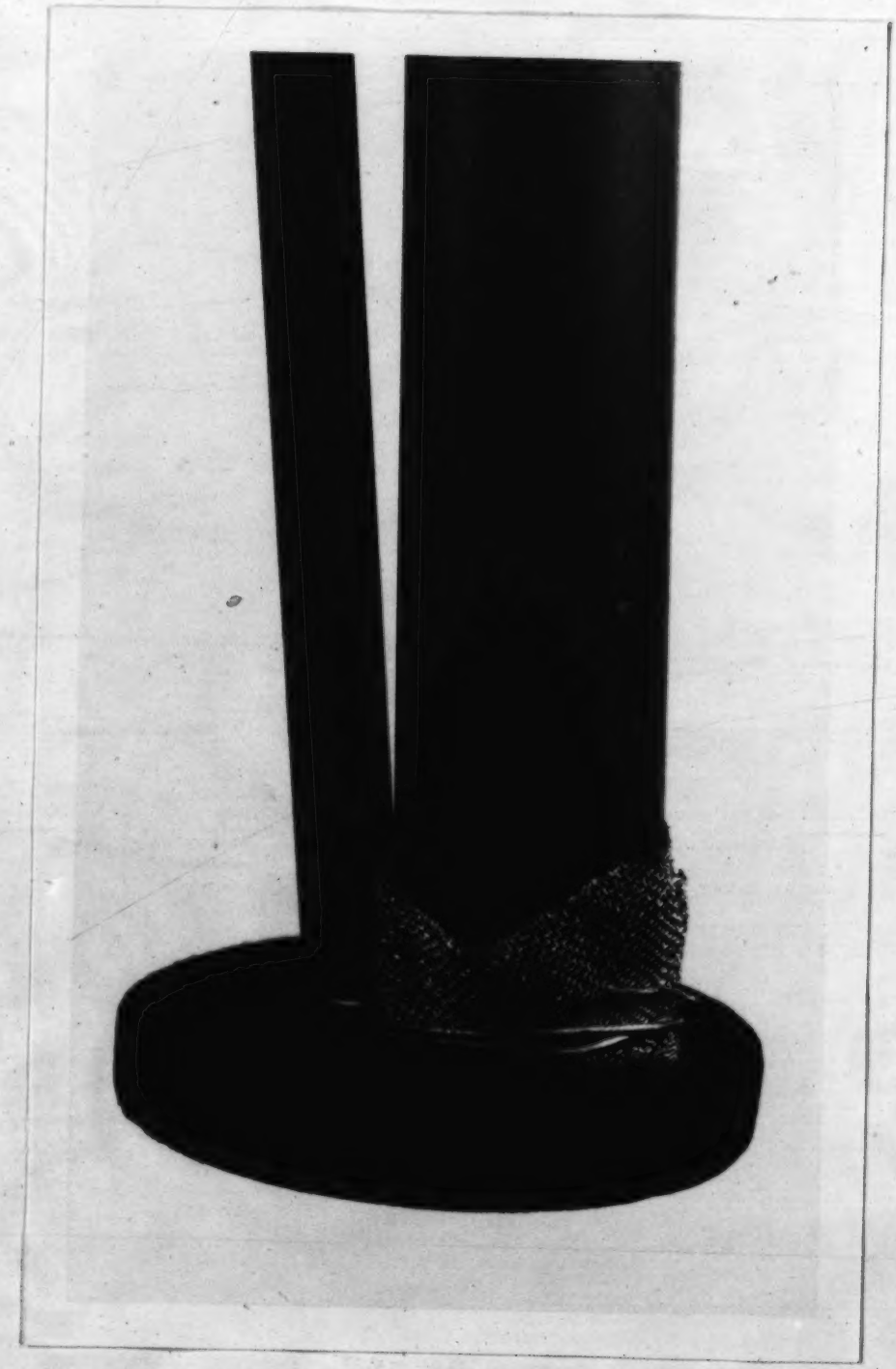

Photograph 6: Anode compartment of evacuated chromium cell.

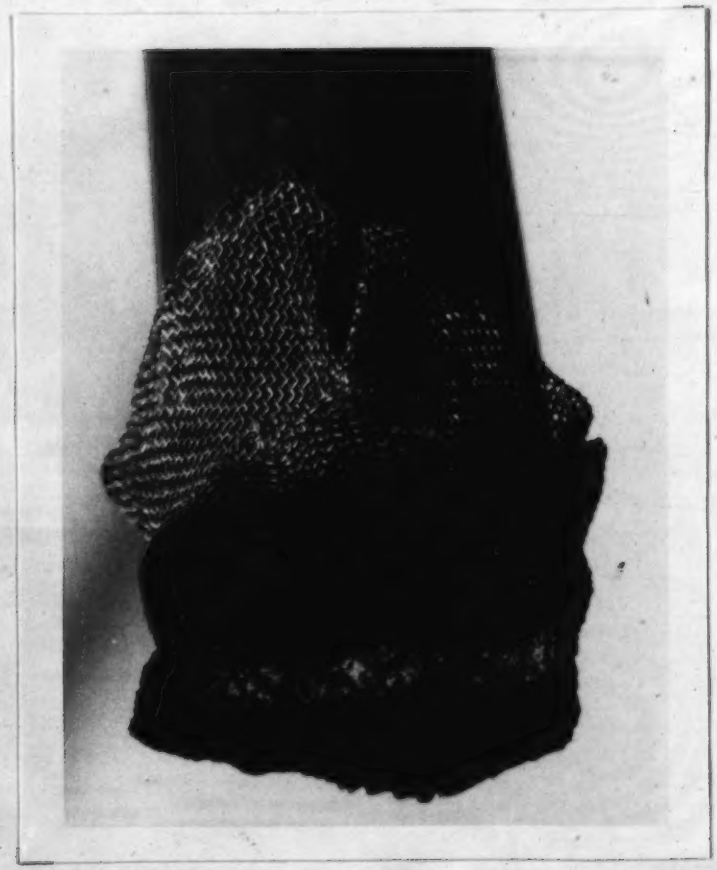

Photograph 7: Bottom of zirconia electrolyte showing sintering of powder.

Photograph 8: Sectioned zirconia electrolyte showing colour gradation.

Photograph 9: Section of electrolyte tube.

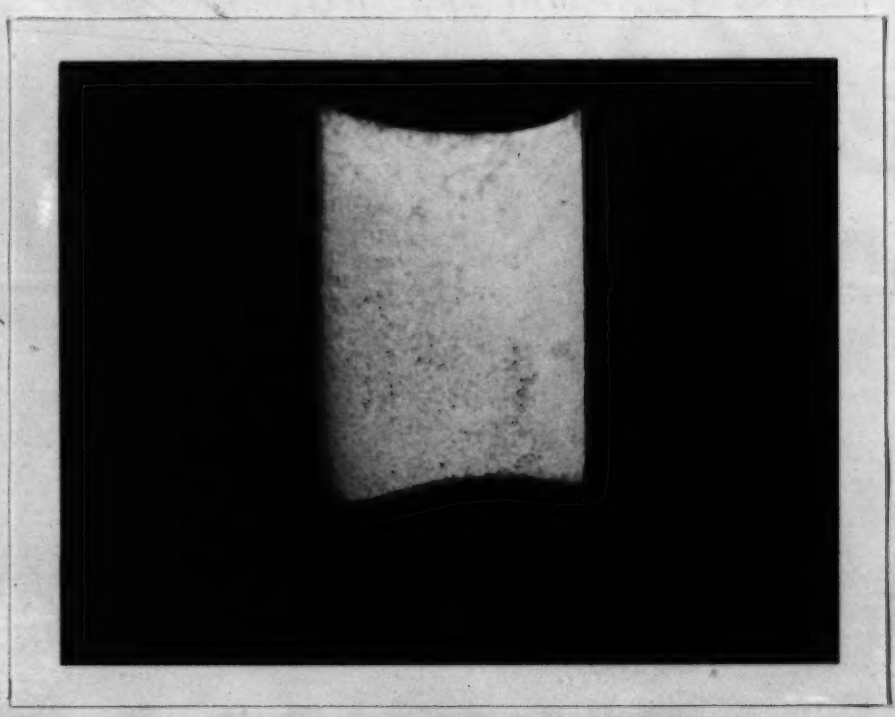

Photograph 10: Polished end of electrolyte tube.

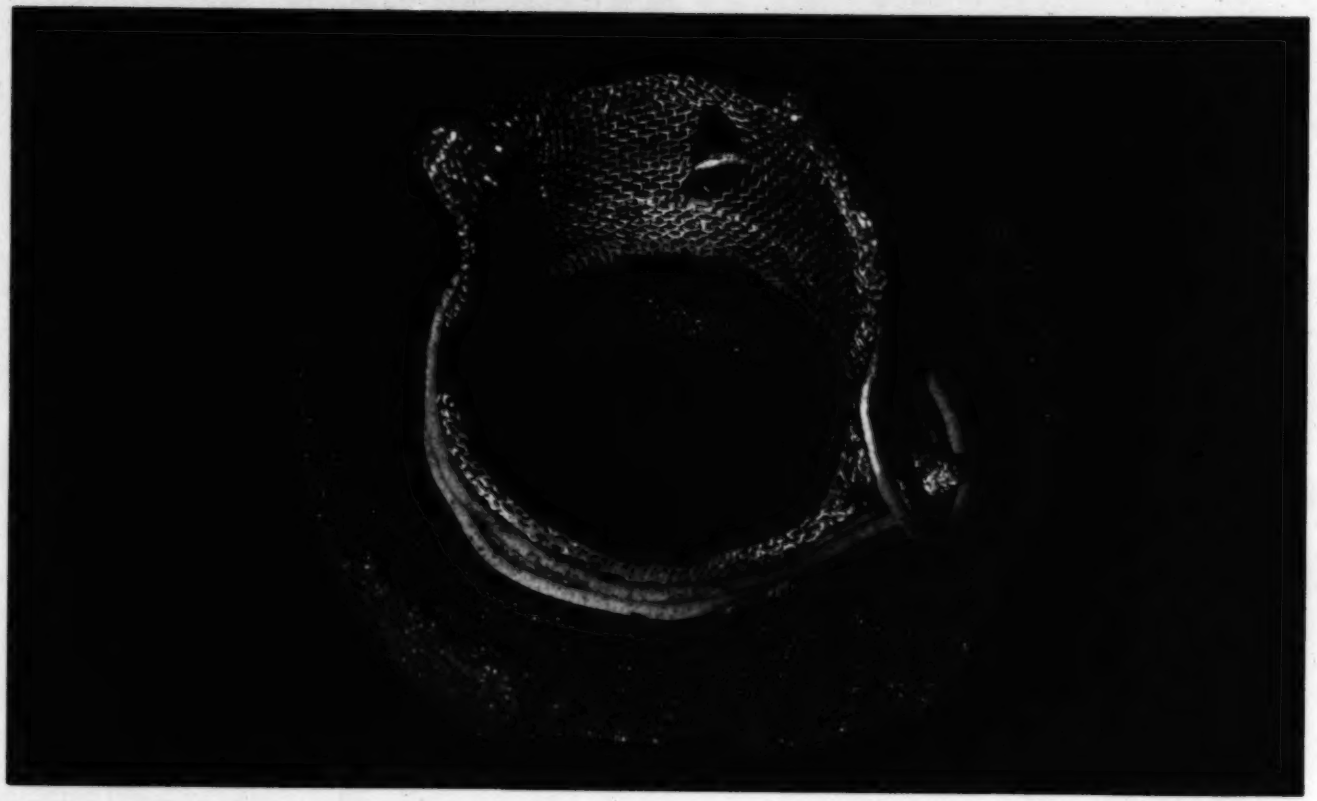

Photograph 11: Anode compartment of molybdenum cell.

BIBLIOGRAPHY

1. K.K. Kelley
   U.S. Bureau of Mines, Bulletin 407 (1937)
2. F.D. Richardson
   J. Iron and Steel Institute, 175, 33 (1953)
3. C.E. Wicks and F.D. Block
   U.S. Bureau of Mines, Bulletin 605 (1963)
4. E.K. Storms
   The Refractory Carbides,
   Academic Press, New York (1967)
5. L.E. Toth
   Transition Metal Carbides and Nitrides, Academic Press, New York (1971)
6. T.B. Reed
   Free Energy of Formation of Binary Compounds: An Atlas of Charts for High-Temperature Chemical Calculations,
   M.I.T. Press, Cambridge, Mass. (1971)
7. O. Kubaschewski and C.B. Alcock
   Metallurgical Thermochemistry, Fifth Edition, Pergamon Press, Oxford (1979) (See also earlier editions)
8. S.R. Shatynski
   Oxidation of Metals, 13, 105 (1979)
9. O. Ruff and T. Foehr
   Zeit. Anorg. Chem., 104, 27 (1918)
10. R Schenck, F. Kurzen and H. Wesselkock
    Zeit. Anorg. Chem., 203, 159 (1931)

11. F. Sauerwald, W. Teske and G. Lempert
Zeit. Anorg. Chem., 210, 20 (1933)

12. R.E. Slade and G.I. Higson
J. Chem. Soc., 105 (1919)

13. I. Barin and O. Knacke
Thermochemical Properties of Inorganic Substances, Springer-Verlag, Berlin (1973)

14. K.K. Kelley, F.S. Boericke, E.H. Huffman and W.M. Bangert
U.S. Bureau of Mines, Technical Paper 662 (1944)

15. F.S. Boericke
U.S. Bureau of Mines, Report of Investigations 3747 (1944)

16. T.Y. Kosolapova and G.V. Samsonov
Zhur. Priklad. Khim. 32, 55 (1959)

17. M. Hansen
Structure of Binary Alloys, First Edition, 345 (1941)
McGraw-Hill Book Co., N.Y.

18. E. Frieman and F. Sauerwald
Zeit. Anorg. Chem., 203, 64 (1932)

19. H. Goldschmidt
J. Iron and Steel Institute, 160, 345 (1948)

20. K.K. Kelley and E.G. King
U.S. Bureau of Mines, Bulletin 592, 35 (1961)

21. A. Westgren and G. Phragmen
Zeit. Anorg. Chem., 187, 401 (1930)

22. H. Moissan
Compt. Rend., 116, 349 (1893)

23. W. DeSorbo
J. Amer. Chem. Soc., 75, 1825 (1953)

24. R.A. Oriani and W.K. Murphy
J. Amer. Chem. Soc., 76, 343 (1954)

25. D.R. Stull and G.C. Sinke
Thermodynamic Properties of the Elements, American Chemical Society, Pub., Washington, D.C. (1956)

26. T.Y. Kosolapova and G.V. Samsonov
Zhur. Priklad. Khim. 32, 1505 (1959)

27. J.F. Elliott and M. Gleiser
Thermochemistry for Steelmaking, Addison-Wesley Pub. Co. Inc., Reading, Mass. (1960)

28. V.I. Alekseev and L.A. Shvartsman
Phys. Metals. Metallog., 11(4), 63 (1961)

29. S. Fujishiro and N.A. Gokcen
Trans. A.I.M.E., 221, 275 (1961)

30. Y.Z. Vintaykin
Phys. Metals. Metallog., 16(1), 127 (1963)

31. R. Speiser, H.L. Johnston and P. Blackburn
J. Amer. Chem. Soc., 72, 4142 (1950)

32. Y.Z. Vintaykin
Dokl. Akad. Nauk. SSSR, 129, 2 (1959)

33. H. Mabuchi, N. Sano and Y. Matsushita
Met. Trans., 2, 1503 (1971)

34. K.K. Kelley
U.S. Bureau of Mines, Bulletin 584, 232 (1960)

35. F.D. Rossini, D.D. Wagman and W.H. Evans
Nat. Bureau of Standards Circ. 500, 1266 (1952)

36. M. Gleiser
J. Phys. Chem., 69, 1771 (1965)

37. A.D. Mah
J. Amer. Chem. Soc., 76, 3363 (1954)

38. A.S. Bolgar, V.V. Fesenko and S.P. Gordienko
Sov. Powder. Met. Metal. Ceram., 2, 159 (1966)

39. O. Heusler
Zeit. Anorg. Chem., 154, 353, (1926)

40. H. Kleykamp
Ber. Bunsen. Physik. Chem., 73, 354 (1969)

41. A.D. Kulkarni and W.L. Worrell
Met. Trans., 3, 2363 (1972)

42. Y.A. Chang and D. Naujock
Met. Trans., 3, 1693 (1972)

43. V.N. Eremenko and V.R. Sidorko
Porosh. Met., 13(5), 51 (1973)

44. H. Tanaka, Y. Kishida , A. Yamaguchi and J. Moriyama
Nippon Kinzoku Gakkaishi, 35, 523 (1971)

45. A. Mah
U.S. Bureau of Mines, Report of Investigations 7217 (1969)

46. K.K Kelley
U.S. Bureau of Mines, Bulletin 582 (1960)

47. L.C. Browning and P.H. Emmett
J. Amer. Chem. Soc., 74, 4773 (1952)

48. C.P. Kempter
J. Amer. Chem. Soc., 78, 6209 (1956)

49. M. Gleiser and J. Chipman
J. Phys. Chem.,66, 1539 (1962)

50. W. Worrell
Trans. A.I.M.E., 223, 1173 (1965)

51. L.B. Pankratz, W.W. Weller and E.G. King
U.S. Bureau of Mines, Report of Investigations 6861 (1966)

52. A. Solbakken and P.H. Emmett
J. Amer. Chem. Soc., 91, 31 (1969)

53. A. Mah
U.S. Bureau of Mines, Report of Investigations 6337, 9 (1963)

54. R.J. Fries

J. Chem. Phys., 46, 4463 (1967)

55. V.I. Alekseev and L.A. Shvartsman

Russian Metallurgy and Fuels, Pt.6, 1 (1962)

56. I. Barin, O. Knacke and O. Kubaschewski

Thermochemical Properties of Inorganic Substances

Supplement, Springer-Verlag, Berlin (1977)

57. M. Gleiser and J. Chipman

Trans. A.I.M.E., 224, 1278 (1962)

58. V.I. Alekseev and L.A. Shvarstman

Russian Metallurgy and Fuels, (1), 41 (1963)

59. H.L. Schick

Thermodynamics of Certain Refractory Compounds,

Academic Press, New York (1966)

60. M.F. Ancey-Moret and M.Y. Deniel

I.R.S.I.D. Report AMC-188 (1971)

61. D.K. Gupta

A Ph.D. Dissertation, State University of New York at Stony Brook (1973)

62. G.W. Orton

Diss. Abst., 22, 527 (1961)

63. T.H. Etsell and S.N. Flengas

Chem. Rev., 70,339 (1970)

64. H. Schmalzried

Z. Elektrochem., 66, 572 (1962)

65. J.W. Patterson
J. Electrochem. Soc., 118, 1033 (1971)

66. T.H. Etsell and S. N. Flengas
J. Electrochem. Soc., 119, 1 (1972)

67. D.A.J. Swinkels
J. Electrochem. Soc., 117, 1267 (1970)

68. W.L. Worrell
Solid Electrolytes, Volume 21 of a series in:
Topics in Applied Physics, Springer-Verlag, Berlin (1977)

69. A. Block-Bolten, personal communication referring to:
Can. Journal of Chemistry, 54(12), 1967 (1976)

70. W. G. Moffatt
The Handbook of Binary Phase Diagrams
General Electric Co., Schenectady, N.Y., (1978)

71. F. A. Shunk
Constitution of Binary Alloys
McGraw-Hill Book Co., N.Y., (1969)